TITLE

BEHAVIOUR OF SELECTED SOUTH AFRICAN COALS IN CIRCULATING FLUIDISED BED(CFB) IN COMPARISON WITH RUSSIAN COAL

AUTHOR

Mohamed Belaid

(Student No. 348629)

A thesis submitted to the Faculty of Engineering and Built Environment, University of the Witwatersrand, Johannesburg, in fulfilment of the requirements for the degree of Doctor of Philosophy

Supervisor(s): Professor Rosemary Falcon

Johannesburg, 2017

DECLARATION

I declare that this thesis is my own, unaided work. It is being submitted for the degree of Doctor of Philosophy in the School of Chemical and Metallurgical Engineering, to the University of the Witwatersrand, Johannesburg. It has not been submitted before for any degree or examination to any other university.

_____

Candidate

_____ Day of _____ Year _____

DEDICATION

To my son, Soheib, the coolness of my eyes

&

In memory of my grandparents and khalu Abdel Kader

ACKNOWLEDGEMENTS

My sincere gratitude goes to the following people who made it possible to achieve this work:

My supervisor Professor Rosemary Falcon, for the guidance and patience, support and friendship.

My Gratitude to Dr Mark Vd Riet for advise, support and valuable input.

To Pasi Vainikka from VTT Finland for the tests conducted at VTT and for sharing valuable information and data for this project; I am indebted to you.

To all VTT employees who made my stay at VTT an enjoyable one.

To Witlab (Coal and Mineral Analysis); VM du Cann (Coal and Organic Petrography) and FINAS (lab service, Finland) for fuel analysis and petrography).

To the International Energy Agency (IEA) for the availability of reports and the permission to make use of these.

To all my friends, colleagues and family who supported and encouraged me through this journey.

To the Dean of the Faculty of Engineering and Built Environment (UJ) Prof Saurabh Sinha and the Head of School, Professor Antoine Mulaba, for support, and for giving me time off to finish this thesis.

To Professor Rafael Santos, Dave Wakeling and Terry Davids from Sheridan College, Toronto, Canada and all their colleagues for welcoming and hosting me during my sabbatical to complete this work.

Last, but not least, to my darling wife Zaheera, who kept supporting, and encouraging me to reach higher.

Thank you all.

ABSTRACT

South Africa (SA) has an energy-intensive coal mining industry, where coal accounts for approximately 72% of total primary energy consumption in the country, particularly in the electricity sector, where 95% of total electricity generated is derived from coal. Pulverised coal combustion has been the preferred technology adopted for power generation in South Africa for many decades. These coal-fired power plants have no flue gas desulphurisation (FGD) equipment fitted at present. Therefore, these plants account for the majority of annual SO_2, CO_2, and NO_x emissions, making them environmentally unsustainable for power generation. Such environmental issues add to the challenges for the power producer, who is required to meet not only energy demand, but also to compete with the export market for quality coals, and to ensure that electricity generation complies with ever-changing air quality standards.

Circulating fluidised-bed combustion (CFBC), a technology for the combustion of coal, biomass, waste, has not been adequately explored or tested in South Africa previously. CFB combustion is currently under intense scrutiny amongst researchers evaluating its potential as an economic and environmentally acceptable technology, in particular for the burning of low-grade coals.

The main objective of this study is to undertake a case study using CFBC technology and to establish its potential for use in South Africa as a clean and cost-effective method in power generating for high-ash, low-grade coals. Experimental tests were conducted in a CFBC pilot plant in Finland, using two high ash coals, discarded coal from South Africa (SA) and a better quality coal from Russia for comparative purposes. A review was conducted of discard coals in South Africa in order to establish an inventory in support of their potential utilisation for power generation in circulating fluidised bed boilers. A further study established a comparison between pulverised coal (PC), and fluidised bed (FBC) technologies as a future benefit analysis.

All four coals proved to have very high combustion efficiencies, despite significant quality differences in terms of petrographic composition and ash content. More specifically, the SA coals achieved combustion efficiencies of 99.6 %, 99.7 % and 99.8 %, where the Russian coal achieved 98.7 percent. The Russian coal was characterised as being low in ash and high in the reactive maceral vitrinite, the two South African coals possessed high ash content (35 to 45%),

one with relatively high vitrinite, and the other very low vitrinite, whilst the South African discard possessed an ash content of 65-70% and extremely low reactive vitrinite content. All these factors lean towards the suitability of SA coals to the CFB technology.

In terms of NOx emissions, all coals tested showed that their NOx and N_2O emission meet the minimum requirements for small plants as set out by the European and SA standards, i.e. <300 ppm for a plant with generating capacity below 100 MW. This result is in agreement with data from the literature.

The emission of SO_2 depends on the sulphur content in the initial coal, which also has an impact on the Ca/S Ratio. SO_2 emitted from the South African coals was higher than the national permitted standard, due to the low Ca/S ratio used. This was especially the case for South African discard.

Vast reserves of discard coal containing from 2MJ/kg to 14 MJ/kg in calorific value have accumulated in South Africa since the last inventory of 2001, i.e. close to 1.5 billion tonnes are in existence. It is apparent that one of the looming challenges regarding discard coal is putting this ever-accumulating material to use. From the combustion results obtained in this research, it is proposed that such materials can be combusted in a CFBC boiler, and that it produces the same efficiency as other coals from South Africa and a clean coal from Europe. Ash distribution within the boiler was found to change in proportion of bed ash to fly ash, subject to the quality of the coal used. This is also likely to change the proportions of sulphur-absorbing sorbents in future. CO_2 emissions from the coals under review were found to be very close, in the region of 12.8 to 13.8 percent.

TABLE OF CONTENTS

List of Tables

List of figures

List of symbols and abbreviations

$	:	American Dollar
$/MWh	:	Dollar per Megawatt hour
APCDs	:	Air Pollution Control Devices
B 2	:	Batch two, coals analysed in Finland
B1	:	Batch one, coals analysed in South Africa
BFB	:	Bubbling Fluidised Bed
C & I	:	Capital and Investment
$CaCO_3$	:	Calcium Carbonate
$CaSO_4$	:	Calcium Sulphate
CFB	:	Circulating Fluidised Bed
CFBC	:	Circulating Fluidised Bed Combustion
CO_2	:	Carbon Dioxide
COE	:	Cost of Electricity
CQA	:	Coal Quality Assessment
CSIR	:	Council of Scientific Industrial Research
DME	:	Department of Minerals and Energy
EPRI	:	Electric Power Research Institute
ESKOM	:	South African National Electricity Producer (South Africa)
FBC	:	Fluidised Bed Combustion
FG	:	Flue Gas
FGD	:	Flue Gas Desulphurisation
FP	:	Fuel Power

FTIR	:	Fourier Transform Infra-Red Spectroscopy
HET	:	Heterogeneous
Hg	:	Mercury
HHV	:	Higher Heating Value
HOM	:	Homogenous
IEA	:	International Energy Agency
IGCC	:	Integrated Gasification Combined Cycle
IRP	:	Integrated Resources Plan
LCOE	:	Levelised Cost of Electricity
LCP	:	Large Combustion Plant
LHV	:	Lower Heating Value
MES	:	Minimum Emission Standards
MF	:	Mass of Fuel
MFF	:	Mass Fuel Flow
Mtpa	:	Million tonne per annum
MWh	:	Megawatt hour
N_2O	:	Nitrous Oxide
NERSA	:	National Energy Regulator of South Africa
NGCC	:	Natural Gas Combined Cycle
NMVOCs	:	Non Methane Volatile Compound
NO_2	:	Nitrogen Dioxide
NOx	:	Nitrogen Oxide
O & M	:	Operation and Maintenance

P	:	Pressure
PC	:	Pulverised Coal
PD	:	Pressure Drop
PF	:	Pulverised Fuel
PM	:	Particulate Matter
QEMSCAN	:	Quantitative Evaluation of Materials by Scanning Electron Microscopy
R & D		Research and Development
RT	:	Riser Temperature
Russ	:	Russian Coal
SABS	:	South Africa Bureau of Standards
SANEDI	:	South African National Energy Development Institute
SCPF	:	Supercritical Pulverised Fuel
SCR	:	Selective Catalytic Reactor
SMME	:	Small Medium Micro Enterprise
SNCR	:	Selective Non-Catalytic Reactors
SA	:	South Africa
SA I	:	South African Coal One
SA II	:	South African Coal Iwo
SA Discard	:	South African Coal Discard
SO_2	:	Sulphur Dioxide
SO_3	:	Sulphur Trioxide
SOx	:	Sulphur Oxide
TC	:	Total Carbon in the discharge (bottom ash + fly Ash bag filter)

TE	:	Thermo-Element
TEs	:	Trace Elements
TIC	:	Total Inorganic Carbon in the discharge
TOC	:	Total Organic Carbon in the discharge
TWh	:	Terawatt hour
VF	:	Volume Flow
VOC	:	Volatile Organic Compound

INTRODUCTION

This chapter provides the background, problem statement, main objectives, significance, and contributions of the study.

The study has two main impacts: namely social and economic, for the generation of power with the use of new technology as CFB in the following areas:

- Enviromental impact
- Power generation cost reduction
- Coal discard valorisation
- Job creation

1.1 Background and motivation

Coal represents at present about 70% of world's proven fossil fuel resources, moreover, coal is also a more delocalised resource, and has a lower cost among the different fossil fuels. The use of coal for electricity generation is increasing rapidly, since coal is a relatively inexpensive energy source. Its energy price is estimated to be about US$ 3.5/MBtu (million British thermal units), whereas natural gas and oil are US$ 12.6/MBtu and US$ 10.1/MBtu, respectively due to a progressive decrease in oil prices pushing contract prices downward from 26.1 US$/MBtu in 2008 to US$ 10.1/MBtu in 2015 [2]. This leads to continuing plans to establish coal-fired power plants as a major source of electricity supply in many parts of the world, in turn resulting in the anticipation of coal consumption above 15 trillion kilowatt-hours by 2030 [2]. Global coal supply is forecast to increase by 752 Mtce (+2.1% per year), from 5 709 Mtce in 2013 to 6 462 Mtce in 2019 [3, 4]. Thus, coal is likely to remain one of the main sources of primary energy for the foreseeable future, playing a strategic role in medium to long-term energy production systems [1].

However, even though coal is a major energy and economic resource, it has an adverse impact on the environment. For example, greenhouse gas (GHG) emissions from the energy sector represent roughly two-thirds of all anthropogenic greenhouse-gas emissions, and CO_2

emissions from the sector have risen over the past century [3]. It has been reported that electricity generation by coal combustion contributes to about 40% of the world's GHG emissions [4]. Effective action in the energy sector is, consequentially, essential to tackling the climate change problem.

Of the number of coal-fired electricity plants, pulverised coal (PC)-fired power plant is the most commonly used in electricity generation plants around the globe as it has the highest reliability and commercial readiness for high electricity production capacity. About 1465 GWe (75% Subcritical PC, 23% Supercritical and 2% Ultra Supercritical) of the world's electricity generation comes from PC-fired power plant whereas only 20 GWe and 1GWe come from fluidised bed power plant and integrated gasification combined cycle (IGCC), respectively [1, 5, 6].

Due to thermodynamic (the use of water) and metallurgic constraints, the efficiency of currently operating pulverised coal fired power plants, is relatively low. Modern pulverised-coal-fired power plants can, however, achieve efficiency of about 38–40% (based on the lower heating value of the fuel) operating at 250–300 bar, and at the maximum temperature of 550–570 °C. Nevertheless, such plants are characterised by high pollutant emissions, especially carbon dioxide (about 800g for each kWh of electric energy produced). For this reason, the construction of PC-fired power plants is not popular, and is going to be increasingly difficult in many countries, unless a higher reduction of carbon dioxide (CO_2) removal can be devised and implemented. Post-combustion capture and storage technologies using chemical absorbents to capture CO_2, followed by compression to a high pressure, transportation and storage in an underground reservoir appear to provide a near-term strategy to resolve this issue. However, there are very few, if any, commercial or demonstration plant using this post-combustion strategy for complete CO_2 capture and storage in Africa [7].

1.2 SA power generation

For many decades, power generation in South Africa has been supplied by coal in subcritical pulverized fuel (PF) combustion plants, as used in the majority of the power stations owned by

Eskom. Currently, two new supercritical coal-fired power plants are under construction, with one near completion.

Usage of coal for power and coal to liquid fuel derived from coal accounts for around 86% of the 420 million tons of carbon dioxide (CO_2) emissions South Africa produces annually (2013 estimate) [8]. This in turn represents around 40% of Africa's total coal-derived CO_2 emissions. Generally about two-thirds of sulphur dioxide, one-third of carbon dioxide emissions and one quarter of the nitrogen oxides emissions in South Africa are produced by coal-burning plants [9].

To date, South African Eskom's coal power plants do not include greenhouse gas (GHG), CO and CO_2 emissions capture or reduction processes. Despite this, in terms of SOx (no GHG) emission, the two new power stations (Medupi and Kusile) will be fitted with flue gas desulphurisation (FGD) plants in due course.

Other technologies designed to reduce GHGs and SOx are available, but have not yet been used for this purpose in South Africa, despite attempts by various researchers and stakeholders to introduce one or more methods in recent years. One such attempt is that of North [10] (who gave a detailed historical review of research undertaken by his team at the Council of Scientific, and Industrial research (CSIR) concerning studies conducted on bubbling fluidised bed for SOx reduction. Currently, the South African National Energy Development Institute (SANEDI) is planning a pilot-scale borehole to establish the feasibility of CO_2 storage in one or two land-based rock formations, however, less than 1.2% of land storage is considered to be suitable rock receptacles [11].

Fluidised bed combustors (FBCs), both circulating (CFBCs) and bubbling (BFBs) have been developed internationally as combustion technologies that are useful for widely different fuels such as coal, wastes and biomass. To date in South Africa, small-scale (<60MW) BFBC plants have been developed for various industries, but large-scale Circulating Fluidised Bed Boilers (CFBC) have not been recognised or explored previously [12].

Nevertheless, CFB technology is rapidly emerging as the most suitable technology as it offers various significant advantages. Eskom is currently considering this as a long-term process technology, given that: (i) the reducing qualities of coal, which are now being supplied to, and are unsuitable for, the current suite of PC power stations; and (ii) Eskom's challenge of not meeting energy demand and therefore the need for more power stations in future. Against this background, a number of Independent Power Producers (IPPs) are now emerging most of which are considering the establishment of CFBCs to produce their power using the country's poorer qualities of coal and related waste materials.

In the longer term, the Department of Energy (DOE) plans to increase energy production using renewable energy, thereby to reduce the dependence on coal as a major source of energy. The National Energy Regulator of South Africa (NERSA),regulate the processes including tariffs. Nevertheless, coal reserves, discard coal stockpiles and reduced process technology cost will strengthen the case for the combustion of both coal and coal discard for electricity production for the next 50 to 60 years.

1.3 Problem statement

South Africa is characterised by a shortage of electricity; this together with anticipated future increases in the price of the utility and the aging of the Eskom power plants present a serious challenge to South Africa. The electricity generation capacity came under pressure since 2008, which warranted blackout and load-shedding. The electricity generation capacity versus the demand is depicted in Figure 1.1 below.

Furthermore, Eskom is facing ever-increasing constraints with regard to air quality and emissions, with which none of the current power stations can comply. The most recent air quality came into effect in 2015, due to local and international pressure to deal with global warming and the commitment made by the SA government to the international community to embark in the emission reduction campaign [13, 14].

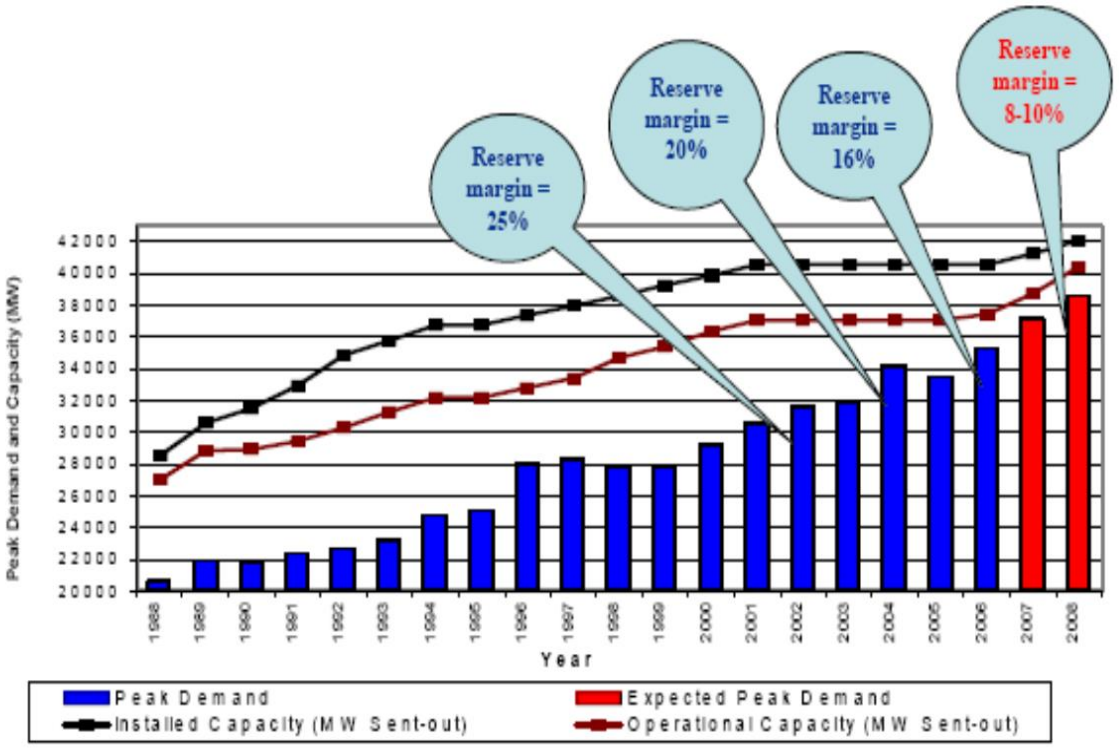

Figure 1. 1 Power demand and capacity in South Africa up to the peak crisis in 2008 [15].

A third point of concern in this problem statement is the quality of South Africa's remaining reserves of coal. Most of the easily accessible good quality coals have been mined out, and only the lower grades are available for production. Furthermore, once mined, the coals that are washed produce a Low Grade product suitable for India and the Far East, at 20-23% ash, leaving behind a much lower grade and higher ash discard material (30-75% ash). Such material is unsuitable for the current PC boiler plants, as they were originally designed for better qualities of coal [16].

In addition to currently mined coals, South Africa holds over 1,5 billion tons of historically discarded coal material from exports in earlier decades. i.e. started to export coal in the early 1970s. The international customers required low ash products for blend coking and high-grade steam generation (7% ash and 10-12% ash), and for the first time, the South African industry started to wash its products in large quantities. Once the prime products were taken off, the discarded material (known as "discard") was then dumped. This has resulted in the accumulation of reasonable reserves of potentially useful discarded coal, where some mines have also practiced double-washing, thereby producing two grades of saleable products and

dumping the remainder of the discarded material. These discards are considered as lower quality coals, with considerably high ash content [17].

As little attention was paid to finding ways of beneficiating this discarded material in the past, such material has continued to accumulate over the years, occupying potentially useful land and polluting the environment i.e. spontaneous combustion and ground water contamination.

Today's challenge is to understand the composition and quantity of this material, and hence, to investigate ways in which such discard coal can be best utilised – whether beneficiated or not, in order to extend the coal-fired energy resources of the country and to eliminate the environmental hazards that discard dumps present. No boilers currently operating in the country can utilise such material. Investigating the potential for using such material in a process technology of the future is the primary goal of this research.

1.4 Study objectives

The major objectives of this study are:

- To study the comparison between bubbling fluidised bed (BFBC) and circulating fluidised bed (CFBC) technologies followed by the pulverised coal (PC) versus circulating fluidised bed (CFBC) technologies, in relation to the use of the technologies and application to South African (SA) coals.

- To compare the combustion behaviour of three selected high ash SA coals with Russian coal in Circulating fluidised bed (CFB) in terms of the following:
    - study of the combustion efficiency;
    - study of the behaviour of minerals and ash found in SA coals;
    - study of the formation of NOx and N_2O;
    - study of the formation of SOx; and
    - study of CO_2 emission and trace elements.
- To undertake a review of South African (SA) coal discard inventory and its potential utilisation for power generation in circulating fluidised bed boilers.

1.5 Significance

This study proposes the following significance:

- An indication of how three specific South African (SA) coals combust in CFB boilers;
- A comparative analysis of PF and FBC technologies for power generation;
- Proof/indications and results that PF technology could be replaced by CFB technology;
- Evidence that coal discards could be an efficient and cost effective combustible material in CFB boilers for power generation;
- Calculations that suggest that CFB application will contribute to the reduction of electricity costs in South Africa; and
- Evidence to suggest that emission reduction in CFBC is both efficient and cost-effective.

1.6 Contribution and benefit of the research to industry and academia

The thesis makes an original contribution to the literature on SA coals combustion in CFB in the following ways, presenting:

- Results in the form of real combustion tests of SA coals in CFB;
- SA coal performance in CFB versus the Russian coal;
- The difference in the combustion temperature and the ignition patterns;
- SA coal's suitability to CFB application;
- An emission study;
- SA coal discard testing and valorisation; and where
- The thesis results provide a methodological platform for the process optimisation and application of CFB for power generation in South Africa.

1.7 Thesis outline

The thesis is structured into five chapters as follows:

Chapter One: Introduction

This section outlines the background with regard to South Africa's power generation situation, and the reasons for this study, followed by the objectives and the anticipated outcomes, as well as their significance arising from this work.

Chapter Two: Literature survey

This section gives a detailed account of PF/PC and CFB technologies, stating the major differences and challenges facing these technologies and highlighting the advantages of CFB over BFBC and PF, in addition to a detailed study on South Africa situation with regard power generation and environmental concerns.

Chapter Three: Methodology

This section outlines the coal samples that were used in this study, the analyses that were undertaken on them, and the specific pilot-scale test equipment in which the coals were combusted.

Chapter Four: Results and Discussion

All test results and their analyses are presented in this section, followed by detailed discussion using the literature for critical analysis.

Chapter Five: Conclusion and Recommendations

This chapter encompasses two sections, namely the conclusion and recommendations. In the first, all major conclusions will be highlighted, followed by major recommendation for future research and application purposes.

CHAPTER TWO LITERATURE REVIEW

This chapter provides a review of the background issues pertaining to this research and a review of previous work conducted in the fields pertinent to the technologies used in this study.

2.1 Background

Power in South Africa is predominantly generated by Eskom's 14 power stations using subcritical boilers and pulverised coal (PC) as the source material for combustion leading to steam generation, where two new coal-fired power stations with supercritical PC boilers are currently being near full commissioning. While other technologies for coal-fired power generation are known and available, namely Fluidised Bed Technologies, these have not been introduced into South Africa for large-scale base-load purposes, due to their historic limitations in size, scale and output. This is no longer the case, as modern, fluidised bed technologies are now being stalled with capacities of up to 600 MW or more per unit, i.e. equal to the capacities of Eskom's current PC boilers of 600^{+} MW. Such fluidised bed boilers are specifically found in the form of Circulating Fluidised Bed (CFB) technology.

Of the two forms of fluidised bed, circulating fluidised bed is rapidly emerging as the most suitable technology for large scale power generation due predominantly to its capacity to handle large quantities of feed material in an extended boiler configuration which, when turned down (not fluidised), can withstand the weight of such loads [18].

Fluidised bed combustors (FBCs), both circulating (CFBCs) and bubbling (BFBs) have been developed to accept widely different fuels from a wide range of grades of coal to variable municipal and industrial waste materials and biomass [12].

Of particular significance to South Africa, is the fact that CFB boilers can effectively handle wide variations in coal quality, such as can exist even within coals from the same mine. Furthermore, given the flexibility of feed intake, and in an attempt to minimise the operational costs, utilities could well seek to utilise cheaper, lower-grade coal, including discards with high moisture, ash and sulphur contents. Lower-grade coals have already been used in CFBC power production in Poland, in the Turow, Jaworzno and Lagisza power stations, where lower grade coal and washed discards have proved to be valuable sources of energy [19].

The proven high efficiency of the circulating fluidised-bed (CFB) technology also offers an excellent partial solution for CO_2 reduction, both in retrofitting existing coal fired power plants and in greenfield power plants [18]. CFB technology, with its excellent fuel flexibility, offers the opportunity to further reduce CO_2 emissions by co-combusting coal with biomass [20]. Foster Wheeler has also developed CFB gasification technology for biomass applications. An example of this technology is gasification of biomass with a pressurised gasifier to produce syngas, which can be used for biodiesel production to address the reduction of CO_2 emissions from vehicles [19, 21].

2.2 Fluidised Bed Technologies and Fluidisation Principles

2.2.1 Background

Fritz Winkler was the first to demonstrate the gasification of coal in a fluidised bed. He did this by introducing gaseous products of combustion into the bottom of a crucible containing coke particles on 1921. The mass of the particles was lifted by the drag of the gas to look like a boiling liquid [22].

This experiment initiated the process of fluidisation, namely the art of making granular solids behave like liquids. This experiment paved the way for the development of fluidised bed technology and its uses for various applications, especially in combustion and gasification processes.

In 1950, Lurgi [23] constructed the first reactor for roasting of sulphur bearing materials, based on the principles of fluidised bed technology. The new system was quickly adopted by industry, where fluidised bed roasters increasingly replaced multiple hearth furnaces and rotary kilns, thereby ensuring enhanced product quality and significantly reduced plant emissions.

Fluidised bed combined with efficient heat recovery and off gas treatment, including the process of converting the off gas to sulphuric acid, became state-of-the-art technology for processing sulphur bearing ores [23].

The circulating fluidised bed (CFB) was developed more recently in the last 40 years or so, for the high temperature treatment of fine and light particles [24]. A variety of other CFB applications followed, with more than 170 industrial plants worldwide [24, 25]. The CFB has been successfully applied for coal combustion, roasting of gold containing ores, direct reduction of iron ore fines, and other uses [23]. Therefore, the development and refinements of CFBC units continue to grow to this day.

2.2.2 Fluidisation principles

Fluidisation is a process in which solids are caused to behave like a fluid, by blowing gas or liquid upwards through the solid-filled reactor [26]. When a liquid or a gas is passed at very low velocity up through a bed of solid particles, the particles do not move, and the pressure drop is given by the Ergun equation. If the fluid velocity is steadily increased, the pressure drop and the drag on individual particles increases, and eventually the particles start to move and become suspended in the fluid. The terms "fluidisation" and "fluidised bed" are used to describe the condition of fully suspended particles, since the suspension behaves like a dense fluid. When the frictional force acting on the particles, or pressure drop, of the flowing air through the bed equals or exceeds the weight of the bed, the powder particles become suspended and the bed exhibits liquid-like behaviour, as shown in Figure 2.1 below. At gas flowrates less than the fluidisation velocity, the bed is a fixed bed and there is no movement of particles. At flowrates above minimum fluidisation, the bed expands and bubbles appear [27]. The minimum fluidisation velocity can be found graphically as shown in the graph of Figure 2.1 below, with the use of the Ergun equation.

Ergun equation

$$\frac{\Delta P}{L} = 150\frac{(1-\varepsilon_{mf})^2}{\varepsilon_{mf}^3}\frac{\mu U_{mf}}{(\phi_s d_p)^2} + 1.75\frac{(1-\varepsilon_{mf})}{\varepsilon_{mf}^3}\frac{\rho_g U_{mf}^2}{\phi_s d_p} \qquad 2.1$$

Where ΔP is the pressure drop

U_{mf}: minimum fluidisation velocity

μ: fluid viscosity

ε_{mf}: void fraction, it was estimated for many systems as: $\varepsilon_{mf} \approx (14\ \varphi_s)^{-1/3}$ where φ_s is the particle sphericity

ρ_g: density

dp: particle diameter

L: bed height

The air velocity corresponding to a pressure drop that just equals the weight of the bed is referred to as the minimum fluidisation velocity. At this air velocity or flowrate, all of the bed particles are completely suspended by the air stream. For a given system, minimum fluidisation velocity can be determined from a pressure drop vs. air velocity diagram, as shown in Figure 2.1. As air flow is increased above the minimum fluidisation velocity, the bed may exhibit behaviours ranging from smooth fluidisation to bubbling fluidisation to dilute fluidisation, in which powder can be transported by the air stream. Smooth fluidisation is desirable for optimal performance in the powder coating process [26, 27].

The liquid-like nature of the fluidised powder bed allows for high heat and mass transfer rates between the gas phase and the solid phase. As a result, fluidisation is widely used in many applications [28].

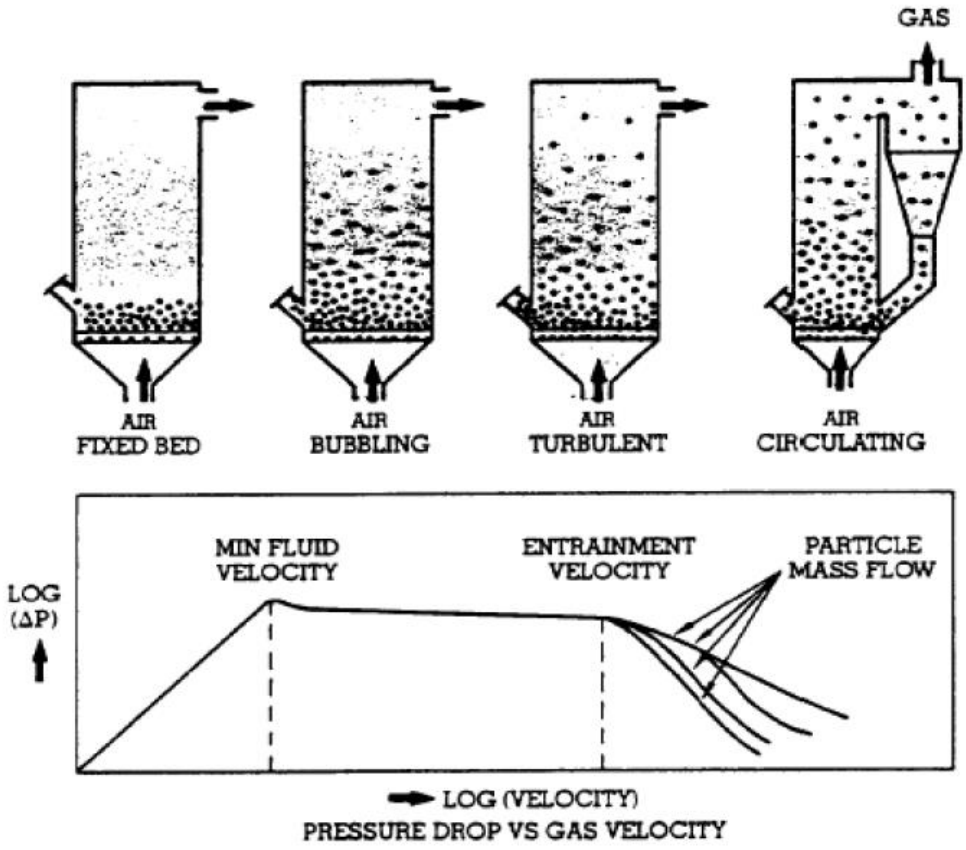

Figure 2.1: Principle of fluidisation [29]

Fluidisation is widely used in commercial operations. Their applications can be roughly divided into two categories, i.e.:

a. physical operations, such as transportation, heating, absorption, mixing of fine powder, etc.; and
b. chemical operations, such as reactions of gases on solid catalysts and reactions of solids with gases, etc.

The fluidised bed is one of the best-known contact methods used in the processing industry, for instance in oil refinery plants. Among its chief advantages are that the particles are well-mixed, leading to low temperature gradients, suitable for both small and large scale operations, allowing for continuous processing.

There are many well-established operations that utilise this technology, including cracking and reforming of hydrocarbons, coal carbonisation and gasification, ore roasting, Fisher-Tropsch synthesis, coking, aluminium production, melamine production, and coating preparations. The

application of fluidisation is also well-recognised in nuclear engineering as a unit operation, for example, in uranium extraction, nuclear fuel fabrication, reprocessing of fuel and waste disposal [30].

Fluidisation depends largely on the particle size and the air velocity. The mean solids velocity increases at a slower rate than does the gas velocity. The difference between the mean solid velocity and mean gas velocity is called as slip velocity. Maximum slip velocity between the solids and the gas is desirable for good heat transfer and intimate contact [31, 32].

2.2.3 Gledart Classic Classification of Powders

The fluidisation phenomena of gas-solids systems depend very much on the types of powders employed. There are several classifications available in the literature, all based on the original work by Geldart[33]. Geldart [33] classified the fluidisation of particles into four groups which are used extensively in the industry. The following are the major groups:

Group A: The materials have small mean particle size ($d_p < 30$ μm) and/or low particle density <1.4 g/cm^3), and are easily fluidised with smooth fluidisation at low gas velocities and controlled bubbling with small bubbles at higher gas velocities. A point is eventually reached when bubbles start to form and the minimum bubbling velocity, U_{mb} is always greater than U_{mf}. A typical example of this category is the fluid cracking catalysts.

Group B: is called ‘sand like’ particles and some call it bubbly particles, which result in vigorous bubbling fluidisation under these conditions. Bubbles form as soon as the gas velocity exceeds the minimum fluidisation velocity. Most particles of this group have size 150 μm to 500 μm and density from 1.4 to 4 g/cm^3. For these particles, once the minimum fluidisation velocity is exceeded, the excess gas appears in the form of bubbles. Bubbles in a bed of Group B particles can grow to a large size. Typically used Group B materials are glass beads (*ballotini*) and coarse sand.

Group C: materials are ‘cohesive’, or very fine powders. Their sizes are usually less than 30 μm, and are extremely difficult to fluidise, because inter-particle forces are relatively large, compared to those resulting from the action of gas. In small diameter beds, Group C particles easily give rise to channeling. Examples of Group C materials are talc, flour and starch.

Group D: is called 'spoutable' and the materials are either very large or very dense. They are difficult to fluidise in deep beds. Unlike Group B particles, as velocity increases, a jet can be formed in the bed and material, and may then be blown out with the jet in a spouting motion. If the gas distribution is uneven, spouting behaviour and severe channelling can be expected. Roasting coffee beans, lead shot and some roasting metal ores and gasifying coals are examples of Group D materials.

Geldart's classification is clear and easy to use, as displayed in Figure 2.2 for fluidisation at ambient conditions and for U less than about $10 \cdot U_{mf}$.

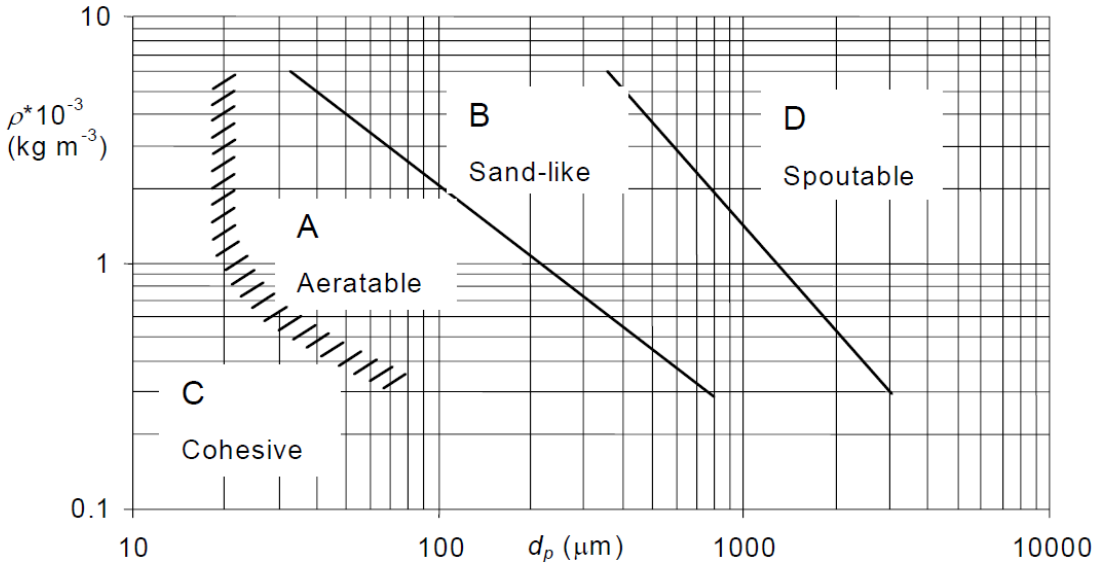

Figure 2.2 Diagram of Geldart classification of particles for fluidisation by air (ambient conditions) [33].

Figure 2.2 shows the Geldart classification for any solid of a known density ρ_s and mean particle size d_p. This graph shows the type of fluidisation to be expected. It also helps predicting other properties such as bubble size, bubble velocity, the existence of slugs etc.

2.2.4 Fluidised bed types

There are three basic types of fluidised bed combustion boilers:

- Atmospheric classic Fluidised Bed Combustion System (AFBC)
- Atmospheric circulating (fast) Fluidised Bed Combustion system (CFBC)
- Pressurised Fluidised Bed Combustion System (PFBC).

A review dealing with CFB technology is provided in sections 2.2.5, 2.2.6, 2.2.7 and 2.2.8 followed by a comparison between CFB and bubbling fluidised bed, which lead to a comparison between CFB and PC technology in sections 2.3 and 2.4, respectively.

2.2.5 Circulating fluidised bed

Given the fact that CFBC technology is the process under review, rather than BFBC, the following section outlines the background of that technology.

A circulating fluidised bed boiler is one in which the fuel is burnt in a fast, extended fluidised bed regime. The gas velocity is sufficiently high to blow all the solids out of the furnace. The majority of the solids leaving the furnace are captured by a gas-solid separator, and are recirculated back to the base of the furnace at a rate sufficiently high to cause a minimum degree of vertical mixing of solids in the furnace.

The process flow and key components of a CFB boiler are shown in figures 2.3 and 2.4, respectively. The primary combustion air (usually stoichiometric in amount) is injected through the floor or grate of the furnace, and the secondary air is injected from the sides at certain height above the furnace floor. Fuel is fed into the lower section of the furnace, where it burns to generate heat. A fraction of the combustion heat is absorbed by water or stream cooled surface located in the furnace, and the rest is absorbed in the convective section located further downstream, known as the back pass [34].

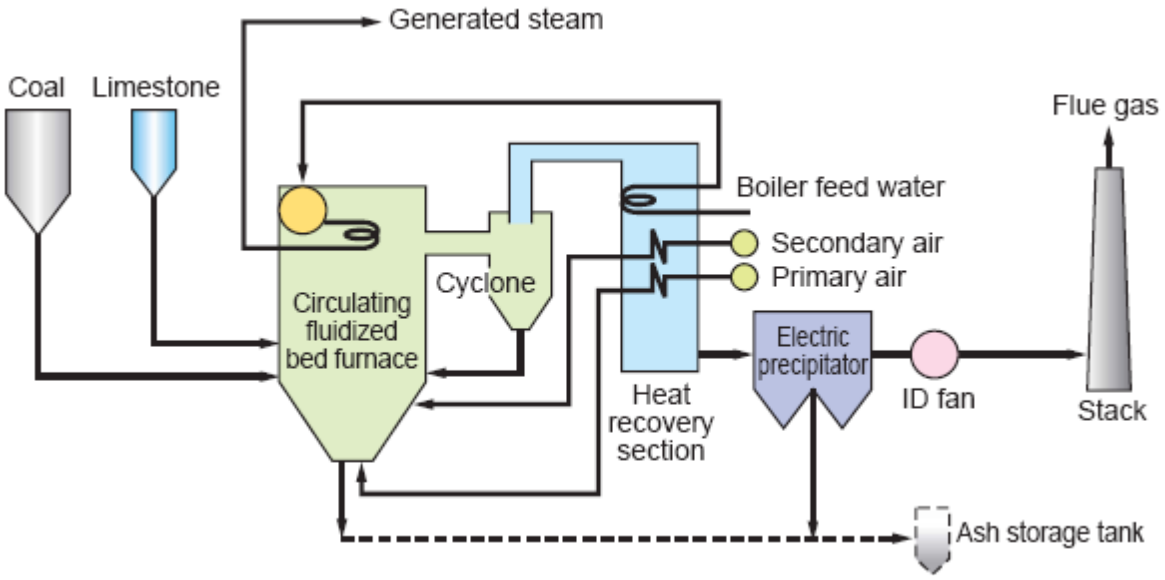

Figure 2. 3 Process flow of circulating fluidised bed boiler (Foster wheeler, Finland) [35].

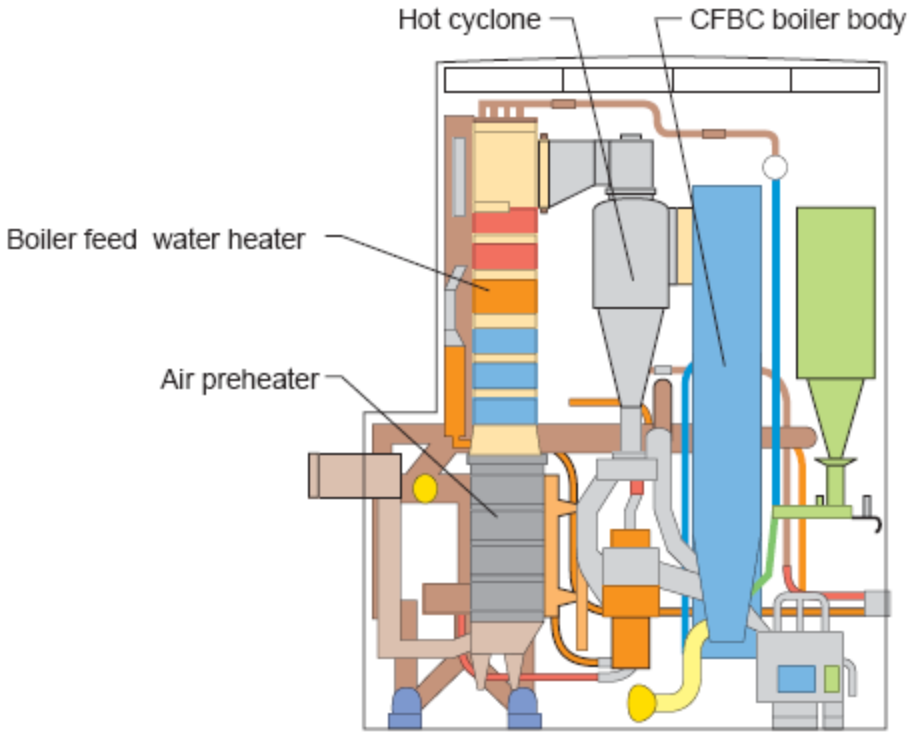

Figure 2. 4 Schematic drawing of CFBC structure (Foster Wheeler, Finland) [35]

In terms of process flow, a circulating fluidised bed boiler can be divided into two sections; the first is the CFB loop made of Furnace or CFB riser, Gas–solid separation (cyclone), Solid

recycle system (loop-seal), External heat exchanger (optional), while the second is the back-pass made of super heater, reheater, economiser, and air heater [19, 36].

At higher gas velocities, the slip velocity increases and the fluidised bed changes its behaviour. The defined boiling surface disappears with the expansion of the fluidised solids. The fluidisation gas has enough energy to entrain solids particles. The entrained particles are separated from the gas by a cyclone and recirculated via an external loop, back into the fluidised bed reactor. In addition, an internal recirculation of the solids in the fluidised bed reactor takes place. Both internal and external circulation results in a homogenous temperature distribution in the CFB system [34, 37].

2.2.6 Merits of CFB

Many researchers and operators confirmed that circulating fluidised bed technology merits are considerably favourable as a technology suitable to various applications with the emphasis on fuel flexibility[36].

The major performance features of the circulating bed system as reported by various authors are as follows [36, 38].

- Fuel Flexibility: FBC boilers can be operated efficiently with a variety of fuels. Even fuels like flotation slimes, washer rejects, agro-waste can be burnt efficiently. These can be fed either independently or in combination with coal into the same furnace.
- Ability to Burn Low Grade Fuel: FBC boilers would give the rated output even with an inferior quality fuel. The boilers can fire coals with ash content as high as 62%, and have calorific value as low as 2,500 kCal/kg. Even carbon content of only 1% by weight can sustain the fluidised bed combustion.
- Ability to Burn Fines: Coal containing fines below 6mm can be burnt efficiently in the FBC boiler
- High processing capacity, due to the high gas velocity through the system.

- The temperature of about 820 ºC -870 ^{o}C is reasonably constant throughout the process because of the high turbulence and circulation of solids.
- The low combustion temperature in the bed 820 ºC -870ºC also advantageous for the suppression of NOx emission. However the FBC generate a significant proportion of the NOx as N2O which has a high global warming potential.
- Sulphur present in the fuel is retained in the circulating solids in the form of calcium sulphate, and removed in solid form. The use of limestone or dolomite sorbents allows a higher sulphur retention rate, and limestone requirements have been demonstrated to be substantially less in a CFBC unit than in BFBC combustor.
- The combustion air is supplied at 1 to 1.1 atm, rather than 1.2-1.3 atm, as required by bubbling bed combustors.
- It has a better turndown ratio than the bubbling bed system.
- Erosion is still a concern, and is only reduced to a certain extent by the heat transfer surface in the combustion chamber, since the surface is parallel to the flow. In a bubbling bed system, the surface generally is perpendicular to the flow.
- High Efficiency: FBC boilers can burn fuel with a combustion efficiency of 95-99%, irrespective of ash content.
- Reduction in size: high heat transfer rate over a small heat transfer area immersed in the bed results in overall size reduction for the boiler.
- Pollution Control: SO_2 formation can be greatly minimised by addition of limestone or dolomite for high sulphur coals.
- Low corrosion, the effect is less due to lower combustion temperature, softness of ash and low particle velocity (around 1 m/sec).
- The heat and mass transfer rates are high.
- Good temperature control can be achieved.
- Lower temperature operation increases refractory life.
- As there are no moving parts (excluding the fans to fluidised the bed) in the furnace, the maintenance costs are low.

- The lower operating temperature of CFBC boilers (820°C-870°C) reduces the risk of fouling and agglomeration.
- Easier Ash Removal – Low Clinker Formation: Since the temperature of the furnace is in the range of 750°C -900°C in FBC boilers, even coal of low ash fusion temperature can be burnt with less clinker formation. Ash removal is easier as the ash flows like liquid from the combustion chamber. Hence less manpower is required for ash handling.
- The CO_2 in the flue gases will be of the order of 14-15% at full load.
- Simple Operation, Quick Start-Up: High turbulence of the bed facilitates quick start up and shut down. Full automation of startup and operation using reliable equipment is possible.
- High Reliability: The absence of moving parts in the combustion zone results in a high degree of reliability and low maintenance costs.
- Reduced Maintenance: Routine overhauls are infrequent and high efficiency is maintained for long periods.
- Quick Responses to Changing Demand: FBC can respond to changing heat demands. This makes it very suitable for applications such as thermal fluid heaters, which require rapid responses.

2.2.7 Disadvantages of CFB

A potential disadvantage of fluidised bed FBC combustion or gasification is that, due to the lower temperature in the FBC bed, combuster/gasifier, the carbon conversion is lower than in PC boilers for combustion, and entrained flow gasifiers for gasification, both of which operate at a higher temperature. A further point of concern is the formation of N_2O in the lower temperatures operating in FBCs, although the production of NO/NO_2 is lower than PC boiler at these temperatures [39].

NOx emissions may exceed current stringent standards in some areas when the boilers are operated at less than full load. Further to this, the nature and impacts of CFB residues (primarily ash) are not fully understood, and therefore, their disposal requires careful consideration [18].

2.2.8 Barriers to wider adoption of CFB technology

The Energy International Agency IEA[3] compiled a report on energy outlook, and made the following concluding remarks about CFB technology: "with around 20-23 GW operating worldwide, CFBC units can demonstrate significant operating experience". They have the ability to accept a variety of fuels, including a range of coals from lignite to anthracite, waste coal and biomass. They exhibit low emissions of conventional pollutants and show the potential to be designed for oxy-firing. Though there is a need for research, development and demonstration (RD&D) to progress to higher steam conditions over time, there are no obvious barriers to CFBC other than the size of the market[40]. However the report compiled by IEA in 2013 [18] concluded that the poorer economy of scale and lower efficiency of the CFBC plants in subcritical boilers result in higher plant costs, and thereby the assumption at that time was made that CFBC has limited deployment [18].

2.3 Comparison between Bubbling Fluidised Bed and Circulating Fluidised Bed

The main objective of fluidised bed technology was burning solid waste, where small units were installed as incinerators, since the technology had a major development in many industrial applications, which made the technology to be known for accepting different types of fuels with low calorific value and high ash content, other advantage emission control and high combustion efficiency. These attributes go for both bubbling fluidised bed (BFB) and circulating fluidised bed (CFB), the first one was the first version, which comes under severe competition from CFB. This section summarises the major differences (advantages, disadvantages, and operating concepts) between the technologies using literature where each technology has been going through major research and development, especially in the last three decades.

A summary is provided in Table 2.1 below:

Table 2.1: Comparison between CFB and BFB up to year 2007 [34, 41].

Parameter	BFB	CFB
Fluidisation velocity (m/s)	1-3	3-10
Combustion temperature °C	760-870	800-900
Combustion efficiency %	Low: 85 High: 98.5	Low: 90 High: 99
Ratio of unburnt carbon in bottom ash (%)	≤ 3	0.2- 4
Ratio of unburnt carbon in fly ash (%)	High	4-9
Particles concentration	High in bottom, low in freeboard	Gradually decreasing along furnace height
Solid circulation	minimal	Yes
Fuel flexibility	Yes	Yes
Emission control	Yes (lime stone addition)	Yes (lime stone addition)
Lime stone demand	High	Low, higher if its low reactive
SO_2 capture efficiency (%) @ 6 % O_2 dry; Ca/S=2; high reactive limestone	90	70
Emission of NOx @ 6% O_2 (mg/m^3 n dry)	100-160 Increases if the temperature is increased to 900 °C	250-320
Emission of N_2O (mg/m^3n) @ 6% O_2 (mg/m^3 n dry)	75-250 Decreases if the temperature is increased to 900 °C	50-200
Cost	Not available for larger plant	Competitive with PC
Scaling-up factor	0.62	0.81
Steam flow (kg/s) (range)	36 (13-139)	60 (12-360)

Steam temperature (°C) (range)	466 (150-543)	506 (180-580)
Steam pressure (bar) (range)	72 (10-160)	103 (10-275)
Maximum power output (MW)	≤ 150	≤ 550 850 in the near future
Number of installed unit worldwide	Over 2000	Below 1500 About to change in the near future
Installed unit in Africa (South Africa)	Yes (limited)	No

As can be seen from Table 2.1 above, CFB boilers outperform BFB boilers in many parameters, both operational and output-related. The following figures represent the maximum output of both technologies and major development for periods of 30 and 40 years for CFB and BFB, respectively. The data in Figure 2.5 (up to 2007) is for bubbling bed technology, whilst Figure 2.6 and 2.7 include major development in the fluidised bed technology on the CFB especially where supercritical boilers came on line in Poland (Lagsiza), Korea (Samcheok), and China (Baima), with boilers capacity of 460 MW (2009), 550 MW (2015), and 600 MW (2013), respectively.

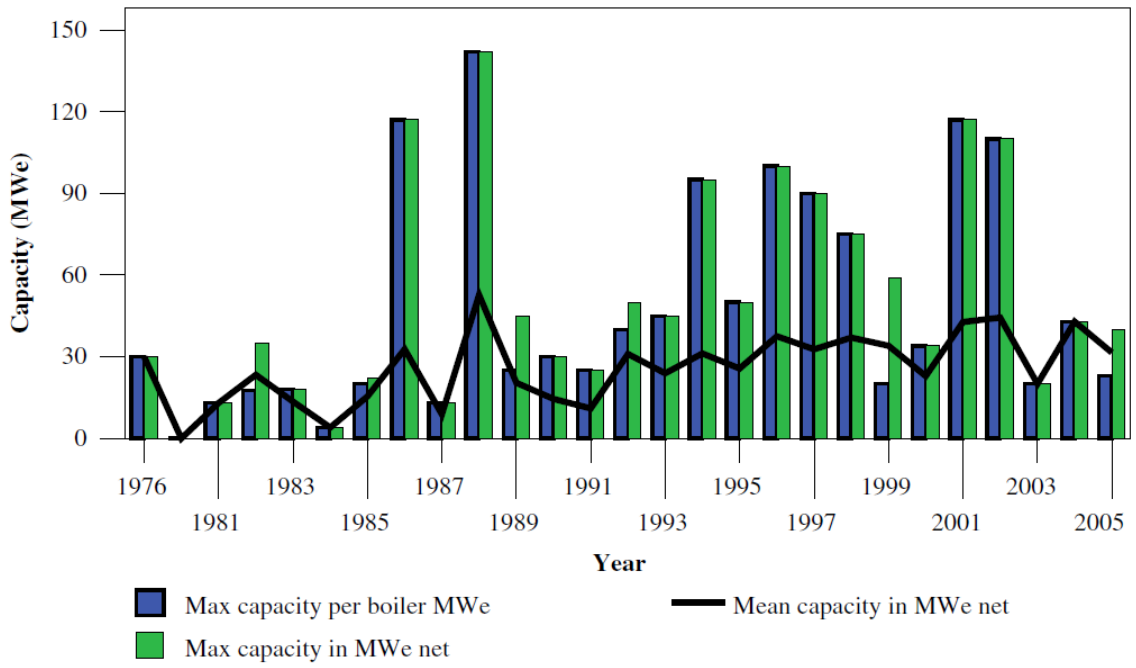

Figure 2. 5 Maximum designed capacity of bubbling fluidised bed boilers up to 2007 [41].

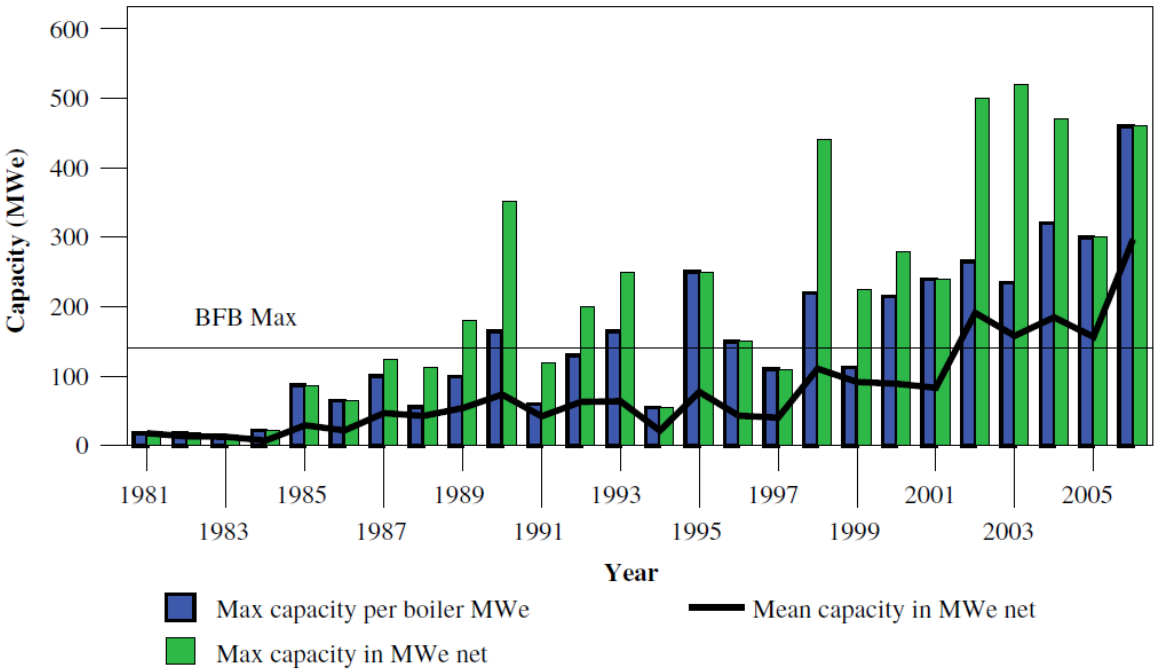

Figure 2. 6 Maximum designed capacity of CFB boilers over time [41].

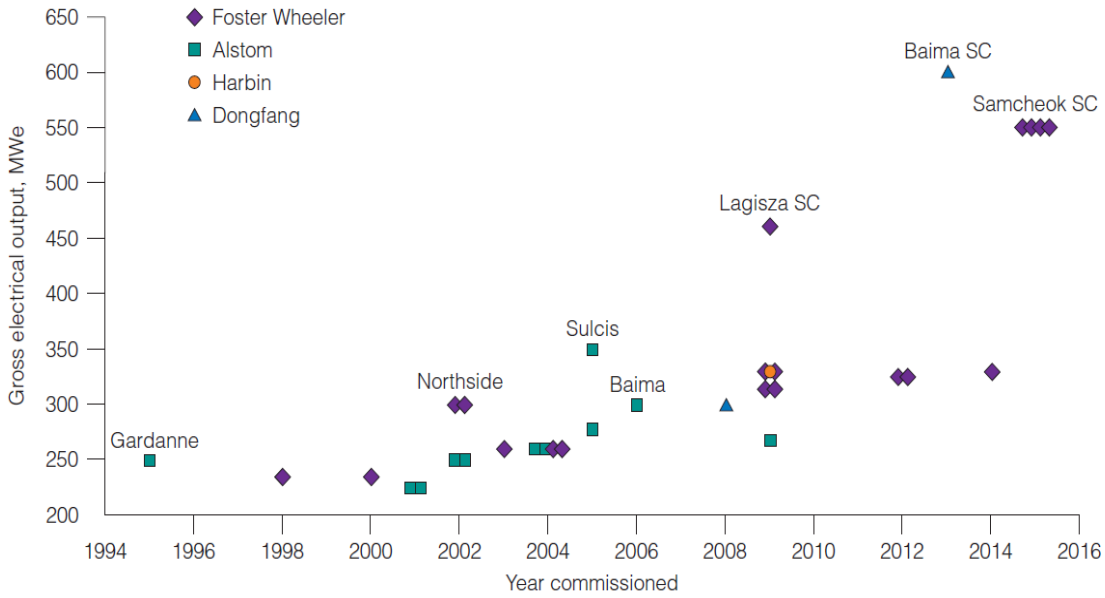

Figure 2. 7 Scale up of CFB boiler capacity in the last two decades installed and design capacities by major fluidised bed companies [42].

Figures 2.5, 2.6 and 2.7 Shows the major differences in installation and design capacity in recent times between the two technologies, this being due primarily to the overriding benefits that CFBC has over BFBC as shown in Table 2.1. Both BFB and CFB technologies have advantages and disadvantages, some of which are common, and some of which distinguish CFB over BFB. In the current study, the focus is on CFB versus PC in the context of a South African power utility. Sections 2.4 presents a detailed comparison between CFB and PC in addition to sections 2.2.6 and 2.2.7 above, highlighting the major merits and limitation of CFB [34, 41, 43].

2.4 Comparison between pulverised coal (PC) and circulating fluidised bed (CFB)

2.4.1 Background

Various firing methods for the burning of coal are used: cyclone furnaces, stokers, pulverised coal, and fluidised bed. Of these applications, pulverised-coal firing is the dominant method in use today in terms of the quantity of coal burned. Pulverised-coal (PC) firing is predominant on the large, highly efficient utility boilers that are used to provide the base-loaded electric capacity in utilities throughout the world.

Circulating fluidised bed technology has been overtaking other combustion technologies in some parts of the word with the same fuels, where it is particularly effective when burning reactive fuels with low heating values, as well as high moisture and ash contents. The development of the fluidised bed technology has allowed for the achievement of higher efficiency levels, while reducing emissions and increasing fuel flexibility, which are key under current global market and environmental conditions. Technology employed for the utilisation of coal in South Africa consists mainly of Pulverised coal combustion (Eskom and Sasol), fixed-bed coal gasification (Sasol) and grate-fired boilers (industry)[15, 40, 44]. South Africa has abundant resources of high-ash and other low-quality coals.

The comparison between PC technology and fluidised bed technologies, with a focus on CFB, rather than all other fluidised bed technologies.

Circulating fluidised bed technology has gradually succeeded in bubbling fluidised bed, therefore it is gaining some momentum for boiler design and installations for power plants. This section looks at the technology of circulating fluidised bed versus pulverised coal.

A detailed comparison between the two technologies, PC and CFBC in particular, now follows. Factors including operating concepts, capacity/output, coal combustion kinetics, efficiency, environmental impact, costs, as well as the advantages and disadvantages of each technology will be considered.

An initial brief comparison between the two technologies as presented in Table 2.2 below.

The results displayed vis-à-vis in the table below are general for the two technologies, and not necessary achieved at all times for all boilers using the two technologies. For example, in the case of the PC boilers in South Africa, neither the boiler efficiency nor the combustion efficiency reach the data as prescribed for the technology in Table 2.2 below.

Table 2.2: Physical features of CFB and PC boilers [34]

	CFB	**PC**
Bed height (m)	10 to 30	Variable, up to 100m
Fuel burning zone (m)	10 to 30	27-45
Coal size (mm)	6-0	<0.1
Combustion efficiency %	95-99	99-99.5
Boiler thermal efficiency (%)	Subcritical 25-35 Super critical 35-39 Ultra-supercritical 39-44	Subcritical 25-37 Super critical 37-41 Ultra-supercritical 41-44
NO^*_x (ppm)	50-200	400-600
SO_2 capture in furnace %	80-90	None Requires FGD in post combustion

**the data do not include N2O, which is higher in the CFBC than in PC technology due to the low temperature*

From the table above it can be noted that a CFB unit would be smaller in size, can accept larger particle sizes (thereby eliminating pulverising milling), produces lower NOx, and can reduce SOx to a significant degree in-bed rather than require an expensive FGD unit at the back end

of a PC boiler. Both technologies have same range of combustion efficiency and both technologies can achieve 37 to 43% boiler thermal efficiency in sub-critical and ultra-critical boiler, respectively [42].

2.4.2 Operating concepts of CFB and pulverised coal technologies

2.4.2.1 Pulverised coal technology

Pulverised coal remains a relatively simple technology, converting a little more than one-third of the fuel's energy potential into useful electricity [45]. With the unit system of pulverisation, each boiler is equipped with one or more pulverising mills through which the coal passes on its way to the burners. The coal is fed to these pulverising mills by automatic control to meet the steam demand. No separate drying is necessary, because heated air from an air preheater is supplied to the pulveriser mill, where drying takes place. This stream of primary air carries the fine coal from the pulveriser mill through the burners and into the furnace. Combustion starts as the fuel and primary air leave the burner tip. The secondary air is introduced around the burner, where it mixes with the coal and primary air. The velocity of the primary and secondary air creates the necessary turbulence, and combustion takes place with the fuel in suspension. Modern pulveriser systems for boilers are direct-fired systems, and consist of the following major features [5]:

- A raw coal feeder that regulates the coal flow from the coal bunker to the pulveriser;
- A heat source that preheats the primary air for coal drying, either the boiler air heater or a steam-coil air heater;
- A primary air fan that typically is located ahead of the pulveriser (pressurised mill) or after the pulveriser (suction mill);
- A pulveriser;
- Piping that directs the coal and primary air from the pulveriser to the burners;
- Burners that mix the coal and combustion air, both primary and secondary; and
- Controls.

Figure 2.8 below illustrates the operation and different stages of a PC boiler

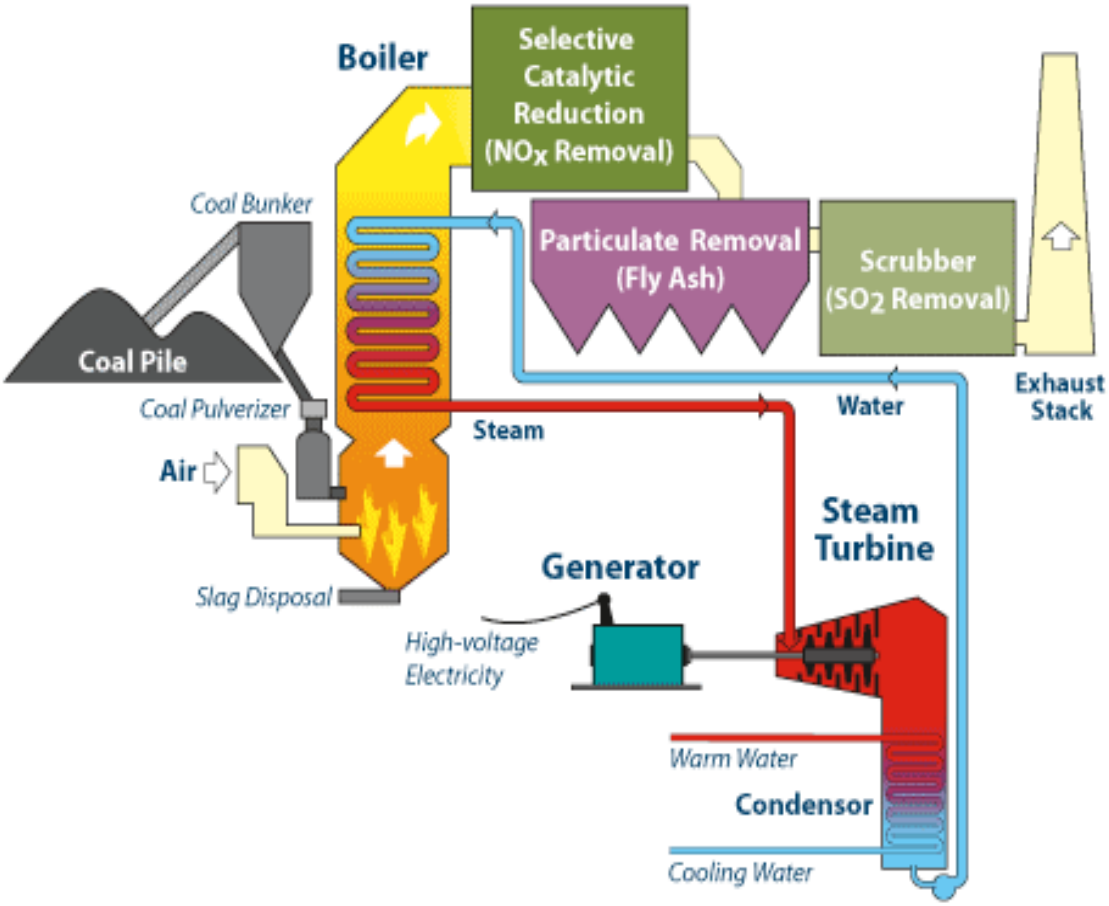

Figure 2.8 Operation stages of PC boilers [46].

As described by Basu [34], the coal is ground (pulverised) to a fine powder, the technology uses much smaller particle sizes, which allows high combustion rates, and, therefore, it is significantly different from the other coal combustion technologies. The total particle surface area controls the combustion rate of coal. Less than 2% is +300 µm and 70-75% is below 75 µm, for a bituminous coal. The pulverised coal is blown with part of the combustion air into the boiler plant through a series of burner nozzles. Secondary and tertiary air may also be added. Combustion takes place at temperatures between 1300-1700°C, depending largely on coal type and rank. Steam is generated, driving a steam generator and turbine. By pulverising coal, the coal can be burned completely in 1 or 2 seconds, thus particle residence time in the boiler is typically 2-5 seconds. Particles must be small enough for complete burnout to have taken place during this time, as is the case with burning oil and natural gas [47]. When coal particles enter the furnace their surface temperature increases. This is due to heat transfer from the furnace gases and other burning particles. As the coal particles' temperature increases, the contained moisture is vaporised, and the volatile matter in it is released. This volatile matter ignites and

burns almost immediately, and this further raises the temperature of the particle, which now consists primarily of carbon and mineral matter (ash). The particle is then consumed at high temperature, leaving the ash and a small amount of unburned carbon.

In the combustion of pulverised coal, the following are said to be important influences on the process [48].

- *Volatile matter*: This is critical for maintaining flame stability and accelerating the particle burnout. Coals with low volatile matter, such as anthracite and low-volatile bituminous, are difficult to ignite, and require specially designed combustion systems.
- *Coal particles*: The rate of combustion of the coal particle depends on its size and its porosity.
- *Moisture content*: Moisture content in the coal influences combustion behaviour. Pulverised-coal-fired systems convey all the moisture to the burners, unless preheating is used in the fuel-preparation (pulverisation) phase. The moisture, if present in significant quantities, presents a challenge to coal ignition because the water in the coal must be vaporised, as the volatile matter in the coal particles is burned. It is because of this problem that coal drying is done in the pulverisation process with the use of preheated air. Not all the moisture in the coal is eliminated, however.
- *Mineral matter (ash)*: The mineral matter or resulting ash in the coal is inert, and dilutes the heating value. Consequently, with coals of higher ash content, more fuel is required to meet the heat input required in the furnace for a particular steam capacity. The ash absorbs heat and interferes with the heat transfer to the coal particles, thus deterring the combustion process with high-ash coals. The type of ash varies in coal, and this reflects the tendency for slagging, which must be accounted for in the boiler design [49].
- *Organic matter in coal (resulting in forms of char)*: Coal contains organic matter in the form of fragments (macerals) derived from matter accumulating in the original peat swamp, which has decomposed and passed through a series of chemical and physical changes over time, and in response to additional factors such as temperature and pressure. The latter process results in increasing rank or

maturity of coal, and is seen as the reduction of volatile matter in some reactive organic components in coal (vitrinite and liptinite macerals). Relatively inert organic matter also accumulates in coal (inertinite macerals), which have low volatile contents, higher density than the reactive organic components, are general associated with high mineral/ash contents, and are difficult to ignite and burnout. The type of organic matter varies significantly in coal, and this determines the nature of the flame, the speed of ignition of each particle, and the length of time it takes to burn out [50].

The PC technology is well developed, and there are thousands of units around the world, accounting for well over 90% of coal-fired capacity. However, PC technology can only use a limited variety of coals, and it is not always appropriate to use for those coals with high ash content, unless the boiler is specifically designed for that quality of coal. In terms of SOx and NOx emissions, PC boilers require a Flue Gas Desulphurisation unit for the reduction of Sulphur Dioxide, and an ammonia-based selective catalytic process for NOx capture and reduction. Also, around 15% of coarse ash collects at the bottom of the furnace, and the balance (80 to 95% of the ash in the form of fly ash) is captured in electrostatic precipitators or bag filters at the backend of the boilers.

CO_2 can be captured from the off-gas duct and from the plume of pulverised coal plants and then sequestered in geological formations, but this process is relatively expensive, especially for retrofit applications [51].

There is considerable variation in the pulverised-coal fineness requirement. Coals with low-volatile content must be pulverised to a higher degree of fineness than those with higher-volatile content. For normal conditions, bituminous coal will burn satisfactorily when 70 percent will pass through a 200-mesh sieve. In order to minimise unburned carbon loss, which is contributed to by coarse particles, the amount passing through a 200-mesh sieve is often increased to 80 percent. It is a waste of energy to pulverise coal finer than required to obtain satisfactory combustion [49].

2.4.2.2 Circulating fluidised bed technology

Circulating fluidised bed (CFB) combustion is currently under intense scrutiny, in view of its potential as an economic and environmentally acceptable technology for burning low-

grade coals. As in all FBC technologies, CFBC combustion occurs when coal and a sorbent, such as limestone, are suspended through the action of primary combustion air distributed upwards from below the combustor floor. Fluidisation on its own offers the advantage of good heat transfer and good fluid flow. CFB has considerable advantages over PC technology; it is best for firing multi-fuels with high moisture content, and significantly higher efficiency up to 95%[34, 49]. Coal with ash contents up to 70% can be utilised [52].

Figure 2.9 below illustrates the operation and stages of electricity generation using a CFB boiler.

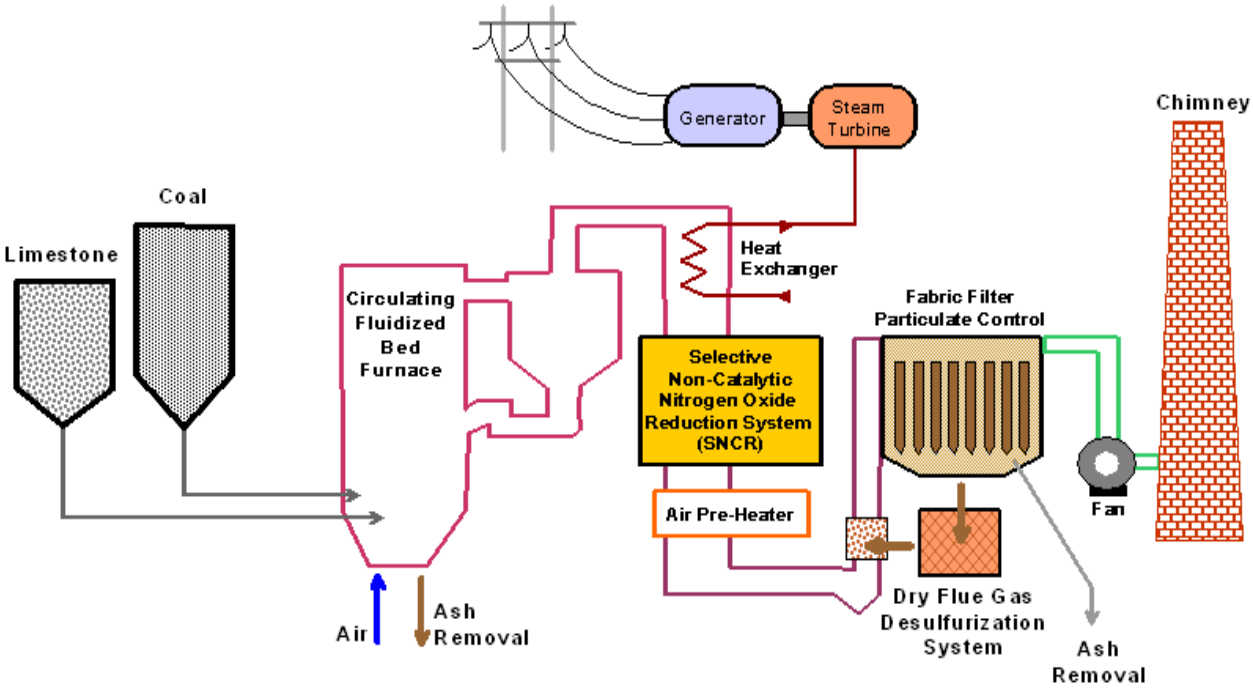

Figure 2. 9 Operation stages of CFB boilers [46].

The operation setup of CFB as shown in Figure 2.9, include fuel and limestone/dolomite feeders. The boiler contains the following: a riser, cyclones, air inlet (combustion/fluidisation). There is also provision for ash removal in the form of a fabric filer, and particulate control and additional FGD at the back-end of the process, if required. The combustion temperature of a FBC boiler (800°C - 900°C) is significantly lower than a PC-fired boiler (1300°C - 1700°C), which results in lower NO_X (NO and NO_2) formation. CFBC also has the ability to capture sulphur dioxide (SO_2) with limestone injection into

the furnace. The calcium in the sorbent/limestone combines with SO_2 gas to form calcium sulphite and sulphate solids, and the solids exit the combustion chamber.

Despite the typically low combustion temperature of a CFB boiler, the circulation of hot particles provide efficient heat transfer to the furnace walls and allows longer residence time for carbon combustion and limestone reaction. This results in good combustion efficiencies [51].

In order for the bed to be well fluidised, the recommended gas velocity in the CFBC bed is greater than three times the minimum fluidising velocity (U_{mf}) of the char particles [53]. CFB uses coal crushed to sizes of around 3 to 6 mm. The time, energy and facility required to crush coal is much less than that of pulverising coal [18]. FB uses higher-pressure primary air for fluidising which is 60% of the combustion air. The total air for combustion and the balanced draught system is the same in both PC and CFBC systems. In CFB boiler, limestone addition in the furnace reduces the sulphur dioxide during combustion itself. This requires only a simple limestone storage and handling unit. In CFB boilers, the collection of coarse ash at the bottom reduces by almost 50% lessening the load on the electrostatic precipitators [46].

2.4.3 Fuel flexibility

When selecting a combustion technology, fuel flexibility is one of the major points to be considered. Higher fuel flexibility will allow advantage to be taken of many low-cost, opportunity fuels that other technologies cannot easily accommodate.

Figure 2.10 below provides information on the fuel range versus the burning difficulty for both CFB and PC.

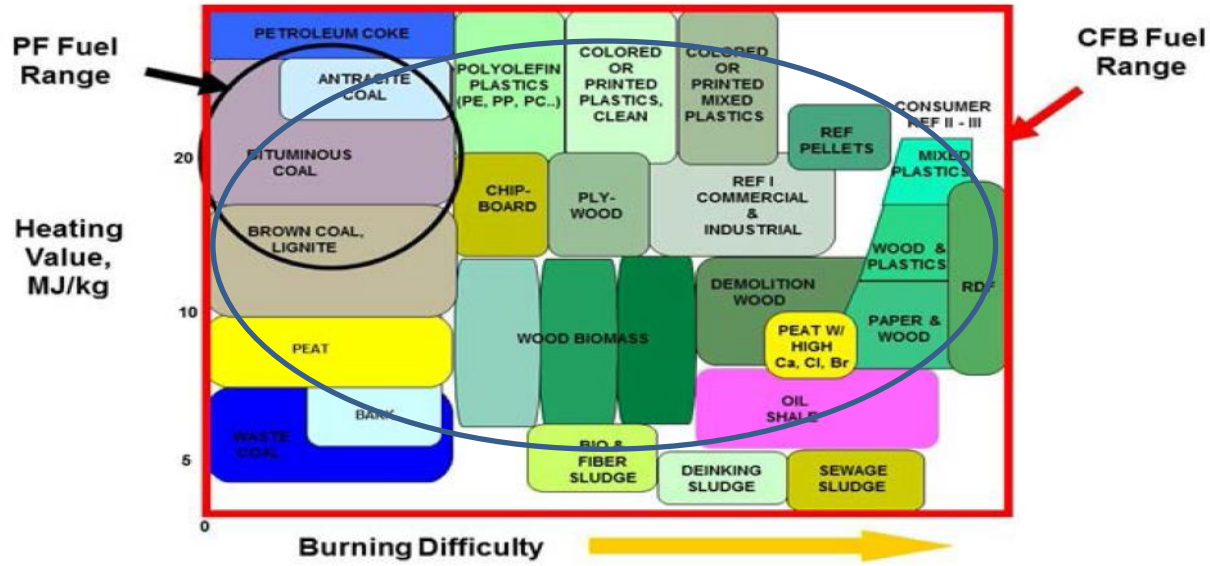

Figure 2.10 Fuel range comparison [54].

2.4.3.1 Circulating Fluidised Bed feedstocks

As shown in Figure 2.10 above, fluidised bed technology has the capacity to tolerate considerable flexibility with regard to feedstocks. This technology can burn any rank, grade or type of coal including coal discards, and additional carbonaceous products such as coke, petroleum coke (a carbonaceous solid derived from oil refinery Coker units or other cracking processes) and biomass, without significant modifications [47].

Fresh fuel and combustible matter make up less than 3% by weight of the hot solids present in the bed. This large source of thermal energy provides an extremely steady combustion environment that is relatively insensitive to variations in fuel quality. The fuel particles fed to the furnace are quickly dispersed into the large mass of bed solids, which rapidly heat the fuel particles above their ignition temperature, without any significant drop in the temperature of the bed solids. This feature makes it possible to burn almost any fuel without the use of auxiliary fuels, and it permits the combustion of several different fuels together without major changes in the hardware. One limitation, however, is that fluidised bed technology cannot burn high alkalis content materials, because of resulting bed agglomeration and corrosion issues. For these reasons, a detailed case-by-case fuel characterisation and evaluation is needed to ensure acceptable combustion performance [55].

2.4.3.2 Pulverised coal-fired boiler plant feedstocks

Pulverised coal boilers are specifically designed for a certain type and grade of fuel [56]. If the quality varies beyond a specific level, the boiler efficiency decreases. There are many factors that affect the efficiency of PC boilers from the type of coal that is fed into the boilers, to the operating conditions used to combust the coal. Plant design factors also come into play in order to achieve maximum efficiency, in addition to the feeding patterns and ratios of coal injected into the furnace. The fuel ratio of coal refers to the weight ratio of fixed carbon to volatile matter in a raw coal [49].

2.4.4 Kinetics

The kinetic study of combustion for both CFB and PC is a complex parameter due to a multitude of factors, including the number of reactions taking place in conjunction with the changing conditions in the different sections of both the fluidised bed and pulverised coal. Often, kinetic studies are done using modelling tools such as computational fluid dynamic (CFD) and ASPEN.

The combustion of coal in both CFB and PC is characterised by various stages, i.e. de-volatilisation, followed by volatile ignition and combustion; char formation and char combustion, to total consumption during combustion, to final burnout. The production of NOx, SOx and greenhouse gases (CO and CO_2) takes place in the hot combustion zone in PC combustion. In CFB combustion, the presence of limestone or dolomite in the bed leads to the absorption of sulphur (SO_2) and the production of $CaSO_4$, a solid ash product, which can be removed from the bed. Lower NOx is formed at the low temperatures in the CFBC bed although another form of N gas does arise as N_2O. These reaction steps occur in the different regions of the riser, which can be divided into a number of individual reactors [57].

The reactivity of coal in the furnace, including the combustion efficiency and the mechanism of formation of NOx and SOx, depends on various parameters (coal properties, combustion temperature, particles residence time and so on). The kinetic studies for both technologies are of great interest to design engineers as it provides a guide with regard to the operation perspectives. There are numerous studies in literature on the kinetic aspects focusing on NOx,

and SOx formation, but very few on the comprehensive kinetics on the full range of processes in both combustion and gasification technology (not the subject of this study). Various researchers have developed models using two approaches, either a generic kinetic model for the whole process taking place in either technology (combustion or gasification), or using a model for each of the reaction taking places in the various stages of the process. Examples of these studies are the collections of the kinetic studies in CFB and PC respectively models established by Sotudeh [57], Dieter [58] and other researchers . Kinetics and modelling are not discussed further in the body of this thesis as this lies beyond the scope of the current study.

2.4.5 Technologies output

Original Engineering Manufacturers (OEMs), such as Babcock Engineering and Scientific Design, have installed a number of BFBC plants for industrial users, including the pulp and paper industry. It was realised during the development and operation of BFBC technology that, due to the low lateral dispersion coefficient of coal, the maximum bed area of these plants is about 60 m^2, which limits the thermal output to less than 100 MW [41]. For large PC power stations such as those operated by Eskom, unit capacities of 600 MW(e) are required to achive econmy of scale . Internationally, this limitation of the BFBC resulted in the development of circulating fluidised bed (CFB) technology. Higher thermal outputs are possible with CFB boilers since they operate at a higher fluidising velocity, which improves coal dispersion and mixing [34]. Currently, the capacity of CFB subcritical boilers ranges from 25 to 350 MWe. The largest atmospheric CFB boiler in operation to date includes a 460 MWe unit at a power plant owned by the Polish utility company Południowy Koncern Energetyczny in Lagisza, Poland (Foster Wheeler North America Corp, 2009)[24], and a 4X550 MW units in South Korea [4, 18]. These new larger CFBC plant are super critical boilers with higher efficiency than subcritical ones. By way of comparison, the satisfactory performance of the pulverised-coal system depends to a large extent on mill operation and reliability. The pulveriser mill should deliver the rated tonnage of coal, have a nominal rate of power consumption, produce a pulverised coal of satisfactory fineness over a wide range of capacities, give dependable service with a minimum of outage time, and operate with low maintenance cost [46].

Msibi [59], from The South African Department of Minerals and Energy compiled a report that concluded that PC boilers in South Africa have been built to match steam turbines, which have

outputs of between 50 and $^{+}$650 MWe. In order to take advantage of economies of scale, newest PC boiler units have therefore been rated at over 300 MWe, but there are relatively particularly large ones three (Majuba), Six (Medupi) and three more (Kusile) in completion phase with outputs from a single boiler/turbine combination of over 700 MWe . This limitation is due to the substantial effects such units would have on the distribution system if they unexpectedly shut down [59, 60].

2.4.6 Boiler and Combustion Efficiency

There is a clear distinction between boiler efficiency and combustion efficiency, where the first is referred to as thermal efficiency which represents the difference between energy input and energy output; and the second is an indication of the burner's ability to burn fuel and the ability of the boiler to absorb the heat generated. The amount of unburned fuel and excess air in the exhaust are used to assess a burner's combustion efficiency.

Combustion efficiency basically refers to the ability of a combustor to burn carbon as close to completely as possible [61]. Estimation of combustor efficiency involves the heat losses owing to incomplete combustion and the quantity of unburnt carbon contained in fine ash particulate matter emitted at the back end of a boiler, a value that can be chemically determined. Losses due to (i) flue gases to ambient; and (ii) the bed to wall heat transfer, are taken into account for the estimation of combustor efficiency. Studies have shown that efficiency of coal combustion depends on design variables such as bed height, bed diameter as well as operating conditions such as combustor load, temperature in the bed, residence time of coal particles, excess air values, combustible gases, and the quality of fluidisation. Additional factors include the quality of the coal, which needs to match the design and operating conditions in a combustor. Efficiency decreases as the combustion losses increase with increasing excess air values. In coal-fired power generation, efficiency is an important performance parameter. Raising efficiency offers benefits such as:[54].

- Reduction of carbon dioxide (CO_2) emissions;
- Reduced emissions of conventional pollutants; and
- Resource preservation through reduction in consumption of coal [54].

PC efficiency plays an important role in the future production of electricity from coal. This is specifically the case with the potential for high efficiency power generation to reduce CO_2 emissions. Improving efficiency levels increases the amount of energy that can be extracted from a single unit of coal. Increases in the efficiency of electricity generation are essential in tackling climate change. Zhai and Rubin [62] reported on the work done by IEA research has shown that single percentage point improvement in the efficiency of a conventional pulverised coal combustion plant results in a 2-3% reduction in CO_2 emissions [62]. The overall thermal efficiency of some older, smaller units burning, possibly, poor quality coals can be as low as 25 percent. A commonly used assumption for the average efficiency of larger existing plants with subcritical steam burning somewhat higher quality coals is in the region of 35-36 percent. New plants, however, with supercritical steam can now achieve overall thermal efficiencies in the 43-45% range [63]. Elliott and Von Fredersdorff [64] published findings stating that efficiencies for PC plants is usually around 37 percent. Supercritical plants use higher pressure and temperatures to boost efficiency to 40% or more. Ultra-supercritical (USC), using still higher pressures, achieves 42-45% efficiency [54].

Efforts to develop advanced USC technology, which claims to lower emissions to 670g CO_2/kWh (a 30% improvement), is underway. Such deployment of advanced USC is expected to begin within the next 10 to 15 years [65]. Highly efficient modern supercritical and ultra-supercritical coal plants emit almost 40% less CO_2 than subcritical plants [66].

An additional advantage that CFB has over the PC technology is high efficiency for combustion, due to the ability to utilise a variety of solid fuels and fuel mixtures [67, 68].

According to a report by the Energy International Agency, the thermal efficiency of CFBC units is similar to that of PC units [4]. However, the real potential in steam generation using PC lies with super critical and ultra-super critical boilers that achieve around 45% efficiency.

Kavalov [68], mentioned in his report for JRC Institute for Energy that power generation efficiency for CFB is in the same range as that of PC, which is normally between 38-40 percent. Franco [1] reported that currently available efficiency for CFB is lower than 40% subcritical and higher than 40 % supercritical (Lagisza) , and that many problems during operation have been evidenced in the various experimental facilities [1].

A summary on both boiler efficiency and net plant efficiency for CFB and PC technologies for some of the commissioned plants worldwide is shown in Table 2.3 below.

Table 2. 3: Comparison of PC and CFB technology efficiency[42].

	Country	**Power output per single unit , MW**	**Start-up**	**Manufacturer**	**Fuel**	**Boiler efficiency, %**	**Thermal efficiency**
CFB Technology							
Gardanne	France	250	1995	Alstom	Bituminous	91.6 (LHV)	37.5 (HHV)
Turow 1-3	Poland	235	1998-2000	Foster Wheeler	Lignite	91.2 (LHV)	40.8 (LHV) 37 (HHV)
Turow 4	Poland	261	2003	Foster Wheeler	Lignite	93.19 (LHV)	41.9 (LHV) 39 (HHV)
Lagisza SC	Poland	460	2009	Foster Wheeler	Bituminous	–	43.3 (LHV)
Baima SC	China	600	2013	Dongfang	Bituminous	>91 (LHV)	43 (LHV)
Samcheok SC	South Korea	550	2015	Foster Wheeler	Bituminous	–	42.4 (LHV)
PC Technology							
Esbjerg SC	Denmark	415	1992	Stein	Bituminous	95 (LHV)	45.5 (LHV)
Staudinger 5 SC	Germany	510	1992	Borsig	Bituminous	–	43 (LHV)
Majuba 1	South Africa	657	1997	Steinmuller	Bituminous	90.26 (LHV)	35 (LHV)
Genesee 3 SC	Canada	495	1998	Hitachi	Subbituminous	87.5 (HHV)	41 (LHV) 40 (HHV)
Suratgarh	India	250	1998	BHEL	Blend	87.78 (HHV	37.1 (LHV) 35.1 (HHV)
Wangqu 1	China	600	2006	Hitachi	Anthracite	93.72 (LHV)	41 (LHV) 40 (HHV)

The table agrees with most of the findings in the literature that efficiency for CFB and PC are close to 1 % in advantage to PC boilers , regardless of the latter being sub-critical or supercritical. Other parameters would then need to be considered, and be the determining factors in choosing technology.

The electrical output versus the energy input and taking in consideration of all losses is better expressed with the use of Sankey's diagram, as shown in Figure 2.11 below.

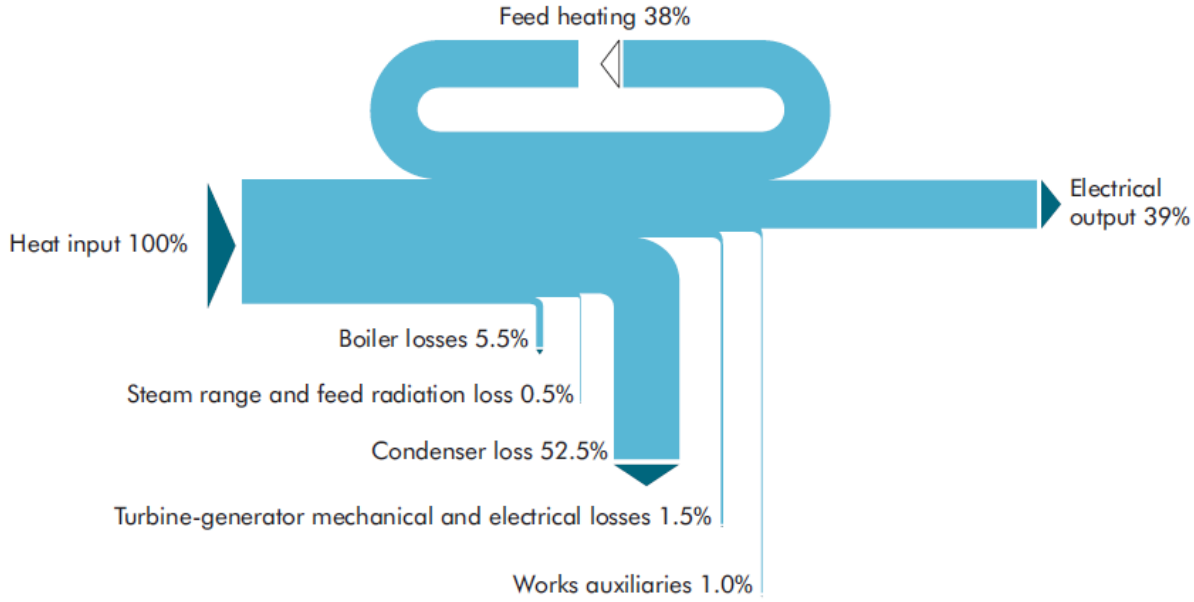

Figure 2. 11 Sankey's Diagram: Example of energy flows in PC [69].

This diagram is for a typical 500 MW subcritical PC coal boiler, and shows that the thermodynamic of the steam cycle which influences electrical output (39 %) and not the fuel combustion process. The heat losses to the cooling water is 52.5 % whilst the boiler loss is 5 percent [69].

2.4.7 Cost

Cost for plants are often difficult to establish, because they are not usually publicly available. Estimates can be made based on equipment costs provided by vendors or accessed from equipment cost databases. However, a number of power plant building project budgets were forecast using various economics aspects, including the running cost of power stations.

According to author Jim Chu Xiang from World Coal association [66], PC construction cost estimates for new coal-fired power plants are very uncertain, and have increased significantly in recent years. This would mean a cost of well over $2 billion for a new 600 MW coal plant, when financing costs are included. The costs associated with CFB and PC could be estimated using a budget drawn up by Kavidass model [38]. This author quoted that the experience in Europe and North America suggested that for a Sulphur fuel (> 0.5 % S) and less than 150 MW, a CFB boiler has 8-15% lower capital costs as well as 5-10% lower operating costs than a PC-fired boiler, because of the FGD system added to the PC boiler [38].

The Florida Power and Light [66] summarised the costs for clean coal technologies (USCPC, SPC, CFB, and IGCC) in the Figure 2.11 below. They used the a levelised Busbar cost analysis that was performed using several sets of data, which included economic criteria provided by FPL, fuel forecasts provided by FPL. The PC and CFB cases were run with 40-year book and 20-year tax lives. The IGCC case was run with 25-year book and 20 tax lives.

Performance was based on the annual average day conditions. The capacity factors for the PC, CFB, and IGCC units were assumed to be 92, 88, and 80 %, respectively.

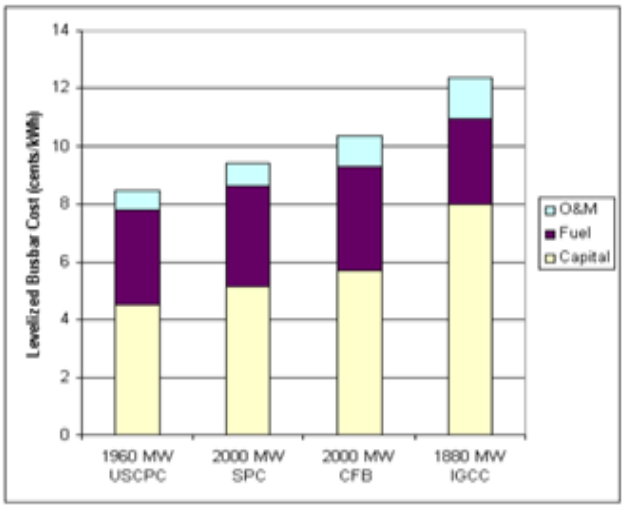

Figure 2. 12 Busbar Cost Component Analysis without Emissions [66].

The typical cost evaluations for both CFB and PC technologies as reported by Kavadiss are summarised in Table 2.4 below.

Table 2. 4: Typical economic evaluation for 125MW CFB vs. PC with FGD based power plant [38].

Description	Units	CFB-Based	PC with FGD-Based
Unit size (gross)	MW	125	125
Unit size (net)	MW	112	112
EPC price	$	120,000	134,375
Capacity factor	%	85	85
Coal heating value	kcal/ kg	5,550	5,550
Coal cost	$/MT	35	35
Limestone cost	$/MT	8	8
Ash disposal cost	$/MT	10	10
Annual O&M cost	$	3,000	3,300
% financed	%	100	100
Debt payment term	years	10	10
Description	Units	CFB-Based	PC with FGD-Based
Interest rate	%	9	9
Discount rate	%	10	10
Tariff to yield 20 years, 10% ROI	($/MWh)	39.5	41.6
Payback period, at $45/MWh	years	6.8	7.6

The results presented above indicate that CFB is able to provide low emission control costs and that the owner profit margin increases and payback period improves with 6.8 years compared to 7.6 years for PC as shown in Table 2.4 above. Costs not included in Table 2.4 are items such as land, project development, permitting, escalation, taxes and owner's costs, since these costs are common for both PC and CFB-based power plants.

2.4.8 Environmental concerns

2.4.8.1 Background

The combustion of fossil fuels in stationary and transportation systems is the main source of air pollution. Various boilers, furnaces, and engines burning fossil fuels emit gaseous pollutants, such as SOx, NOx, CO, Hg, and volatile organic compounds (VOC). Besides these, fossil fuel-fired plants also emit greenhouse gases including CO_2 and N_2O, which are perceived to add to global climate change. In an environmentally conscious society, it has become desirable, as per regulation drivers, to minimise the emission of these pollution-causing gases from fossil fuel-fired boilers, and much research is being undertaken in this regard, as concerns about climate change have heightened the need for such reduction of greenhouse gases [34].

Many countries have imposed ceilings on the emission of harmful gases and particles from pollution sources. These ceilings are in different forms. Some stipulate maximum emissions from individual units, while others put an overall ceiling across a region or an entire country. Some countries impose a tax on the amount of pollutant generated. New or larger capacity boilers may have more stringent emission standards than do smaller or older ones. Individual states or provinces may also have a ceiling lower than the national ceiling.

Emission limits for large combustion plants for most developed countries are generally as follows [70]:

- Particulates, 50 mg/m^3n;
- Sulphur dioxide, 200 mg/m^3n @ dry, 6% O_2;
- Nitric oxide, 200 mg/m^3n @ dry, 6% O_2; and
- Carbon monoxide, 40- 250 mg/m^3n dry, 6% O_2.

The specific emission limits of some countries are given in Table 2.5 for comparison. These values depend on the capacity of the plant, as well as whether it is a new or old plant. Some countries allow higher emission limits for older plants for economic reasons. The USA stipulates a cap and allows trading of emission allowances within the cap (EPA, 2005)[71]. While a significant reduction in sulphur dioxide emissions has been achieved in many industrialised countries, significant growth in industrial activities in some large countries is adding to the global sulphur dioxide emission at an increasing rate. Since gaseous pollutants

do not follow any national boundary, the rising emission in one country is a concern for all, and especially for neighbouring countries.

Table 2.5 below depicts national standards including South Africa, where a detailed focus on South Africa is discussed in Section 2.4.

Table 2.5: Emission limits for existing and new power plants in selected countries/region mg/m^3 Source [14, 70, 72, 73]

Region	SO_2 mg/m^3		NOx mg/m^3		PM mg/m^3	
	Existing	New	Existing	New	Existing	New
China	200 - 400	100	200	100	30	30
European Union	200 - 400	150 - 400	200 - 450	150 - 400	20 – 30	10 – 20
United States	160 - 640	160	117 - 640	117	23	23
India	200 - 600	100	300 - 600	100	50 – 10	30
Indonesia	750	750	850	750	150	100
Japan	-	-	123 - 513	123 - 513	30 - 100	30 - 100
Mexico	550 - 2 200	30 - 2 200	110 - 375	25 - 375	60 - 450	60 - 450
Philippines	1 000 - 1 500	200 - 700	1 000 - 1 500	500 - 1 000	150 - 200	150 - 200
South Africa*	3 500	500	1100	750	100	50
Korea	286	229	308	164	40	20-30
Thailand	700 - 1 300	180 - 360	400	200	80 - 320	80
Vietnam	1 500	500	1 000	650 - 100	400	200

* For 10% O_2 guideline; the rest of the table values are set for 6% O_2 guidelines.

The South African emission limit and compliance are detailed in Section 2.4.

Emissions emitted by CFBCs and PC boilers and the means whereby they can be reduced or eliminated have been investigate by various authors. The summary is presented in Table 2.6.

As can be seen from Table 2.6, the emission of both SOx and NOx are much higher for PC technology than for CFB technology, due to the fact that in the first, where the combustion takes place at very high temperature and there are no measures for SOx reduction. Unlike CFB technology, SOx are reduced by limestone, and the efficiency of removal depends on Ca/S ratio, in addition to the combustion at low temperature, which doesn't favours the formation of NOx, even though there is formation of N_2O at a higher rate than PC.

Table 2.6: Emissions from Typical Circulating Fluidised Bed and Pulverised Coal Fired Boilers Firing Bituminous Coal [74].

	Peak temperature (^oC)	NOx (mg/m^3)	SO_2 (mg/m^3)	Fly Ash	N_2O (mg/m^3)
Circulating fluidised bed	862	133	397 at Ca/S 2.5	4-65 opacity	74
	901	197	366 at Ca/S 3.5		26
Pulverised coal	1600	480-950	2000-2500		<10

Further confirmation of what is reported in Table 2.6 above, Franco from University of Pisa[1] reported on tests done to monitor gas emissions from different coal technologies. The following table gives the outline of gases emitted from PF, PF with desulphurisation, CFB as well as IGCC plants. Emission levels of these technologies are given in Table 2.7 below:

Table 2.7: Emission level of NOx and SOx for various advanced coal plants[1].

	PF	PF+FGD	SCPF	CFBC	IGCC	NGCC
SOx (mg/m^3)	2250	200	150	150	25	0
NOx (mg/m^3)	650	200	150	220	45	45

From this table it will be noted that CFB proved to be second lowest gas emitter from coal combustion, as indicated above. PC technologies gave the highest emissions, which can be minimised with the use of FGD, which would incur extra costs to the plant. Existing plants in South Africa could incorporate the FGD at an additional cost, but based on the above results obtained from experimental tests; it is advisable to base new power stations on CFB, as it can easily reduce SO_2 to lower limits, while PC requires the use of FGD with new scrubbers that can remove SO_2, as per regulations.

Kavidaas [34] showed that SOx and NOx emissions obtained from CFB in comparison to the World Bank Emissions requirements. See Table 2.8.

Table 2. 8: Emissions from CFB compared to the World Bank emissions requirement[38].

Description	World Bank Emission Requirements	CFB emissions
Sulphur dioxide (SO_2) ppm	730	<200
Nitrogen oxides (NO_2) ppm	365*	<100
Particulate matter, mg/Nm^3	50+	50

*coal with 10% volatile matter, NOx is 730ppm; + less than 50 MWe, plant P.M limit is 100 mg/Nm^3

The above results further support Franco's[1] findings on CFB low emissions of polluting gases. According to the above results, CFB is capable of emitting SOx, NOx and PM below the emission requirement.

2.4.8.2 NOx Emission

NOx are major air pollutants emitted by coal-fired boilers as this family of gases is said to be stronger at influencing global warming than CO_2. Uncontrolled NOx emissions from conventional PC-fired boiler are in the range of 0.8 to 1.6 mg/MJ[75]. For these reasons in addition to health, acid rain and regional limits, strict legislation (Table 2.6) on the reduction of NOx is being considered, or has been implemented, by many countries in the Northern Hemisphere. The designer of a fluidised bed boiler or PC technology is required to ensure that the emission level is below the regulatory guidelines. If the operator uses innovations like a low NOx burner, over-fire air or re-burn, the NOx might be reduced by 20-79 percent. If ammonia is injected as in selective non-catalytic reactors (SNCR), the NOx emissions may reduce by 20-50 percent. The greatest reduction is obtained by the use of a selective catalytic reducer (SCR) downstream of the boiler, where ammonia is injected just prior to passing the flue gas over a stack of catalyst. The SCR can reduce the emission by 80 to 95%, but it is a relatively expensive retrofit and needs replacement of expensive catalysts[34].

Nitric oxide is formed through oxidation of the following:

- Atmospheric nitrogen (giving thermal NOx)
- Fuel-bound nitrogen (giving fuel NOx)
- Prompt NO formation

During combustion, the nitrogen of the combustion air is oxidised to thermal NOx, but it is significant only above 1540 ^{o}C [75]. Thus, it is a minor contributor (10%) to the NOx generated in fluidised bed boilers, where the combustion temperature rarely exceeds 900^{o}C. The char nitrogen is oxidised to NO through a series of reactions. The volatile nitrogen appears as NH_3 or HCN. Ammonia (NH_3) may decompose into NO being catalysed by CaO or char, while the HCN is primarily converted into N_2O [76]. Approximately 77% of the fuel nitrogen is oxidised to NO by the above reactions [77], and the rest appears as NH_3, which in turn is partly converted to nitrogen. A large number of complex chemical reactions are involved in the formation and destruction of nitric oxide from either char or volatiles. Some of these reactions are catalysed by calcined limestone (CaO), spent limestone (CaSO4), and char.

2.4.8.3 N_2O Emission

The formation of N_2O is more prominent in CFB boilers than PC technology due to lower furnace temperature 850-900°C. The rise of large CFB units installation calls for technology control of N_2O emission [78].

At a higher temperature, N_2O is thermally instable and it decomposes to

$$N_2O \longrightarrow N_2 + \tfrac{1}{2} O_2 \qquad (2.2)$$

It is desirable to drive the decomposition of N_2O in the CFB through different operating condition using coal properties as mentioned by Svoboda, Who attribute the formation of N_2O to the following [79]:

N_2O Formation in the CFB depends on the following:

- Coal properties coupled with char content within;
- Coal rank;
- Operating pressure;
- Operating temperature;

- Product gases H_2O, CO_2;
- Excess air;
- Lime stone ratio and increase of coal particles size increased the formation of NOx and decreased the formation of N_2O; and
- The presence of oxygen even with small amount could deteriorate the catalytic decomposition of N_2O over the circulating ash.

Circulating ashes, the circulating bed material in CFB boilers are generally of narrow size distribution, larger specific area and less carbon content than those bed materials residing in the furnace, and could be excellent catalyst to accelerate decomposition. The interaction of NH_3 could be of great importance in the usage of N_2O decomposition, which justifies its introduction through the cyclones.

The formation mechanism includes the homogenous oxidation of hydrogen cyanide, heterogeneous oxidation of fixed nitrogen in char residue and reduction of NO with char or with CO. About 10-50% of the volatile Cyan and cyanide compound of the fuel nitrogen such as HCN are oxidised homogenously to N_2O through the following simplified reaction path, as the reaction mechanism is a much more complicated one [39]:

$$HCN + O \longrightarrow NCO+H \quad (2.3)$$

$$NCO + O \longrightarrow NO + CO \quad (2.4)$$

$$NCO + NO \longrightarrow N_2O+CO \quad (2.5)$$

Nevertheless, the rate of formation of N_2O is larger than its destruction in the furnace, where the increase in the formation of N_2O increases with the increase of the furnace height.

Bernhard Bonn [80] conducted a study on a 200 MW plant using different types of boilers. He found the following:

- Conventional boiler: N_2O = "less than " 30 mg/m^3;
- Stationary fluidised bed: 33-108 mg/m^3;
- Circulating fluidised bed: up to 380 mg/m^3;
- Effect of N_2O emission: temperature, and excess air; and
- Factors with no effect: lime stone addition and the variation of primary and secondary air.

Scaling up the kinetics data obtained in the laboratory fixed bed reactor to the N_2O conversion measured in the secondary cyclone of CFBC shows that the N_2O conversion can be explained by thermal decomposition in the gas phase. In the recirculation cyclone, N_2O decomposition is enhanced by composition on solid particles [80].

The emission of N_2O is more dominant in CFB than in PC boilers, which is one of the major issues with CFB boilers. Various studies were conducted in view to minimise or decompose N_2O in CFB furnace. One of the ways studies for the minimising of N_2O emission by co-combustion of coal and biomass. They concluded that for the high nitrogen content, coal co-combustion can be adopted to decrease the emission of N_2O, due to the fact that the quick devolatilisation of wood chips and rice husks results in the formation of char with high porosity and higher reactivity compared to that of coal which encourages the decomposition of N_2O and NOx [78, 81].

2.4.8.4 SOx Emission

SO_2 emission from power plants is one of the main issues for the environmental protection. During the combustion of coal, the sulphur is oxidised to the pollutant, SO_2. Sulphur dioxide produced during combustion processes if not controlled or minimised, just like nitrogen oxides, combines with water in the atmosphere to create acid rain. Acid rain acidifies the soils and water, killing off the plants, fish, and animals that depend on them. Often PC boilers have a desulphurisation plant added as an end of pipe process to deal with sulphur capture, this comes at an additional cost. On the other hand, the advantages of the circulating fluidised bed combustion technology of coal is in-situ SO_2 capture by added sorbents, usually limestone ($CaCO_3$). The majority of the sulphur in the coal is captured by limestone that is injected into the furnace; about 90-95%[18]. Limestone ($CaCO_3$) of the bed materials is converted to CaO, which reacts with SO_2 producing $CaSO_4$. Thus, instead of leaving the combustor as a gaseous pollutant, sulphur is discharged as a solid residue. Numerous experimental and theoretical studies about the sulphur retention in CFBs are present in the literature [49]. Some models have already been proposed for predicting the sulphur retention in CFBC. Considering the natural resources, especially fossil fuels, usage of CFBs will have a crucial importance in the future. A well-designed CFB combustor can burn coal with high efficiency and within acceptable levels of gaseous emissions. In some theoretical reviews and modelling processes [82], the effects of operational parameters such as sorbent particle diameter, emission could be estimated

using a previously developed dynamic 2D model for CFBs. As a results of these reviews, the following holds:

- Air-staging strongly influences the concentration and distribution of Sulphur compounds in the combustion chamber of fluidised beds;
- Feeding limestone with high proportion of fines into the combustor causes high Sulphur retentions;
- It is observed that operational bed velocity has better effect on SO_2 emission; and
- An increase in the Ca/S ratio gives a significant increase in the Sulphur retention reached in the combustor.

2.4.8.5 CO_2 emission

Carbon dioxide (CO_2) is a greenhouse gas produced by the combustion of fossil fuels. Global warming is mainly caused by carbon dioxide emissions and is responsible for at least half of the global warming [49].

CO_2 emissions from pulverised coal-fired power plants amount to 37.5% of global CO_2 emissions or an annual figure of 2100M tpa [83]. CO_2 concentrations in power plants vary depending on the type of plant. For a gas turbine plant the CO_2 concentration amounts to about 4% and for a pulverised coal-fired plant. This concentration is roughly 14%; 10% more than the gas turbine power plant [54].

A number of solutions have been developed to tackle the problem of high levels of CO_2 emissions from pulverised coal fired plants. These include the increase of plants efficiency; this helps in decreasing the levels of CO_2 that are emitted from coal combustion. There are three procedures or steps that have been developed for the management of CO_2 from coal fired plants. Figure 2.13 below illustrates these procedures [84]:

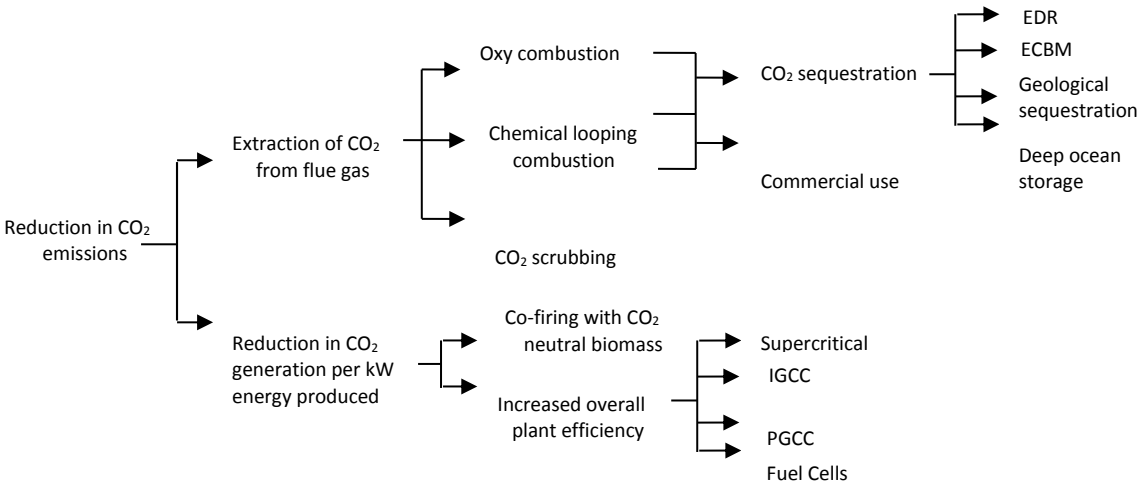

Figure 2. 13 Means for reduction of CO2 emissions from coal-fired power plants [84].

These steps or procedures are as follows:

Carbon Capture

Carbon capture involves:

- Pre-combustion, where the CO_2 is separated from the fuel before burning it; and
- Combustion, which is constituted by two main methods:
    a. Oxy-fuel combustion

This is where the nitrogen content is reduced by the addition of oxygen to the combustion air or to burn the fuel in pure oxygen [84]. This is done because oxygen in the air serves as an oxidant for combustion and as a result high levels of nitrogen make it unsuitable for CO_2 sequestration [40], and Figure 2.14 below serves as an illustration of this method.

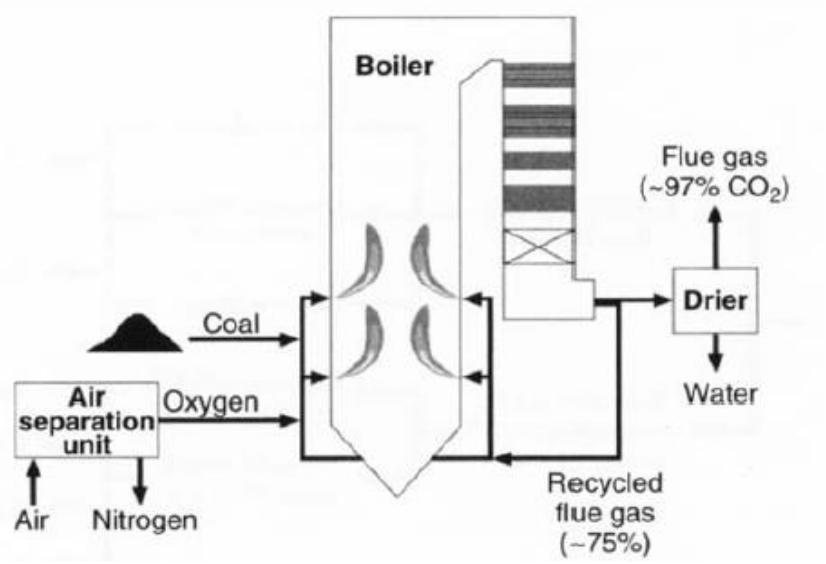

Figure 2.14 High concentration CO2 steam producing using oxygen fuel combustion [84].

b. Chemical looping combustion

This method involves the use of a metal oxide, which provides the oxygen needed for combustion. As a result of this method; pure CO_2 and nitrogen are produced and as shown by Figure 2.15 below.

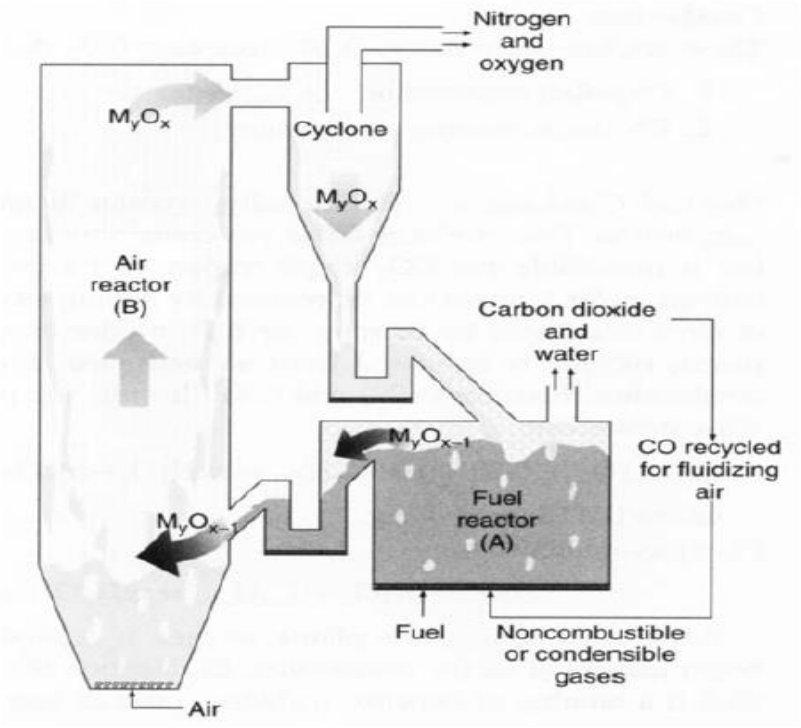

Figure 2. 15 Chemical Looping combustion [74].

- Post combustion

This step is involved with the separation of CO_2 by making use of sorbents/solvents. This is "achieved by passing the gas through a reaction chamber in contact with a liquid or solid sorbent that is capable of capturing CO_2" [84]. Membrane separation can also be used; this uses physical or chemical differences of the different substances in a gas mixture to separate CO_2. Separation by Cryogenic distillation is also another way of separating CO_2 and it works by using relative volatilities or boiling points; where CO_2 boils at -78°C at 1atm and nitrogen boiling at -196°C at 1 atm as well. Figure 2.16 below illustrates carbon capture using amine as a solvent.

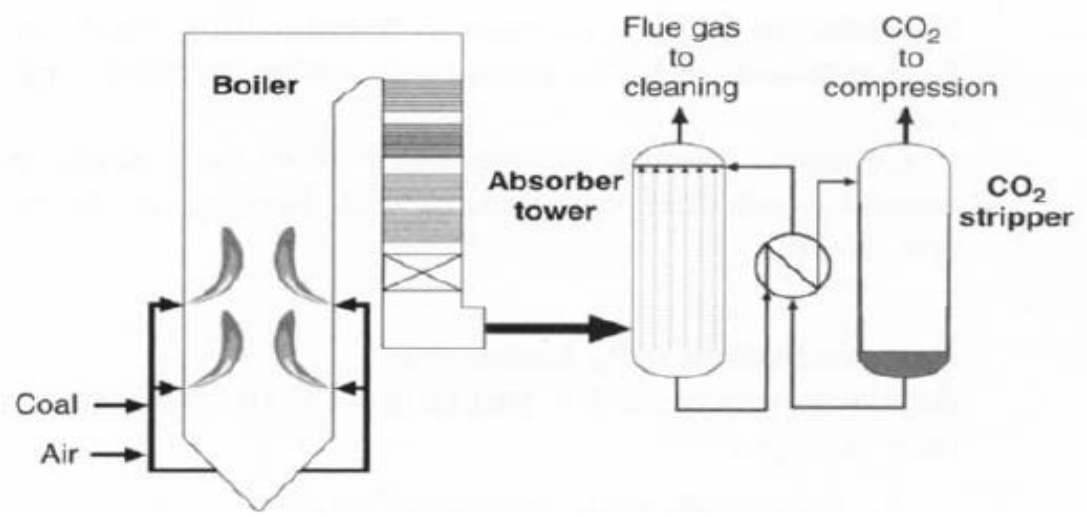

Figure 2. 16 Carbon capture using sorbent/solvent [84].

Transportation

Carbon dioxide (CO_2) can be transported using pipelines, which are used when dealing with amounts of CO_2 greater than 40 million tpa over short distances. Ships can also be used to transport captured CO_2; this usually applies for small amounts of CO_2 that need to travel long distances for instance, overseas.

Sequestration and utilisation

This step attempts to prevent CO_2 from being emitted into the atmosphere. It is achieved by storing the carbon dioxide underground and at the bottom of the ocean. To get the CO_2 to the bottom of the ocean; it is liquefied between temperature of -56.5°C and 31.1°C, by means of compression. This allows for high pressures to exist, where, as a result, the risk of CO_2 being emitted into the atmosphere is reduced. Figure 2.17 below represents the sequestration option.

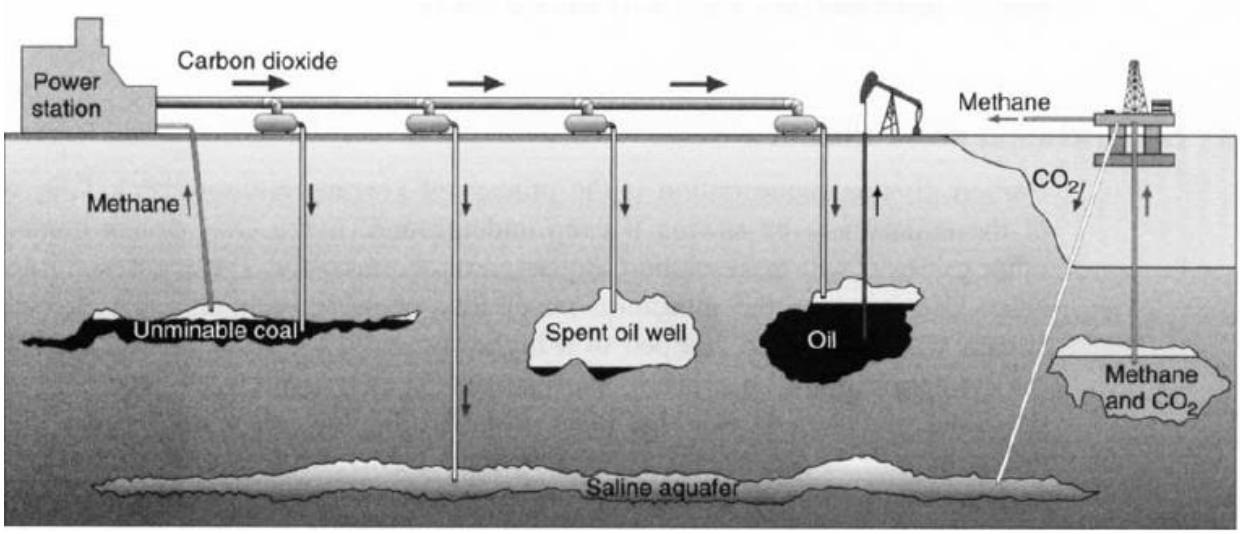

Figure 2. 17 CO2 sequestration option [84].

Circulating fluidised bed combustion technology is of the new technologies capable of reducing CO_2 emissions in the repowering of coal-fired and Greenfield power plants [85]. This is done by increasing the boiler efficiencies and by co-combusting coal with biomass. Circulating fluidised bed combustion technology is ideally suited for oxy-fuel combustion, and this is when the fuel is burnt in a mixture of pure oxygen and re-circulated flue gas, instead of air. By doing so, it allows for high concentration of CO_2 to be produced without the presence of nitrogen and due to this fact, it makes it easier to separate the CO_2. Figure 2.18 below represents an oxy-combustion power plant flow diagram.

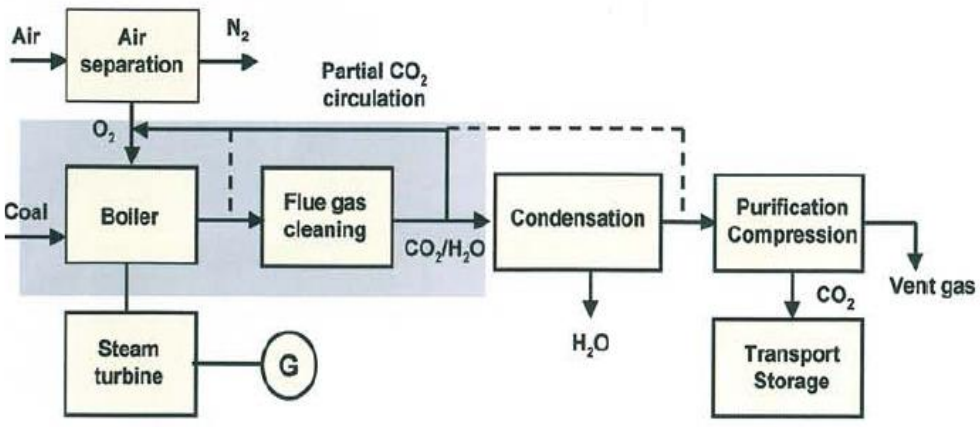

Figure 2. 18 Oxy-Combustion Power Plant [86].

Circulating fluidised bed and pulverised coal combustion have the potential to reduce CO_2 emissions with the optimisation of the plant, biomass co-firing or increasing steam temperature and pressure. However CFB has better fuel flexibility [87]. Also because of its ability to give high boiler efficiencies, CFBC technology uses this to its advantage in terms of reducing CO_2 emissions. The ability of the CFBC boiler to use co-firing of solid fossil fuels with CO_2 neutral fuels also accounts for the reductions of carbon dioxide emissions.

2.4.8.6 Mercury (Hg) and other trace elements emission

Mercury (Hg) is one of the most important environmental contaminants, which has aroused global concern due to its toxicity, long-range transport, persistence and bioaccumulation in the environment. Coal combustion is believed to be the main source of mercury emissions to the atmosphere, accounting for 60%, or even more, of the total mercury emissions [88]. Pirrone et al. [89] suggested that the change of global anthropogenic Hg emissions may range anywhere from −4% to +96% by 2050, depending on future implementation of best available technology (BAT) in coal-fired utilities and energy demand [90].

Mercury is present in coal in trace amounts (0.01– 0.5 mg/kg). At the high temperatures in combustion zone of boilers, combustion releases the Hg in coal into the exhaust gas as elemental mercury (Hg_0). This vapour may then be oxidised by HCl, $SO_,$ and fly ash in flue gas due to thermo-chemical processes [89]. Oxidised mercury (Hg^{2+}) is soluble and has a tendency to associate with the particles in flue gas to form particulate-bound mercury (Hg0). Therefore, typical air pollution control devices (APCD) may efficiently control emissions of Hg2+, such as electrostatic precipitators (ESP), fabric filter (FF), and flue gas desulphurisation (FGD) systems [91]. However, because the relative proportions of Hg^{2+}, Hg_p and Hg^0 can vary widely, the corresponding reductions in total mercury achieved by APCD vary. For example, the removal efficiency of Hg from the flue gas by a combination of cold side ESP and wet FGD range from 24 to 70% [89]. Emission speciation is an important source of uncertainty when assessing the atmospheric fate of mercury because Hg^{2+}, Hg_p and Hg^0 have very different physico-chemical characteristics, and consequently, different atmospheric lifetimes [88, 92].

Mercury control R&D includes sorbents and oxidising agents that can change gaseous mercury into solids, which can be captured. The oxidising agents work inside wet flue gas scrubbers to capture mercury in sulphate by products. Hg capture with existing controls depends on coal

and technology type, being more difficult to control Hg from low-rank coal-fired boilers. Sorbent injection is an emerging Hg control technology.

2.4.9 PC Vs CFB summary

In summary, the two technologies have been the subject of many comparisons highlighting, costs, benefits, environmental concerns, operating parameters. A typical plant ≤ 150 MW using either of the two technologies was the subject of study conducted by Kavidas [38], who summarised the main benefits of adopting CFB over PC as depicted in Table 2.9 below:

Table 2. 9 Benefits of CFB over PC in a plant (≤ 150 MW) [38].

Description	PC	CFB	Benefits of CFB
Fuel size	< 75 µm	6-12 mm	Crushing cost reduced
Fuel range (ash + moisture)	Up to 60%	Up to 75%	Accept wider range of fuel
High Sulphur fuel (1-6 %)	FGD plant required	Limestone/ dolomite injection	Less expensive SO_2 removal
Auxiliary fuel support (oil and gas)	Up to 60%	Up to 20-30%	Les oil and gas consumption
Auxiliary power consumption	lower	Fractionally higher	IF FGD used in PC, CFB power is lower
*SO_2 (ppm)	< 250 with FGD	< 200	Lower emission in the process
NO_2 (ppm)	< 100 with SCR	< 100	No SCR required
Boiler efficiency	Same range	Same range	No difference
O& M cost (85% CF)	5-10% higher	5-10% lower	Lower for less movable equipment
Capital cost	5-10% lower without FGD and SCR	5-10% higher	

	8-15 % higher with FGD and SCR	8-15 % lower	

*It could be lower than 250 ppm with FGD for the new plant.

2.5 South Africa's situation

2.5.1. Background

About 95% of the electricity produced in South Africa is generated by burning fossil fuel coal [66]. Coal in South Africa is found in coalfields lying on the periphery of the large ancient Karoo Sea in the Free State, Mpumalanga and KwaZulu-Natal provinces, and in smaller coalfields in the Limpopo Province in the Waterberg, Springbok Flats and Soutpansberg coalfields. The coal reserves are at an estimated capacity of 35 billion tons, which are considered to be enough to last until the end of the century, subject to rate of consumption and continuity of use. The latter proviso relates to the ever-increasing call to reduce fossil fuel combustion in order to reduce greenhouse gases, and thereby, their perceived impact on climate change [93]. Coal remains a major energy source due to its abundance and low cost, as compared to the alternatives which are natural gas, renewable-wind, solar energy and nuclear energy, which also contribute to the primary energy supply.

Pulverised coal combustion is the technology adopted for power generation in South Africa for many decades. The power generation is controlled by the state owned company ESKOM, the main power producer using PC boilers.

Usage of coal and liquid fuel derived from coal accounts for around 86% of the 420 million tons of carbon dioxide emissions South Africa produces annually (2011 estimate)[9], and represents around 40% of Africa's total coal derived CO_2 emissions[8]. Generally, about two-thirds of sulphur dioxide, one-third of carbon dioxide emissions and one quarter of the nitrogen oxides emissions in South Africa are produced by coal burning.

South African coal plants currently have no flue gas desulphurisation (FGD). NOx reduction equipments (low NOx burners) are fitted in all Eskom fleet at present. Therefore, these plants account for the majority of annual SO_2, and CO_2, emissions in the country.

There are other technologies available, but these have not yet been used for this purpose in South Africa, despite various attempts by several researchers and stakeholders. North [10] has given a detailed historical and current account of research undertaken by his team in CSIR and others since 1983, referring to the studies done on bubbling fluidised bed.

The combustion of coal in CFBC, a process technology that has not been recognised or explored in South Africa previously. Fluidised bed combustors (FBCs), both circulating (CFBCs) and bubbling (BFBs), have been developed as combustion technologies that are useful for widely different fuels such as coal, wastes and biomass. Nevertheless, CFB is rapidly emerging as the most suitable technology, as it offers various advantages.

Eskom's challenges of not meeting energy demand and having lower reserve margins paved the way for independent power producers (IPP) initiatives. Khanyisa and Kuysa projects are great examples in addition to diversified plan by the energy regulator NERSA, and of which the plan is to increase energy production using renewable energy and reduce the dependence on coal as a major source of energy. In addition to the initiative under the integrated resources, plan of South Africa (IRP). Related to this plan, a report was prepared by the Electric Power Research Institute (EPRI)[94] of the United States of America (USA), which provided a detailed costs, resources and technologies that can be evaluated by the department of Energy to form part of the IRP envisaged for the 2015-2030 period and beyond. Nevertheless coal reserve, discard coal stock piles and technology cost will strengthen the case of combustion technologies using both coal and coal discard for electricity production for the next 50 to 60 years [95, 96].

2.5.2 PC boilers and current challenges in South Africa

In April 2010, **Minimum Emission Standards** were published in terms of the National Environmental Management: Air Quality Act, as shown in Table 2.10 below. There are standards for an 'existing plant', which came into effect in April 2015, and more stringent 'new plant' standards which come into effect by April 2020. Existing plants are to comply with new plant standards by 2020 [72].

Table 2.10: South Africa Emission compliance targets [72].

	2015 existing plant limit (mg/Nm^3 at 10 % O_2)	2020 new plant limit (mg/Nm^3 at 10 % O_2
Particulate matter PM	100	50
Sulphur Dioxide SO_2	3500	500
Oxide of nitrogen as (NOx as NO_2)	1100	750

A postponement of the compliance time frames of not more than five years may be applied for according to the Minimum Emission Standards, and an exemption from the Standards may be applied for in terms of section 59 of the Air Quality Act [14].

There must also be compliance with National **Ambient Air Quality Standards**. PM10 is the greatest air quality problem in South Africa, but, when operating at normal emission levels, power stations make only a small contribution to total ambient levels. Power stations are the major source of SO_2 in the Mpumalanga Highveld, and a major source of NOx, although ambient levels are well below NOx limits.

Masekoameng et al. [97], have estimated mercury emissions to air from South African sources for the time period 2000-2006. By using a combination of annual information on activity in combination with South Africa, specific emission factors and UNEP-toolkit based emission factors mercury emissions to air were estimated from each activity. Overall, there was an estimated increase in total atmospheric mercury emissions from around 34 tonnes in 2000, to 50 tonnes in 2006. Coal-fired power plants were the largest contributor of mercury emissions, 38.9 tonnes, followed by cement production, with 3.9 tonnes in 2006. This emission inventory for South Africa is in close agreement with that presented in the UNEP/AMAP work for both the total emissions and almost all individual sectors considered [98].

In terms of emissions abatement control on Eskom's plants, the focus to date has been primarily on particulate control.

With the advent of the minimum emissions standards, focus is now moving toward De-SOx and De-NOx abatement. Kusile (new build) will be Eskom's first coal fired power station to

employ wet flue gas desulphurisation (FGD). Medupi (new build) will be retrofitted with a wet-FGD during the first general overhaul seven years into commissioning. Eskom also made an application for both Medupi and Kusile (new build) for postponement, in order to comply with the air quality new limits. As far for NOx limits for new plant from inception (low NOx burners plus over-fire air) are installed.

Medupi will be fully compliant with all the MES when the FGD retrofit is completed, which will be by April 2027 at the latest. Nevertheless, the Eskom's emission reduction plan for the rest of the fleet provides useful context. Eskom considers that it is not practically feasible or beneficial for South Africa (when considering the full implications of compliance) to comply fully with the MES by the 2015 and 2020 time frames stipulated. As a result, Eskom prefers to adopt a phased and prioritised approach to compliance with the MES. Highest emitting stations will be retrofitted first. Reduction of particulate matter (PM) emissions has been prioritised, as PM is considered to be the ambient pollutant of greatest concern in South Africa. In addition, Eskom proposes to reduce NOx emissions at the four highest emitting stations [99].

In addition to the compliance challenge, Eskom have to deal with the plants age where more than half the number of plant have already reached half-life or below as illustrated in Table 2.11 below.

Table 2.11: SA Power plants life and emission compliance [72].

		Current compliance with existing plant standards			Compliance with New plant standards		
Plant Name	Decommissioning Date 50 years $^{+}$ life	PM	NOx	SO_2	PM	NOx	**SO_2**
Kusile	50 +	**Y**	**Y**	**Y**	**Y**	**Y**	**Y**
Medupi	50+	**Y**	**Y**	**Y**	**Y**	**Y**	*****
Majuba	2046-2051	**Y**	**N**	**Y**	**Y**	**N**	**N**
Kendal	2048-2053	**Y**	**Y**	**Y**	**N**	**Y**	**N**
Mathimba	2047-2051	**Y**	**Y**	**Y**	**N**	**Y**	**N**
Lethabo	2045-2050	**Y**	**Y**	**Y**	**N**	**N**	**N**

Tutuka	2045-2050	**N**	**N**	**Y**	**N**	**N**	**N**
Duvha 1-3	2040-2044	**Y**	**Y**	**Y**	**Y**	**N**	**N**
Duvha 4-6	2040-2044	**Y**	**Y**	**Y**	**N**	**N**	**N**
Matla	2039-2043	**N**	**N**	**Y**	**N**	**N**	**N**
Kriel	2036-2039	**N**	**N**	**Y**	**N**	**N**	**N**
Arnot	2031-2039	**Y**	**Y**	**Y**	**Y**	**N**	**N**
Hendrina	2030-2036	**Y**	**Y**	**Y**	**Y**	**N**	**N**
Grotvlei	2021-2023	**N**	**Y**	**Y**	**N**	**N**	**N**
Camden	2025-2028	**Y**	**Y**	**Y**	**N**	**N**	**N**
Komati	2024-2028	**Y**	**N**	**Y**	**N**	**N**	**N**

*: No (not compliant), will comply in 2027, Y: yes (compliant), N: No (non-compliant)

Decommissioning date: Grey (plants passed mid-life), 2040-2044 and onwards (plant in Mid-life, new and relatively new)

Eskom's greatest challenge is replacing the power plants nearing the end of their life cycle, while in addition making provision for the electricity demand in the next two decades, and meeting the ever changing air quality control standards, bearing in mind that both current and new power plant standards are far more relaxed than the more stringent European standards.

In order to be fully compliant, Eskom will have to invest huge sum of money to install abatement retrofit techniques namely:

- Flue gas desulphurisation (FGD)
- Low NOx burners (LNB)
- Fabric filter plants

2.5.3 Current CFB initiative in South Africa

Coal quality currently being mined is reducing in quality and therefore approaching the grade found in some good quality discard. The beneficiation of coal discard would have been better option in addressing the quality challenges and reducing the mining cost.

2.5.3.1 Khanyisa project

Khanyisa project: IPP, Anglo American Witbank Emalheleni Mpumalanga region

A 450 MW plant (three modular plants at 150 MW)

The supply of energy in South Africa is characterised by a shortage of electricity and future increases in the price of the utility. These circumstances give investors good reason to build new power-generating capacity in the country. Anglo American has a competitive advantage over many other potential players in this market, with exclusive access to fuel (in the form of discard coal) at very little cost, and its operations in South African demand continuously high, stable power. KhanyiSA IPP will exploit these advantages. Its location, furthermore, can take advantage of Anglo American's Emalahleni Water Reclamation Plant for much-needed water, the tender for which went public in 2011.

Of the environmental and social impact assessments, the licensing process and the interconnection arrangement with Eskom, the first of three 150-MW CFB boilers could have been commissioned in 2015 [95].

2.5.3.2 Kuyasa project

Kuyasa Mining (Pty) Ltd. of South Africa (Kuyasa) is planning to develop a multi-phased mine-mouth coal-fired power project with a total generating capacity of 2,400 MW (gross). The first phase of this proposed project will be the development of a 600 MW (gross) power plant project, which will be constructed on a site located approximately 80 km east of Johannesburg and about 20 km southeast of Delmas. The proposed project will be fuelled by low-quality coal produced by Kuyasa's Delmas Coal Mine, and will employ commercially available fluidised-bed-boiler technology capable of burning low-quality coal or discard coal without sacrificing boiler performance. The 600 MW (gross) power plant configuration will consist of four units each capable of producing 150 MW (gross) electrical power. Each unit will consist of one circulating fluidised bed (CFB) boiler supplying steam to a 150 MW (gross) steam turbine generator. In addition, the unit will also include all associated material handling systems for coal, sorbent, and ash, as well as all other auxiliary systems [96].

2.6 Literature Review Summary

2.6.1 Coal qualities in South Africa

Coals sold for thermal and general power generation purposes are costed on the basis of heat content. For this reason, coals in in this country are categorised by Falcon [53] into five grades or SABS standards, viz. special, A, B, C and D, where each grade is characterised by calorific value, ash content and volatile content, to name few. Special (top) grade coals have a calorific value greater than 28 MJ/kg, medium grades A, B and C possess calorific values ranging from 25 to 28 MJ/kg, while Grade D has a calorific value below 25 MJ/kg.

Special Grade and Class A are almost depleted, while there is a competitive market for the other grades, with the increase demand both internally and external for export to India and China in particular, where even a low-grade coal is sought after, which leaves the local industry under severe pressure to beneficiate and use coals with Grade D specs. Similarly South Africa has a stock pile of over a billion tonnes of coal discard, where the quality and the properties are close to that of Grade D. Beneficiation of the coal discard will create an opportunity for its usage in power generation using technologies other than pulverised coal technology currently widely used in South Africa [16].

2.6.2 Case for CFB usage in South Africa

Based on the literature presented, it is apparent that no significant work has been undertaken on the effect of South African coals in CFBC, and that both energy security and emissions reduction will be major issues for the country in the near future. CFB technology is proven technology and, with its fuel flexibly, it is likely to offer an alternative to the use of beneficiated SA coal discard in power generation. Experience has indicated that operating and maintenance costs are generally lower than PC fired boilers, due to the ability to burn lower grade fuels, thus reducing fuel cost-escalation uncertainty. Since maintenance areas are said to be minimal in the CFB boiler, the availability of the boiler is likely to be relatively higher. The CFB design should also allow emissions reduction without significant capital cost, since SO_x removal occurs in bed and low or no NO_x production occurs in the typically low temperatures of the CFB combustion process usually with the use of SNCR as well [38].

It is for these reasons that this research study seeks to investigate the potential for CFB as an alternative solution to South Africa boilers and power generation challenges.

CHAPTER THREE: RESEARCH METHODOLOGY

This chapter provides information concerning the source of the coals tested, the different analysis conducted on the fuels tested, the nature of the CFBC test facility, the methodology and programme of testing in the test facility, the monitoring of the combustion tests, data collection and the methods used to calculate cost factors and economical evaluations.

3.1 Materials

Three South African (SA) coals and one Russian coal were tested in the CFBC pilot scale test facility. The SA coals were from specific collieries currently supplying power stations in South Africa, as indicated below.

- SA I: South African coal from a Free State colliery (Run-of-mine thermal feed to power station L)
- SA II: South African coal from a Limpopo colliery (Middlings product, middle density coals extracted in the washing process, used as thermal feed to power station M)
- SA discard: South African coal from a Limpopo colliery (Discard product, material left after washing out export and middlings products; unused, stockpiled)
- Russ: Russian coal, thermal coal sold on the European market.

Additive: Limestone

The objective of this work was to study the behaviour of SA coals in CFB with some focus on additives such as limestone or dolomite, to explore the option of SOx reduction in-bed. A detailed study on the calcium-sulphur ratios used features in Chapter Four. The limestone was provided by the test facility at VTT, where the characterisation and properties of limestone and dolomite does not form part of the current study.

3.2.Preparation

The coal samples were crushed and prepared to pass -3mm. They were then separated into a number of representative bags in preparation for analysis and combustion tests. The bags were stored in nitrogen to prevent oxidation.

3.3.Characterisation

All coals were analysed as follows:

i. Proximate analyses (inherent moisture, volatile matter, ash and fixed carbon content reported on an air dry basis)
ii. Ultimate analyses (C, H, O, N and S)
iii. Petrographic and mineralogical analysis including:
   Maceral analysis
   Mineral distribution
   Rank by vitrinite reflectance
   Abnormal condition analysis
iv. Particle size analysis
v. Ash composition
vi. Trace element analyses

3.3.1 Proximate, ultimate analysis

The coals were analysed in two batches, Batch 1 in South Africa and Batch 2 in Finland.
B1: batch one coals were analysed for proximate analyses, ultimate analysis without oxygen, nitrogen, carbon content and hydrogen in addition to ash composition on the four coals.
B2: coals for proximate analyses, ultimate analyses and trace element composition.
Both analyses for Batch B1 and B2 were outsourced to external companies, namely, Witlab Laboratory in South Africa and FINAS in Finland, respectively. All analyses were undertaken according to ISO standards.

3.3.2 Petrographic analyses

OBJECTIVES

The main purpose of the petrographic analyses was to assess the coals in terms of their fundamental petrographic properties (rank, organic (maceral) composition, mineral groups and general condition).

3.3.2.1 Background and information

Coals are complex combustible sedimentary rocks formed from consolidated plant remains, which have undergone extended periods of time, temperature and pressure. The latter processes lead to a maturing process which results in the original peats swamps passing through phases from lignite through sub-bituminous coal to bituminous coal and anthracite, according to their degree of maturation in the continuous evolution towards a pure carbon structure, graphite.
Coal petrography is the microscopic examination used to identify the organic (maceral, vegetable fragments) and inorganic (mineral) components as well as the level or maturity (rank) in coal. The data so obtained, together with the interpretation of the conventional chemical analytical data, can provide valuable fundamental information regarding the full characterisation of a coal, which is vital for gaining insight into the behaviour of a coal in any technological process.

Because of the highly variable compositional (petrographic) nature of the South African coal in contrast to the very consistent coals in Europe and America, (a fact which cannot be identified by simple chemical analyses alone), such additional analyses were considered vital for the full characterisation and understanding of the combustion behaviour of the coals in the current research.

3.3.2.2 Classification

Petrographically, coals can be classified according to three major fundamental and independent parameters.

Organic composition or Type:

This relates to the **microscopically discernable organic components of coal that are termed 'macerals',** and which are analogous to minerals in inorganic rocks.

Three maceral groups are recognised - *vitrinite, liptinite and inertinite*. These are distinguished from one another under the petrographic microscope by differences in reflectance, morphology, colour, shape, size, polishing hardness and fluorescence. Their optical, physical, chemical and technological characteristics alter as the coal matures.

Rank:

This refers to the **degree of maturation**, i.e., the stage in the evolution or coalification of the plant remains.

Grade:

This relates to the inorganic (minerals-ash) impurities present, conveniently represented by the ash yield (incombustibles remaining after burning).

The organic composition (i.e. the relative proportions of the macerals), the rank and the grade of a coal, together with the process conditions applied, are all influential factors governing the technological performance of the coal.

3.3.2.3 Reactivity to heating

When bituminous rank coal is heated to temperatures above approximately 350°C, vitrinites, liptinites and some inertinites start to soften, become plastic, and expand. The rest of the inertinites and most of the minerals remain unchanged. The degree of expansion is influenced by the heating rate and the final temperature applied. As the volatiles are released, vesicles may be formed in the reactive coal macerals. Reactives-rich components in bituminous coal increase in volume on heating to form cellular structures producing porous coke/char. These products then provide greatly increased surface areas for reactions to occur. Most inertinites however, and particularly fusinites, do not soften, degasify or develop into porous structures, but form dense solid carbon-rich chars, which often pass right though a boiler without any change in structure at all.

3.3.2.4 Experimental Petrographic Techniques

Each coal sample was prepared into a block containing thousands of particles embedded into gum with the surface polished ready for petrographic analysis. This is conducted in accordance with ISO Standard 7404 - 2, [100]. Maceral analysis (to determine the organic composition of coal) and reflectance measurements (to determine the rank) were carried out. The group maceral analysis was carried out in accordance with the ISO Standard 7404-3, [101]. Vitrinite random reflectance measurements (100 over the polished surface of each particulate petrographic block) were taken in accordance with the ISO Standard 7404-5 [102]. Microlithotype, carbominerite and minerite analyses (to determine the organic/inorganic associations) were conducted in accordance with the ISO Standard 7404-4 [103]. Mineral group and condition analyses were also performed on the coal samples. In both of these types of analyses, the components were quantified using a 500 point-count technique as described in the ISO Standard 7404-3 [101].

3.4 Experimental setup

The combustion experiments were carried out with a pilot scale CFB (Figure 3.1) housed by VTT, Finland. The fuel power of the pilot is 40-60 kW depending upon operating conditions. The height of the riser is 8 m and the inner diameter 167 mm. The combustor is equipped with several separately controlled electrically heated and water/air-cooled zones in order to control the process conditions (for example oxygen level, temperature and load) almost independently. Several ports for gas and solid material sampling are located in the riser area. The circulating matter is separated from the combustion gases in the primary cyclone and fly ash is separated from the gases in the secondary cyclone, gas cooler and bag house filter. The combustor is controlled with a computer, on which all measurement data is saved. The experimental set up is illustrated in Figure 3.1 below.

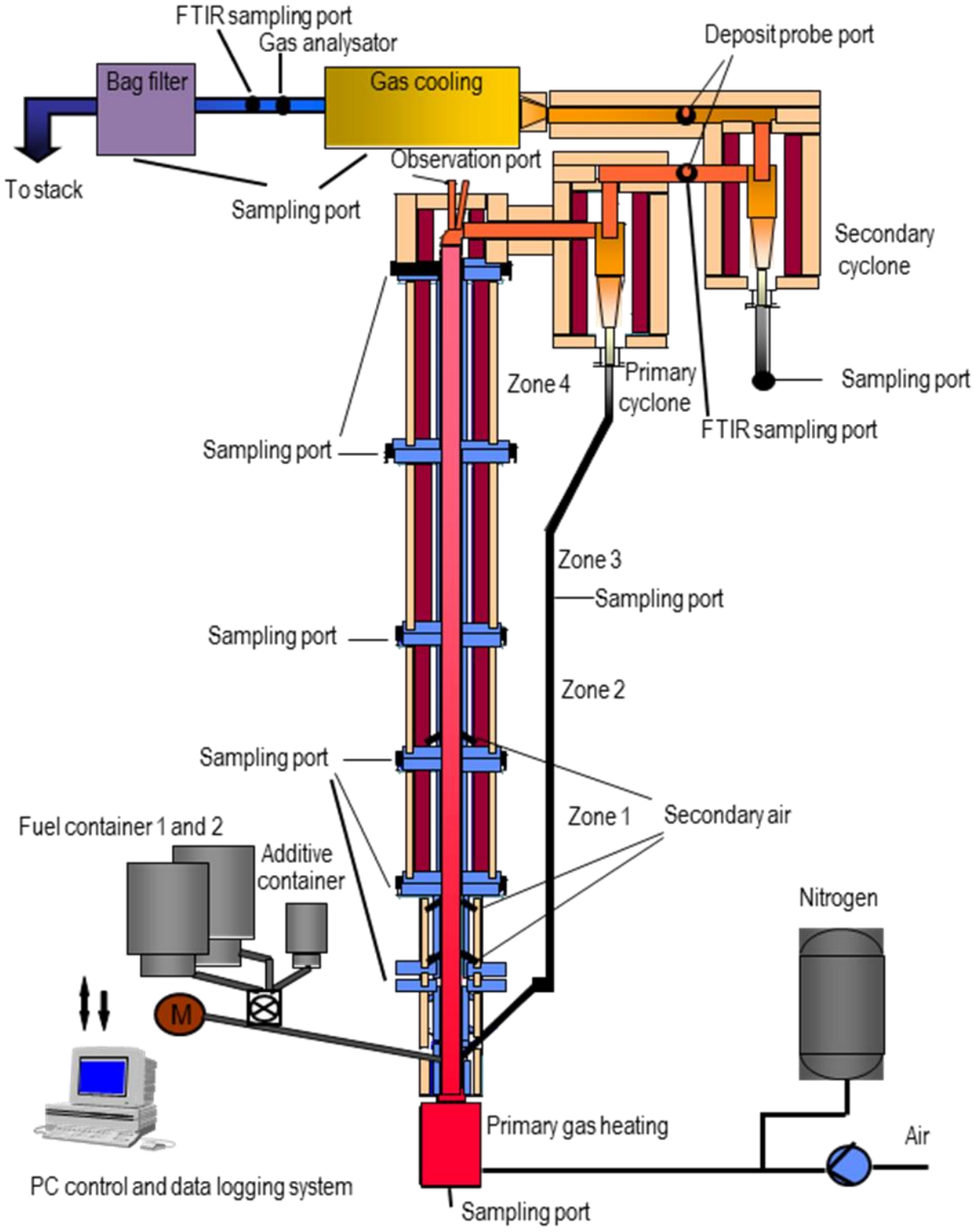

Figure 3.1: Experimental setup (VTT Finland)

As shown in Figure 3.1, the system is comprised of a riser, primary cyclone, a secondary cyclone, fuel feeder, additive container, gas cooling, gas analyser and a bag filter.

The riser is sectioned into four zones as follow:

Zone one: 3.2 m above the grate: this is the bottom section, where the fuel feeder and the additive container are located. Primary gas heating takes place in this zone, and primary and secondary air are introduced into the bed in here. Also, the return loop and recirculating material and gas entrance to the bed is fed back into the bed at this point. The bed material is in the bottom of this zone. This zone is often referred to as the dense bed.

Zone Two: 4.655 m above the grate: provision for tertiary air can be introduced in this zone; combustion takes place and gases are produced. This zone is often referred to as the furnace

Zone Three: 6.15 m above the grate: also known as the furnace section, full combustion continues to take place.

Zone Four: 8.3 m above the grate: This section is often referred to as the dilute section.

In addition to external components where the gas cooling occurs, bag filters, gas sampling equipment and cyclones are located.

Different probes and thermos-elements are placed along the riser in various monitoring spots as displayed in Table 3.1 below. The grate is the reference or zero level.

Table 3. 1: Thermo-element distance from the grate (the grate is considered to be zero level)

Thermo-element	**Distance from the grate (m)**
TE 1	Below the grate
TE 2	Below the grate
TE 3	Limit point/grate zero level
TE 30.1	**0.065**
TE 30.2	**0.265**
TE 30.3	**0.420**
TE 31	**1.095**
TE 32	**2.000**
TE 33	**3.200**
TE 34	**4.400**
TE 35	**6.150**
TE 36	**7.900**

3.5.Tests Methodology and Measurements

3.5.1 Experimental methodology

The coal samples were fired in succession with a minimum of three-hour intervals for system cooling and final ash collection. The Russian coal was fired first as a reference coal. During the experimental work, a steady state was maintained apart from the three-hour interval. At the end of the steady state period, the different solid streams were weighed and analysed for unburned carbon content (the bed was drained, and the bag filter sampled).

Primary gas grid velocity (fluidisation velocity) was maintained as a constant in each test run corresponding to 3.6 m/s and 0.6 s residence time before the gas-sampling probe. The average gas velocity after the secondary air feed was 2.4 m/s. And fluidisation velocity was kept constant by adjusting primary airflow with nitrogen. These factors contributed in maintaining a steady state during the combustion process. The steady state was also monitored by the recorded outgoing gases and the readings over that period formed the core of the data reported

in the thesis. Primary air was fed through the grate with 1100 evenly distributed 1 mm holes. The secondary air was fed at different levels of the combustor. In this test work, secondary air was applied at the lowest feeding point (1.3 m above the air grid)[104]. The bed material was sand with a particle size between 0.1 and 0.3 mm. Mean gas velocity in the reactor was 3 m/s. The share of primary air was 63%. Temperature in the riser was kept around 870°C max during the experiment.

Fuel was fed into the combustor through two separate fuel-feeding lines. One used for the main feed, and the other for additional feed (feed adjustment) or it could be used as a separate feeder for fuel feed switch from one type of fuel to another. There is also a feeder for solid additives. The additives were mixed with the fuel before being fed in the furnace with an option to spray a liquid chemical additive in the furnace if required. Fuel flow was measured from the weight loss of the fuel silos. The rotation speed of this screw feeder was kept constant [105, 106]. Excess air was set at 5-15 % and 10-20 % for primary and secondary air, respectively. The overall stoichiometry over the reactor was maintained by increasing secondary airflow in proportion to nitrogen dilution in primary air. Flue gas oxygen concentration at the outlet of the reactor remained rather constant during all the experiments by adjusting secondary air flows between the tests.

The combustor was equipped with a FTIR gas analyser and traditional on-line analysers for main flue gas compounds. Gas samples were taken to FTIR from different levels of the riser and flue gas ducts. In these experiments, it was taken from between the primary and secondary cyclone at approximately 780 °C. Traditional on-line analysers were connected to the flue gas duct between the gas cooler and bag house filter. Flue gas composition measured after the gas cooling includes O_2, CO_2, CO, NO, NO_2, N_2O and SO_2 measurements (Servomex 4900, (Gfx) IR)[104, 107].

All process variables were recorded in continuous data form and processed by the control system. A sample was continuously extracted from flue gases before the bag filter and sent to the on-line flue gas analysers (O_2, CO_2, CO, N_2O, NOx, CH_4, SO_2 and HCl). The sample had to be relatively clean and dry before entering the analysers so it was filtered and condensed.

3.5.2 Measurements and monitoring

As shown in Figure 3.1 in section 3.4, the system was equipped with a computer for continuous monitoring and data collection for the experimental parameters, as taken at different points spread across the four zones.

i. Temperature

The following temperature readings were recorded:

- the grate primary gases temperature
- riser temperature at different levels as per table 3.1
- riser cooling temperature
- cyclone temperature
- cyclone cooling temperature
- circulating material temperature
- mass deposit temperature

The thermo-elements were placed in different sampling points (ports), these thermos-element were coded as per Table 3.1 below.

ii. Pressure

- riser pressure, and cyclones circulating material return pipe pressure, in addition to circulating material return pipe pressure drop)
- pressure general (Air)

iii. Gas flow

- air flow (primary, secondary and tertiary)
- nitrogen flow

iv. Mass flow rate

v. Fuel power

vi. Gas monitoring gas analyser (FTIR)

The gas analyser using Fourier Transform infra-Red (more details about FTIR technique see Appendix B, for CO, CO_2, SO_2, NO, NO_2, N_2O and other gases. The monitoring, reading and data storage was set to one-minute intervals. In addition, the system was equipped with coal/ash sampling [107, 108].

3.5.3 Ash sampling points

Fly ash in the CFB combustor is separated from the flue gases in three stages: i.e.

- A primary cyclone separator;
- A secondary cyclone separator in the flue gas cooler; and finally
- The bag filter.

Fly ash samples from these locations were combined to form one for each experiment based on their relative accumulated amounts. The cut size of the primary cyclone is approximately dp0.9=110 μm.[106].

The bottom ash sampling was done at the end of each experiment, where the bed material was drained, weighed, and inspected for agglomerates.

3.5.4 Deposit sampling

Deposits were collected on 15 mm diameter 300 mm long air-cooled AISI 321 steel tubes. The side facing the combustion gas flow was held at 500°C at combustion gas temperatures 780°C and 700°C between the cyclones and after the secondary cyclone, respectively. After three-hours exposure without any intermediate cleaning the probes were removed from the furnace and the deposits accumulated on the tubes were sampled at three locations along the circumference: on the side facing the flow (‘wind’), 80° (‘side’) and 180° (‘lee’) along the circumference. Deposit material was carefully removed from the surface of the deposit layer at each location with a surgery knife. The sampling time was optimised to obtain enough deposit for chemical analyses and weighing, and to let the deposits form their shapes as a result of different deposition mechanisms along the circumference of the probe [105, 106].

3.6.Collation of Data

The data with respect to the analyses of the coals and their carbon (char) and ash products were collated and have been presented in tables and graphically.

The data concerning temperature monitoring and all pertinent operational factors including combustion and air quality results that applied during the tests were captured and collated.

Analytical and combustion tests results were then correlated with comparisons and correlations drawn. The results are presented in Chapters 4 and 5.

3.7 Calculations and presentations

3.7.1 Calculations from experimental data

The experimental work yielded a considerable amount of data through the online system and use of computer for data storage. The most important aspects of the data were used for calculations using different formulas and correlations. The main results are presented in Chapter 4, whilst the calculation methods are collated in the appendices.

3.7.2 Calculation from the literature

This section specifically deals with the correlations used to estimate the SA coal discard stockpile and properties. The correlations were conducted using an excel spreadsheet for the SA coal discards for a period of 10 years, from 2001 to 2011, and the results are presented in section 4.7.5. The 2001 SA coal discard report compiled by the Department of Mineral and Energy Affairs (DME, now called Department of Energy DoE) was used as a reference [17]. The latter is the only known comprehensive survey on coal discard in South Africa.

3.7.3. Economic and costing

In this section data and case studies from literature were used to do the costing of potential plant installation based on CFB using coal discard. Real time costing couldn't be done due to the following factors:

- Instability of the fuel market;
- Electricity costs;
- Volatility of the local currency;
- Difficulty to obtain costing for both equipment and plant set up from suppliers;
- Labour issues; and
- Miscellaneous.

CHAPTER FOUR:

EXPERIMENTAL RESULTS AND DISCUSSION

Chapter 4 presents the results of the detailed analyses conducted on the coals under investigation followed by the results and discussion of the tests undertaken by the CFBC test facility in Finland.

4.1. Results of Conventional Analysis Conducted on the Coal Samples

As presented in Chapter 3, the coals under investigation and their sources are coded as follow:

- SA I: South African Coal One - Free State coal, unwashed run-of-mine
- SA II: South African Coal Two - Limpopo, washed middlings product
- SA Discard: South African Coal Discard - Limpopo, discard product
- Russ: Russian Coal

The coals were analysed in two batches, Batch 1 in South Africa and Batch 2 in Finland. B1 coals were analysed for proximate analyses, ultimate analysis without oxygen, in addition to ash composition on the four coals. B2 coals for proximate analyses, ultimate analyses and trace element composition. The coal analysis were done according toi each country specifics and standards.

4.1.1 Proximate and Ultimate analysis

The results of the conventional proximate and ultimate analyses of the four coals are presented in Table 4.1 and 4.2. The analyses are reported on an air-dry basis.

Table 4.1 Proximate analysis of batches B1 (SA) and B2 (Finland)

Sample	Batch	H_2O (%)	Ash (%)	Volatile (%)	F/Carbon (%)
SA I	**B1**	**4.8**	**47.7**	**17.6**	**29.9**
	B2	7.7	53.7	18.6	20.0
SA II	**B1**	**1.6**	**34.2**	**27.4**	**36.8**
	B2	9.8	35.6	28.1	26.5
SA Discard	**B1**	**0.9**	**73.5**	**12.8**	**12.8**
	B2	2.2	65.27	17.18	15.35
Russ	**B1**	**3.2**	**15.4**	**34.0**	**47.4**
	B2	12.1	13.6	36.3	38.0

The combined results of the calorific values, total sulphur contents and ultimate analyses are presented in Table 4.2 below (apart from hydrogen, nitrogen and carbon content for Batch 1). The analyses are reported on an air-dry basis.

As will be noted in the two tables, the Russian coal has a high calorific value (26,6 MJ/kg) versus the extremely low value for SA discard (5.04 MJ/kg ad). The remaining two South African coals possess 12,9 to 20,9 MJ/kg ad. Similarly, volatile matter is highest in the Russian coal (34) and lowest in the SA discard (12, 8%). The sulphur contents for all four coals are relatively low (below 1%) with the exception of SA II (1,3%). The ash content of all three South African coals are high (between 34,2% and 73,5%), whereas the Russian coals possess an ash content of 15, 4 percent.

The results of calorific value and proximate and sulphur analyses in Batch 2 (Table 4.2) are similar to those in Batch 1, thereby confirming the general trend same trends.

Table 4. 2 Ultimate analysis of batches B1(SA) and B2 (Finland)

Sample	Batch	Cal Value MJ/Kg	T Sulphur (%)	H (%)	N (%)	C (%)
SA I	B1	**12.9**	**0.7**			
	B2	11.8	0.8	2.2	0.7	32.5
SA II	B1	**20.9**	**1.3**			
	B2	19.9	1.4	3.6	1.1	50.3
SA Discard	B1	**5.0**	**0.6**			
	B2	5.6	1.4	1.4	0.3	13
Russ	B1	**26.6**	**0.2**			
	B2	28.9	0.3	4.7	2.2	68.4

Results reported on as fired basis

4.1.2 Ash Properties

The ash composition of the four coals was analysed during the course of Batch 1 tests and the results are presented in Table 4.3.

Table 4. 3 Ash constituents analysis of sample B1

Sample	SiO_2 (%)	Al_2O_3 (%)	Fe_2O_3 (%)	P_2O_5 (%)	TiO_2 (%)	CaO (%)	MgO (%)	K_2O (%)	Na_2O (%)	SO_3 (%)
SA I	65.7	26.2	2.1	0.1	1.3	0.7	1.2	1.3	0.2	1.3
SA II	71.0	14.3	8.8	0.1	1.0	0.0	0.7	1.2	0.10	2.5
SA discard	56.3	36.9	3.0	0.4	0.7	0.0	0.4	1.2	0.11	0.4
Russ	60.7	12.6	8.8	2.6	0.4	3.9	2.9	2.1	1.93	5.4

It will be noted that the Russian coal is characterised by high contents of SiO_2 (quartz), P_2O_5, CaO, MgO and the alkalis, whereas the South African coals have high SiO_2, with moderately high Al_2O_3, indicating the presence of clays in two samples. SA II has a high SiO_2 (quartz) and lowered SO_3 content compared to the Russian coal.

4.1.3 Trace elements analysis

The trace elements content analysed during the course of Batch B2 analysis is presented in Table 4.4 below.

Table 4. 4 Trace element analysis B2

Sample	Hg (%)	Br (%)	F (%)	Cl (%)
SA I	< 0.01	< 0.002	0.004	0.090
SA II	< 0.01	< 0.002	0.008	0.080
SA discard	< 0.01	< 0.002	0.004	0.004
Russ	0.080	< 0.002	0.008	0.039

The results indicate that the Russian coal has a considerably high mercury content than the South African coals. The SA discard coal possesses the lowest chlorine content (0.004%) relative to the other three coals (0.039-0.090%).

4.1.4 Summary of coals conventional analyses

From the tables above, it is apparent that the Russian coal has considerably higher heat value and highest volatile matter content with lowest ash content compared to the SA coals. The South African coals have considerably higher ash contents with variable volatile matter and heat contents. The Russian coal has higher alkali and SO_3 contents with high SiO_2 (quartz), whereas the South African coals have generally high SiO_2 and Al_2O_3 contents (clays) and low alkalis and SO_3.

4.2 Petrographic Analyses

4.2.1 Reflectance Analyses

The rank parameter of the classification is based on vitrinite random reflectance. Reflectance measurements were conventionally taken on the vitrinite maceral telovitrinite in the Medium Rank coals. The vitrinite random reflectance measurements as presented in Table 4.5 below indicate that, according to the ISO 11760-2005 [68] coal classification, the four coals are characterized as Medium Rank coals.

Table 4. 5 The mean random reflectance values

	Rr %	Distribution %	σ	Rank designation
SA I	0.60	V 4 to V 9	0.099	Medium Rank C
SA II	0.68	V 5 to V 8	0.058	Medium Rank C
SA DISCARD	0.68	V 5 to V 9	0.079	Medium Rank C
Russ	0.60	V 4 to V 7	0.060	Medium Rank C

The vitrinite-class distributions of samples 1, 2, 3 and 4 showed standard deviations of < 0.1, typical of non-blend coals (terminology of the ECE-UN[1] International Codification System for Medium and High Rank coals).

4.2.3 Petrographic composition

4.2.3.1 Maceral analyses

The results of the maceral analyses are presented in Table 4.6.

It is notable that:

- Samples 2 and 4 represented high vitrinite coals with 78% and 86% of vitrinite and total reactives (vitrinite +reactive inertinite) of 87% and 91%, respectively (percentages by volume, mineral matter-free basis).
- Sample SA I, was lowest in vitrinite and total reactive matter contents <50%, with total vitrinite and reactive inertinites of 18% and 22%, respectively. Similarly,

sample 3, the SA Discard, possessed relatively low vitrinite and reactive inertinite content of 29% and 19%, respectively.

Table 4. 6 The total reactive maceral contents (mineral matter-free basis).

	Total reactives %	Vitrinites %	Liptinite %	Reactive inertinites %
SA I	45	18	5	22
SA II	87	78	5	4
SA DISCARD	54	29	6	19
Russ	91	86	3	2

For the purposes of the current investigation, reactivity is defined as the propensity of the organic constituents of the coals to react very rapidly to heating.

The considerations that follow are based purely on the characteristics of the products as expressed by the petrographic analyses. These properties, together with the chemical and physical characteristics, give insight into *expected behaviour*. They do not take into account the specific conditions to which the coals may be subjected, nor do they consider the possible kinetics and chemical reactions that may occur in a particular process.

It is generally accepted that the vitrinites and liptinites of bituminous coals are the reactive organic components (macerals), i.e. components that devolatilise, ignite and burnout out very quickly.

Also, certain inertinite group macerals are known to behave in a similar manner to vitrinites. Such reactive inertinites are identified as those inertinites (semifusinites and inertodetrinites) displaying low relief, with colour and reflectance very similar to those of the associated vitrinites in a coal. At sufficiently high temperature, the vitrinites and reactive inertinites of bituminous coals degasify, soften, swell and form porous chars, providing increased surface areas for reactions to occur easily and rapidly.

Inert forms of inertinite macerals, on the other hand, do not degasify, soften and become porous. On heating, these components remain in their normal form, as solid, dense carbon forms thereby becoming known as "dense chars". Generally, these forms undergo delayed ignition, only igniting (if at all) at very high temperatures and they have extended burnout times. Such particles have been shown in recent research to burn at high temperatures (some at 1800^{o}C) and to require increased oxygen to do so (Falcon *per comm*). The expected combustion behaviour of the coals under review is highlighted in section 4.2.3.4.

4.2.3.2 Microlithotypes (maceral/mineral) associations

The results of microlithotype analyses (maceral-maceral and maceral-mineral associations) are illustrated in Tables 4.7 and 4.8. Here the categories of microlithotypes – vitrite, inertites, carbominerite and minerite – are presented as percentages by volume on a mineral matter free basis.

Table 4. 7 Microlithotype (maceral/mineral associations) Results

	Vitrite "pure" vitrinite %	Inertite "pure" inertinite %	Intermediates maceral mixtures %	Carbominerite maceral/mineral mixtures %	Minerite mineral rich %
SA I	4	16	12	46	22
SA II	38	6	18	24	14
SA DISCARD	1	2	2	12	83
Russ	57	7	28	3	5

From the above table it will be noted that:

- The SA discard contains a very high proportion of minerite (rock and mineral-rich) particles (83%), whereas the Russian coal has a minimum quantity (5%). SA I and SA II possess 22% and 14%, respectively.

- In contrast, the SA I and SA II have high carbominerite (organic and mineral matter mixed evenly together), with 46% and 24%, respectively. However, these two coals differ radically in their organic composition: SA I has only 4% particles of pure easily combusting vitrinite-dominated *vitrite* particles, whereas SA II has 38%.

These results indicate that the coals differ significantly from one another in the distribution of their mineral and maceral (organic) matter content, with the Russian coal the cleanest and lowest in rock and high-ash particles (8%), whereas the SA Discard is predominantly composed of high proportions of rocky and high ash material (95%).

In terms of reactive microlithotype forms (vitrite), the Russian coal possesses the highest clean vitrite content (57%) and SA II the next highest (38%), with SA 3 and SA discard coals possessing negligible amounts (4% and 1%, respectively).

These results once again illustrate the significant differences between the organic and inorganic composition of all four coals.

4.2.3.3 Abnormal condition analyses

The abnormal condition and weathering of the coals tested is presented in Table 4.8 below. This analysis outlines the preservation and nature of the coaly material.

Observations undertaken on the coals with regard to any abnormal conditions indicated that:

- The majority of the particles in samples 2, 3, 4, were of a predominantly "fresh" nature. Some particles displaying cracks and micro-fissures were seen (20% or less). Some of these cracks may have developed during handling and preparation due to the brittle nature of the coal at this level of rank.
- Sample 1, contained notable portions of organic particles which exhibited signs of severe weathering and general disintegration (10% to 15%); (30% cracks and fissures with 14% severely weathered) i.e. a total of 44% of the coal in Sample 1 is abnormal in one form or another.

Table 4. 8 Condition/weathering analysis - relative proportions of abnormal particles (% by volume)

	Fresh coal particles	Pyrite		Particles with extensive cracks or fissures	Severely weathered particles	Shrinkage/ desiccation cracks	Particles with oxidised/thermally affected rims or zones	Particles displaying low temperature devolatilisation	Severely heat altered (coke/char)	Total abnormal particles
		normal	altered							
	%	%	%	%	%	%	%	%	%	%
SA I	55	1	0	25	14	5	0	0	0	44
SA II	86	4	0	7	0	3	0	0	0	10
SA Discard	76	10	0	10	2	2	0	0	0	14
Russ	81	1	0	14	1	3	0	0	0	18

4.2.3.4 Summary of the petrography analyses

The summary of the petrographic analyses is presented in Table 4.9 below.

Table 4. 9 Summary of major petrographic characteristics

	SA I	SA II	SA Discard	Russ
RANK (degree of maturity)	Bituminous	Bituminous	Bituminous	Bituminous
ISO11760-2005 Classification of Coals	Medium Rank C	Medium Rank C	Medium Rank C	Medium Rank C
Mean random reflectance of vitrinite %	0.60	0.68	0.68	0.60
Vitrinite-class distribution	V 4 to V 9	V 5 to V 8	V 5 to V 9	V 4 to V 7
Standard deviations	0.10	0.056	0.089	0.06
Abnormalities	None	None	None	None
PETROGRAPHIC COMPOSITION (% by volume) Maceral analysis (mineral matter-free basis)				
Total reactive macerals %	45	87	54	91
Vitrinite content %	18	78	29	86
Liptinite content %	5	5	6	3
Total inertinite %	77	17	65	11
Heat altered (coke, char etc.) %	0	0	0	0
Maceral analysis - Total %	100	100	100	100
Microlithotype analysis				
Vitrite %	4	38	1	57

Liptite %	0	0	0	0
Inertite %	16	6	2	7
Intermediates %	12	18	2	28
Visible minerals				
Carbominerite %	46	24	12	3
Minerite %	22	14	83	5
Microlithotype analysis - Total %	100	100	100	100
Condition analysis				
"Fresh" coal particles %	56	90	86	82
Cracks and fissures %	30	10	12	17
Severely weathered %	14	0	2	1
Particles exhibiting oxidation rims %	0	0	0	0
Particles displaying low temperature				
devolatilisation %	0	0	0	0
Heat altered (e.g., coke/char) %	0	0	0	0
Condition analysis - Total %	100	100	100	100

Based upon the petrographic results listed above, it is anticipated that the Russian coal would be the first coal sample expected to exhibit rapid ignition with high volatiles followed by rapid burnout. Following the Russian coal would be the SA II sample (high vitrinite and vitrite contents). Sample SA I is anticipated to be difficult to ignite (low vitrinite and vitrite contents

with 44% of abnormal weathered and oxidised coals) but once ignited, this coal could provide reasonable extended combustion at relatively high temperatures. Sample 3 is likely to exhibit abnormal and difficult ignition due to very low proportions of organic matter due to the extremely high rock and mineral-rich matter content and the very low vitrite content in the microlithotype analysis.

On the basis of the estimated combustibility of the coals as analysed petrographically, the decreasing order of ease of ignition, combustion and burnout would be as follows:

1. Russian coal - expected to be the fastest to burnout
2. SA II
3. SA I
4. SA Discard

Note:

The petrographic properties should be considered together with the chemical and physical data to confirm the expected behaviour of the coals. It is also critical that the influences of the operating conditions be taken into account in the prediction of the technological performance.

4.3 Mineralogical Composition

4.3.1 Background

The mineralogical compositions of the samples under review are based on the quantitative evaluation of minerals by scanning electron microscopy QEMSCAN (direct measurement) analysis and the Coal Quality Assessment (CQA) model. QEMSCAN mineral identification is based on elemental proportions derived from a 1000 count X-ray spectrum. The elemental proportions are compared to a "mineral identification" standard (COAL SIP) and the "best" fit mineral is identified (refer to "QEMSCAN OPERATION"). The chemical results are the input into the CQA. CQA was designed to determine the mineral composition of coal and not the organic fraction of "coals", which have a significantly high proportion of organically bound inorganic elements such as may be found in peat, lignite and sub-bituminous coals. The assessment still provides valuable results as the comparison between QEMSCAN and CQA indicates the dominant organically bound inorganic elements. See Appendix D.

Particle classification

The individual particles are classified into ten groups:

1. Pyrite/siderite cleats - extraneous pyrite/siderite rich particles (area% pyrite/siderite >60%)
2. Calcite cleats - extraneous calcite rich particles (area% calcite >60%)
3. Dolomite cleats - extraneous dolomite/ankerite rich particles (area% dolomite/ankerite >60%)
4. Carbonate Cleats - extraneous calcite/dolomite/ankerite rich particles (area% calcite/dolomite/ankerite >60%)
5. Sandstone - sandstone fragments with a high proportion of quartz/microcline/muscovite content (>60%)
6. Siltstone - mixture of fine kaolinite and quartz. Kaolinite+quartz (>60%)
7. Mudstone/Shale - Mudstone/shale rock fragments with a high proportion of kaolinite/illite (>60%)
8. Middlings (50-70) - organic matter “coal” material in “middlings” particles. Organic coal proportion varies from 50-70 Area percentage. Included and attached mineral matter make up the balance.
9. Included (80-100) - organic matter "coal" material with some mineral "included" particles. Organic coal proportion varies from 80-99.9 Area percentage. Included mineral matter makes up the balance.
10. Ash Free organic matter coal particles - mineral matter free coal particle.

For each sample the particles are classified and the percent mineral distribution across the particle classification is computed.

Size classification

Size classification is based on the equivalent circle diameter or QEMSCAN unique size classification based on the phase specific surface area (PSSA). Size classes are defined and each particle is classified. The area percentage proportion for each class is computed.

4.3.2 Mineral properties

The following section presents the mineralogical analyses of the four samples under review. These are illustrated in terms of (i) mineral proportions, (ii) particle characteristics (i.e. pure or mixed forms of organic and mineral matter content) and (iii) mineral distribution across the class sizes.

4.3.2.1 Sample SA I Mineralogy Results

SA I coal properties are presented in tables 4.10, 4.11 and 4.12 below

Table 4.10 SA I Mass- percentage mineral proportions

Mass %	QEMSCAN	CQA
Sulphates (Gypsum/Iron- Al-sulphates)	0.2	
Pyrite	1.0	0.3
Siderite	2.3	1.4
Calcite	0.9	0.0
Dolomite/Ankerite	1.0	2.5
Apatite	0.3	0.1
Kaolinite	31.5	30.5
Quartz	14.9	16.1
Illite/Muscovite	0.1	2.3
Muscovite	0.6	1.9
Albite/microcline/plagioclase	0.5	1.4
Rutile	0.6	0.6
Coal - organic sulphur	18.9	43.0
Coal	26.8	

Other	0.5	0.0
Total	100.0	0.0
Mineral Matter	54.2	57.0
Mineral Volatiles	6.8	6.4
Ash percentage Calc (QEMSCAN/CQA)	47.4	50.5
Ash percentage Chemical (DB)	50.1	50.11

Table 4. 11SA I Particle characteristics

	Percent Mineral Distribution							
Particle Type	Mass percentage	Kaolinite	Quartz	Pyrite/ Siderite	Calcite	Dolomite	Coal	Other
Pyrite/siderite Cleat	2.33	0.45	0.21	49.13	0.38	1.42	0.18	20.60
Calcite Cleat	0.08	0.01	0.01	0.01	6.27	0.04	0.02	0.28
Dolomite Cleat	0.27	0.01	0.02	0.00	1.39	17.04	0.07	0.39
Carbonate Cleat	0.07	0.01	0.00	0.00	2.18	2.35	0.02	0.15
Sandstone	3.42	1.84	15.30	1.72	0.08	0.14	0.45	2.82
Mudstone	15.30	39.73	7.60	7.63	0.69	4.54	2.98	6.70
Siltstone	4.57	8.29	9.20	0.54	0.09	6.54	0.78	1.31
Middling 50	26.85	31.34	40.83	28.99	78.37	50.33	16.63	34.99
Middling 60	8.48	8.16	8.04	4.27	6.32	6.18	9.34	8.42
Middling 70	8.56	4.93	9.04	3.51	2.47	6.38	11.46	9.64

Included 80	9.95	3.72	6.64	2.91	1.25	3.23	16.39	7.99
Included 90	13.25	1.52	3.12	1.30	0.51	1.80	26.62	6.71
Ash FreeCoal	6.88	0.00	0.00	0.00	0.00	0.00	15.06	0.00
Total	100	100	100	100	100	100	100	100
	Mass-%	Kaolinite	Quartz	Pyrite/Siderite	Calcite	Dolomite	Coal	Other
Total Cleat	2.74	0.48	0.24	49.13	10.22	20.85	0.30	21.42
Total Stone	23.29	49.85	32.10	9.8 9	0.85	11.23	4.21	10.83
Total Middling	43.89	44.44	57.91	36.76	87.16	62.89	37.43	53.05
Total Included	23.20	5.23	9.76	4.21	1.77	5.03	43.00	14.71
Ash-Free Coal	6.88	0.00	0.00	0.00	0.00	0.00	15.06	0.00
	100.00	100.00	100.00	100.00	100.00	100.00	100.00	100.00

Table 4. 12 SA I Percentage mineral distribution across size classes

Size Class (um)	Volume	Kaolinite	Quartz	Pyrite	Calcite	Dolomite	Coal	Other
>500	15.97	28.31	26.18	18.86	26.39	10.22	9.31	11.72
475-500	1.59	2.14	1.36	0.25	0.04	0.02	1.51	0.53
450-475	3.53	7.92	2.71	0.76	0.34	14.33	2.03	2.10
425-450	1.78	3.77	3.72	0.15	0.02	0.26	0.75	0.40
400-425	2.17	3.02	1.65	0.58	28.19	16.39	1.50	1.55

375-400	2.99	2.88	3.62	24.35	0.22	1.47	2.34	17.54
350-375	3.04	4.93	2.94	1.82	11.71	2.97	2.29	3.98
325-350	2.72	1.97	2.98	8.68	0.06	0.47	2.86	2.66
300-325	3.10	3.37	4.96	8.17	2.47	1.14	2.52	7.14
275-300	3.46	3.09	4.67	0.93	0.01	0.33	3.51	1.54
250-275	3.26	3.23	2.86	2.07	0.23	1.92	3.44	2.18
225-250	3.17	2.85	3.18	7.68	0.40	3.39	3.19	3.78
200-225	3.21	3.12	3.09	6.96	0.46	1.98	3.22	2.61
175-200	3.95	2.44	4.26	4.30	0.80	8.01	4.42	3.22
150-175	5.56	4.85	5.24	1.68	2.19	5.55	6.02	4.34
125-150	5.39	4.06	3.85	1.13	4.05	1.96	6.36	3.57
100-125	6.00	4.46	4.83	1.36	5.26	6.06	6.93	5.31
75-100	6.50	4.34	5.03	2.63	4.52	3.55	7.77	4.80
50-75	6.68	4.12	5.09	2.91	6.22	8.78	8.00	5.87
25-50	8.12	3.73	5.51	3.52	4.37	8.04	10.41	8.32
0-25	7.83	1.41	2.28	1.22	2.03	3.16	11.60	6.83
Total	100.00	100.00	100.00	100.00	100.00	100.00	100.00	100.00

SA I has a high proportion of kaolinite rich mudstone, siltstone and middling 50 particles. Included kaolinite in “middling” and “included” particles will probably facilitate fragmentation. The high ash is attributed to the relatively high proportion of stone (23 mass percentage) and middlings particles (43 mass percentage). This aligns with the petrographic analysis of minerite (22%) and carbominerite (44%) as reported in the previous section.

The mineral distribution in general is typical for a South African coal in terms of high kaolinite and quartz contents. This sample has a comparatively high proportion of siderite relative to pyrite. The calcite, dolomite and carbonate cleats have a higher propensity to react with sulphur compared to included and middling calcite and dolomite. A higher proportion of stone will contribute to a fluidised bed boiler (FBC)'s ballast of sand in the bubbling bed.

4.3.2.2 SA II Mineralogy results

SA II coal properties are presented in tables 4.13, 4.14 and 4.15 below.

Table 4. 13 SA II Mass- percentage mineral proportions

Mass percentage	QEMSCAN	CQA
Sulphates (Gypsum/Iron- Al-sulphates)	0.07	
Pyrite	1.8	2.4
Siderite	0.98	2.56
Calcite	0.35	0.00
Dolomite/Ankerite	0.76	0.66
Apatite	0.03	0.10
Kaolinite	14.55	10.79
Quartz	15.27	18.29
Illite/Muscovite	0.60	1.51
Muscovite	0.75	1.30
Albite/microcline/plagioclase	1.48	0.93
Rutile	0.12	0.35
Coal - organic sulphur	35.79	61.03
Coal	27.08	
Other	0.43	0.00

Total	100.00	0.00
Mineral Matter	37.13	38.87
Mineral Volatiles	4.00	4.31
Ash percentage Calc (QEMSCAN/CQA)	33.14	34.55
Ash percentage Chemical (DB)	34.76	34.76

Table 4. 14 SA II Particles characteristics

	Percent Mineral Distribution							
Particle Type	Mass percentage	Kaolinite	Quartz	Pyrite/ Siderite	Calcite	Dolomite	Coal	Other
Pyrite/siderite Cleat	1.45	0.13	0.12	44.33	0.22	0.39	0.16	7.86
Calcite Cleat	0.26	0.00	0.00	0.00	67.60	0.52	0.03	0.34
Dolomite Cleat	0.60	0.06	0.02	0.00	4.21	66.74	0.15	1.45
Carbonate Cleat	0.06	0.01	0.00	0.00	5.28	4.13	0.02	0.23
Sandstone	5.66	3.52	15.71	0.66	0.09	0.08	1.30	6.74
Mudstone	4.69	19.16	2.88	0.30	0.07	0.15	0.82	1.71
Siltstone	20.52	45.40	33.32	4.55	0.68	0.62	5.83	14.68
Middling 50	16.56	17.43	23.70	35.96	16.35	20.33	11.00	34.48
Middling 60	6.63	5.35	7.98	3.31	1.69	1.41	6.64	8.59
Middling 70	7.88	4.21	7.51	3.72	1.67	2.85	9.77	9.71
Included 80	9.59	3.39	5.93	4.46	0.75	1.76	14.33	8.70

Included 90	17.49	1.35	2.82	2.72	1.40	1.03	32.72	5.52
Ash-free coal	8.61	0.00	0.00	0.00	0.00	0.00	17.23	0.00
Total	100	100	100	100	100	100	100	100
	Mass-%	Kaolinite	Quartz	Pyrite/Siderite	Calcite	Dolomite	Coal	Other
Total Cleat	2.37	0.19	0.14	44.33	77.31	71.77	0.36	9.88
Total Stone	30.87	68.08	51.92	5.50	0.83	0.85	7.95	23.13
Total Middling	31.08	26.99	39.19	42.98	19.71	24.59	27.41	52.78
Total included	27.07	4.74	8.75	7.19	2.15	2.78	47.05	14.22
Ash-free coal	8.61	0.00	0.00	0.00	0.00	0.00	17.23	0.00
	100.00	100.00	100.00	100.00	100.00	100.00	100.00	100.00

Table 4. 15 SA II Percentage mineral distribution across size classes

Size Class (um)	Volume	Kaolinite	Quartz	Pyrite	Calcite	Dolomite	Coal	Other
>500	42.48	43.65	48.43	62.92	2.81	4.31	39.42	30.64
475-500	4.10	2.96	3.36	0.13	0.13	0.23	4.90	1.28
450-475	4.58	8.93	4.31	10.30	1.00	0.05	3.19	7.26
425-450	2.03	2.42	2.70	0.02	0.07	0.09	1.77	0.40
400-425	2.79	3.01	2.20	7.19	0.00	0.05	2.80	0.66
375-400	3.43	4.06	3.82	1.31	0.20	0.07	3.22	2.17
350-375	4.32	3.31	4.84	1.57	0.07	0.86	4.56	2.42

325-350	3.49	3.86	3.07	0.06	0.13	0.03	3.71	0.59
300-325	3.58	2.28	3.18	2.30	6.76	21.25	4.07	3.02
275-300	3.48	4.12	2.10	0.56	0.13	0.10	3.95	1.08
250-275	2.06	1.84	1.49	0.09	0.94	41.82	2.25	0.66
225-250	2.92	2.09	2.61	0.56	0.20	0.09	3.40	0.63
200-225	3.28	2.76	2.61	1.23	0.00	0.09	3.79	1.72
175-200	2.42	3.10	2.59	3.54	6.10	5.45	2.10	3.84
150-175	2.70	2.38	2.67	0.17	2.34	4.03	2.92	0.92
125-150	2.44	2.45	2.35	1.84	2.55	8.68	2.48	1.82
100-125	2.48	2.34	2.46	2.27	1.27	1.36	2.55	1.40
75-100	2.25	1.63	1.96	1.63	34.56	0.14	2.52	3.29
50-75	1.73	1.50	1.61	0.53	25.39	6.15	1.83	3.07
25-50	1.69	1.01	1.24	1.39	9.65	3.09	2.00	9.02
0-25	1.74	0.32	0.40	0.39	5.69	2.06	2.56	24.12
Total	100.00	100.00	100.00	100.00	100.00	100.00	100.00	100.00

The QEMSCAN report for SA II indicates a higher ash content than the "CQA" analysis (the latter being based on the chemical analysis). The quartz content exceeds kaolinite. This is attributed to the high proportion of siltstone and a fair proportion of quartz in "middling 50" particles. A significant proportion of the kaolinite occurs as a siltstone and mudstone.

4.3.2.3 SA discard mineralogy analysis

SA coal discard properties are presented in tables 4.16, 4.17 and 4.18 below.

Table 4. 16 SA discard Mass- percentage mineral proportions

Mass percentage	QEMSCAN	CQA
Sulphates (Gypsum/Iron- Al-sulphates)	0.05	
Pyrite	0.6	1.1
Siderite	0.55	2.40
Calcite	0.46	0.00
Dolomite/Ankerite	0.34	0.78
Apatite	0.04	0.69
Kaolinite	61.48	65.67
Quartz	18.42	7.44
Illite/Muscovite	0.30	3.04
Muscovite	0.96	2.61
Albite/microcline/plagioclase	1.43	1.87
Rutile	0.79	0.49
Coal - organic sulphur	4.58	13.86
Coal	9.76	
Other	0.27	0.00
Total	100.00	0.00
Mineral Matter	85.66	86.14
Mineral Volatiles	9.53	11.50
Ash percentage Calc (QEMSCAN/CQA)	76.13	74.63
Ash percentage Chemical (DB)	74.17	74.17

Table 4. 17 SA discard Particles characteristics

	Percent Mineral Distribution							
Particle Type	Mass percentage	Kaolinite	Quartz	Pyrite/ Siderite	Calcite	Dolomite	Coal	Other
Pyrite/siderite Cleat	0.47	0.02	0.02	32.08	0.05	0.10	0.17	5.30
Calcite Cleat	0.34	0.02	0.01	0.00	62.40	0.72	0.20	0.78
Dolomite Cleat	0.10	0.00	0.00	0.08	0.69	22.35	0.09	0.11
Carbonate Cleat	0.07	0.00	0.00	0.00	2.80	9.98	0.09	0.16
Sandstone	3.41	1.35	8.94	0.79	0.09	0.23	1.43	2.55
Mudstone	47.99	62.35	31.96	20.88	5.28	18.31	22.13	21.46
Siltstone	35.97	31.44	54.03	16.08	2.47	5.23	22.06	24.00
Middling 50	4.99	3.24	3.30	27.90	20.99	34.73	12.28	36.93
Middling 60	1.20	0.67	0.69	0.60	0.96	2.14	4.84	2.61
Middling 70	1.31	0.50	0.56	0.78	3.08	4.21	6.63	3.06
Included 80	1.23	0.30	0.34	0.58	0.95	1.55	7.58	2.08
Included 90	1.78	0.11	0.15	0.24	0.24	0.46	13.45	0.97
Ash-free coal	1.12	0.00	0.00	0.00	0.00	0.00	9.04	0.00
Total	100	100	100	100	100	100	100	100
	Mass-%	Kaolinite	Quartz	Pyrite/Siderite	Calcite	Dolomite	Coal	Other
Total Cleat	0.98	0.05	0.04	32.17	65.93	33.15	0.55	6.35
Total Stone	87.37	95.14	94.93	37.74	7.84	23.77	45.63	48.00

Total Middling	7.51	4.41	4.54	29.28	25.04	41.08	23.74	42.59
Total included	3.02	0.41	0.49	0.81	1.19	2.01	21.04	3.06
Ash-free Coal	1.12	0.00	0.00	0.00	0.00	0.00	9.04	0.00
	100.00	100.00	100.00	100.00	100.00	100.00	100.00	100.00

Table 4. 18 SA Discard Percentage mineral distribution across size classes

Size Class (um)	Volume	Kaolinite	Quartz	Pyrite	Calcite	Dolomite	Coal	Other
>500	13.71	16.37	16.12	10.51	0.94	10.35	4.84	10.60
475-500	1.99	2.19	2.85	0.69	0.03	0.08	0.64	0.50
450-475	1.19	1.37	1.66	0.07	0.00	0.04	0.30	0.34
425-450	1.54	1.93	1.37	4.25	1.29	0.03	0.72	1.81
400-425	2.96	3.12	2.70	1.60	1.93	4.22	2.94	1.43
375-400	2.57	2.55	2.69	0.21	0.06	0.15	2.65	0.76
350-375	3.47	4.01	3.96	1.50	0.52	0.62	1.78	1.50
325-350	2.82	3.09	3.18	12.30	0.40	0.82	1.54	4.92
300-325	3.49	3.83	4.20	1.83	0.07	0.34	2.00	1.29
275-300	3.78	4.13	3.63	0.57	0.07	0.43	3.33	1.66
250-275	4.94	5.37	5.99	2.39	1.21	2.23	2.92	2.21
225-250	4.08	4.23	3.89	0.78	10.17	1.14	3.98	1.38

200-225	5.30	5.31	5.32	4.58	11.41	4.98	5.14	5.81
175-200	5.32	5.35	5.18	3.05	7.49	8.53	5.43	3.47
150-175	5.91	5.78	5.39	6.00	5.67	9.86	6.79	4.53
125-150	6.50	6.24	6.17	5.85	16.08	13.21	7.25	3.89
100-125	7.11	6.65	6.27	6.56	12.51	5.91	9.17	4.03
75-100	7.11	6.55	6.50	9.25	9.54	14.86	8.97	6.48
50-75	7.20	6.28	6.38	13.42	8.38	10.90	10.09	9.54
25-50	6.47	4.70	5.39	11.94	10.22	9.76	11.69	13.75
0-25	2.53	0.95	1.15	2.66	2.01	1.54	7.85	20.09
Total	100.00	100.00	100.00	100.00	100.00	100.00	100.00	100.00

Sample SA 3 is a typical discard product characterised by a high proportion of stone (87 mass percentage). Once again this correlates to the petrographic analysis of 83% minerite. Kaolinite rich mudstone and quartz/kaolinite siltstone is the dominant stone in this sample. The proportion of carbon-rich particles is less than 11.7 percent. This correlates to the 5% coal particles noted in the petrographic analysis with 12% particles comprising carbominerite (mixed coal and mineral matter). It is noted that 46 mass percentage of the "carbon coal" is associated with the rock fragments and the remaining carbon is associated with combustible middlings fraction (23%) and included fraction (30%). This product blended with a low ash coal could provide a good FBC bed.

4.3.2.4. Russian coal mineralogy analysis

The mineralogical properties of the Russian Coal are presented in tables 4.19, 4.20 and 4.21 below.

Table 4.19 Russ coal mass percentage mineral proportions

Mass percentage	QEMSCAN	CQA
Sulphates (Gypsum/Iron- Al-sulphates)	0.03	
Pyrite	0.1	0.4
Siderite	0.55	1.94
Calcite	1.01	0.00
Dolomite/Ankerite	0.78	1.84
Apatite	0.02	1.03
Kaolinite	2.13	3.55
Quartz	5.27	6.74
Illite/Muscovite	3.00	1.22
Muscovite	0.49	1.04
Albite/microcline/plagioclase	3.90	0.75
Rutile	0.03	0.06
Coal - organic sulphur	19.30	81.41
Coal	63.38	
Other	0.00	0.00
Total	100.00	0.00
Mineral matter	17.32	18.59
Mineral volatiles	1.78	2.55
Ash percentage Calc (QEMSCAN/CQA)	15.53	16.04
Ash percentage Chemical (DB)	15.91	15.91

Table 4.20 Russ coal particles characteristics

	Percent Mineral Distribution							
Particle Type	Mass percentage	Kaolinite	Quartz	Pyrite/ Siderite	Calcite	Dolomite	Coal	Other
Pyrite/siderite Cleat	0.09	0.00	0.01	11.47	0.00	0.00	0.01	0.03
Calcite Cleat	0.52	0.14	0.13	1.08	42.84	0.44	0.09	0.26
Dolomite Cleat	0.17	0.03	0.03	0.00	0.50	19.46	0.02	0.05
Carbonate Cleat	0.03	0.01	0.02	0.00	1.27	1.43	0.01	0.02
Sandstone	2.24	5.05	19.18	4.04	0.51	0.41	0.20	1.12
Mudstone	0.16	2.89	0.10	0.05	0.00	0.07	0.02	0.05
Siltstone	0.03	0.38	0.12	0.00	0.00	0.00	0.00	0.01
Middling 50	7.51	22.86	19.29	55.51	27.44	32.85	2.40	77.16
Middling 60	3.75	13.60	10.29	2.69	4.45	9.10	2.35	5.39
Middling 70	6.38	17.91	14.25	7.38	5.84	8.63	4.85	4.78
Included 80	10.46	17.30	15.01	5.15	6.25	9.13	9.83	4.73
Included 90	58.82	19.81	21.58	12.63	10.89	18.48	68.12	6.39
Ash-free coal	9.84	0.00	0.00	0.00	0.00	0.00	12.09	0.00
Total	100	100	100	100	100	100	100	100
	Mass-%	Kaolinite	Quartz	Pyrite/Siderite	Calcite	Dolomite	Coal	Other
Total Cleat	0.82	0.19	0.19	12.55	44.61	21.33	0.13	0.36

Total Stone	2.43	8.32	19.40	4.09	0.51	0.48	0.22	1.18
Total middling	17.63	54.38	43.83	65.58	37.74	50.58	9.60	87.33
Total included	69.28	37.12	36.59	17.78	17.14	27.61	77.95	11.12
Ash-free coal	9.84	0.00	0.00	0.00	0.00	0.00	12.09	0.00
	100.00	100.00	100.00	100.00	100.00	100.00	100.00	100.00

Table 4. 21 Russ coal percentage mineral distribution across size classes

Size Class (um)	Volume	Kaolinite	Quartz	Pyrite	Calcite	Dolomite	Coal	Other
>500	0.22	0.01	0.01	0.00	0.00	0.00	0.24	0.00
475-500	0.96	0.40	0.34	0.05	0.05	0.18	1.03	0.08
450-475	1.18	1.57	1.17	0.20	0.34	1.03	1.20	0.16
425-450	1.49	1.13	0.82	1.03	1.29	1.85	1.56	0.42
400-425	1.83	2.01	4.63	1.03	0.14	0.21	1.70	0.29
375-400	1.53	0.91	0.65	0.58	0.28	0.92	1.63	0.20
350-375	2.74	1.49	1.96	0.40	1.22	2.46	2.88	0.25
325-350	2.61	2.06	2.06	3.44	2.92	0.62	2.70	0.43
300-325	5.93	7.55	8.28	4.14	1.98	8.45	5.82	1.81
275-300	6.27	6.84	7.85	18.45	22.19	2.90	6.12	1.57
250-275	7.84	9.03	8.72	3.51	2.20	2.62	7.86	5.63
225-250	7.77	10.88	8.28	2.06	4.50	2.94	7.76	3.41

200-225	9.24	8.36	8.53	13.16	10.96	5.32	9.41	1.68
175-200	9.44	9.54	8.53	10.44	8.96	28.23	9.47	5.67
150-175	7.38	7.92	6.98	7.33	5.13	2.58	7.46	5.04
125-150	7.27	6.80	7.04	10.22	6.13	11.07	7.30	5.35
100-125	7.47	7.15	7.19	12.48	9.03	7.03	7.53	3.64
75-100	6.33	6.72	6.53	3.67	9.59	10.64	6.29	4.92
50-75	5.46	6.74	7.03	4.92	6.72	8.01	5.20	13.14
25-50	7.04	2.90	3.39	2.89	6.38	2.92	6.83	46.32
0-25	0.00	0.00	0.00	0.00	0.00	0.00	0.00	0.00
Total	100.00	100.00	100.00	100.00	100.00	100.00	100.00	100.00

As expected, the Russian low ash coal has less than 2.5 mass percentage stone (mainly sandstone) and a high proportion of “included” and “middling” particles. The majority of the kaolinite is finely distributed, included in a carbon matrix and will be difficult to beneficiate, fine minerals will not fragment. This coal is characterised by a comparatively high proportion of microcline/albite and K-bearing aluminosilicate (muscovite/illite).

4.4 CFB Experimental Parameters

4.4.1 Background

This section presents the results conducted on the CFBC combustion test facility. Initially various aspects of the experiment parameters are discussed followed by the multiple forms of data gathered through the various sampling points and online systems. Some of these data are presented for information purposes only and other data are the subject of comparison using previous information as quoted in the literature review.

4.4.2 Operating Parameters

This section presents the operating parameters for the combustion of the four coals in the CFB test facility as shown in Table 4.22.

Table 4.22 Operating Parameters

Coal type / operating parameter	Air Pressure (KPa)	Primary air volume flow (Nl/min)	Secondary air volume flow (Nl/min)	Secondary air adjustment volume flow (Nl/min)	Oxygen volume flow rate (Nl/min)	Oxygen adjustment volume flow rate (Nl/min)	Nitrogen volume flow rate (Nl/min)	Main fuel feeding rate (g/s)
RUS	99	606	362	21	5	2	4	2.2
SA I	99	589	351	21	5	2	4	3.8
SA II	99	595	354	21	5	2	4	3.8
SA Discard	99	588	349	21	5	2	4	3.8

The primary, and secondary air are similar for all the SA coals tested as shown in Table 4.22 above, with the Russian coal test having marginally higher primary air flow of 606 Nl/min compared to the other coals 588, 589 and 594 Nl/min for SA discard, SAI and SA II, respectively. The ratio of primary and secondary air are 63% and 37%, respectively. Maintaining that the airflow constant is fundamental for effective combustion.

The oxygen flow rate, both main flow and flow adjustment were maintained constant at five Nl/min and 2Nl/min, respectively. The nitrogen flow rate (4Nl/min) was also similar for all tested samples in order to maintain the fluidisation velocity constant as described in section 3.5.1. Carbon dioxide flow adjustment in zone three was maintained at 8Nl/min.

The other operating parameter that requires consideration is the fuel flow rate and the total thermal power as shown in Table 4.22.

The Russian coal-feeding rate 2.2 (g/s) was lower than the other coals tested 3.8 g/s due to its high calorific value. A small proportion of fuel was added through the second feeder with low amount ranging from 1 % for the Russian coal, SA I and 4% for both SA II and SA discard.

4.4.3 Temperature measurements

As discussed in Chapter Three, the experimental combustion test facility is equipped with thermocouples in the four zones of the CFB. Riser temperatures, both heating and cooling, will be discussed in the following sections.

4.4.3.1 Temperatures readings in the riser

Temperature readings (heating) in the riser also represent the combustion temperatures, which are discussed in more detail in Section 4.5. Riser temperature readings in the sampling points, as taken from the sampling points discussed in chapter three, are presented in tables 4.23 (heating) and 4.24 (cooling) below.

Table 4.23 Riser temperatures readings (heating)

Riser section	RT 1/1	RT 1/2	RT 1/3	RT 2	RT 3	RT 4	RT 5	RT 6	RT 7	Average	Minimum	Maximum	Standard deviation
Coal type / Thermo-element	TE 30.1 (°C)	TE 30.2 (°C)	TE 30.3 (°C)	TE 31 (°C)	TE 32 (°C)	TE 33 (°C)	TE 34 (°C)	TE 35 (°C)	TE 36 (°C)	T (°C)	T (°C)	T (°C)	
RUS	856	855	863	862	870	847	834	824	828	849	824	870	16
SA I	836	841	843	844	843	850	850	846	843	844	836	850	4
SA II	845	852	854	855	859	864	862	858	855	856	845	864	6
SA Discard	832	840	843	826	844	850	851	852	851	843	826	852	9

The temperature readings in the sampling points R1/1 to RT7 showed a similar range of values for all combusted coals i.e. 824-870°C, with the lowest temperature of 824°C recorded for the Russian coal high up in the freeboard at sample point RT 6. The highest temperatures were produced by the Russian coal in low sampling points RT 2 and 3 (862^{o}C and 869^{o}C). The second highest temperature of 864°C was found to be at RT 4 or mid-level in the freeboard for SA II. Initially, the Russian coal exhibited the highest temperatures in the lower sections of the freeboard but these were overtaken by the South African coals in the higher levels (RT4 upwards). The standard deviation for the Russian coal (16) was relatively higher than that of the South African coals, with SA I and SA II having close standard deviation of 4 and 6 respectively, compared to the SA discard of 9 as standard deviations. Within the South African samples, SA II maintained the highest levels up to RT7. These results suggest that the Russian coal ignited and burnt at a high temperature early on, whereas the South African coals only produced their higher heating values further up the freeboard, possibly due to delayed ignition. These apparent combustion profiles fit closely with the expected petrographic results discussed above, namely the rapid ignition and combustion of the low ash, highly reactive Russian coal and the more delayed ignition of the less reactive and more ash-rich SA coals. Finally, all the coals tested combusted at close average temperature in the range of 843 to 856°C.

Figure 4.1 in section 4.5 provides detailed temperature profiles vis à vis the locations of the sampling points relative to distance from the grate. The cooling temperatures recorded in the riser for the combusted coals is shown in Table 4.24 below.

Table 4. 24 Riser temperatures reading (cooling)

	Riser 1 cooling circuit Inlet Temperature	Riser bed cooling circuit flow Inlet temperature	Riser 2 cooling circuit	Riser 3 cooling circuit	Riser 4 cooling circuit	Cooling air temperature
Coal type / Thermo-element	TE 50.1 (°C)	TE 50.2 (°C)	TE 51 (°C)	TE 52 (°C)	TE 53 (°C)	TE 54 (°C)

RUS	23	23	296	120	465	167
SA I	22	22	271	94	446	169
SA II	23	24	282	102	464	170
SA Discard	224	24	270	93	454	186

The cooling temperatures in the outer jackets of the riser recorded in the different sections follow a normal pattern for all the coals on each of the reading points, with some variations in point TE 51, TE 52 and TE 53. The variation in the cooling temperature on these points is split into SA II and Russian coal, while SA I and SA discard fall in the same group. It can be observed that the two sets share the same temperatures within each one of them. That could be due to the respective calorific values ranges.

4.4.3.2 Temperatures readings in the cyclones

The temperature readings in the primary and secondary cyclones at the different measuring points are presented in Table 4.25 below.

Table 4. 25 Cyclone temperature readings

	Primary cyclone	Secondary cyclone	Dust temperature after the 2nd cyclone
Coal type / Thermo-element	TE 37 (°C)	TE 38 (°C)	TE 67 (°C)
RUS	831	788	31
SA I	843	789	28
SA II	854	765	30
SA Discard	850	796	44

The cooling effect in the cyclones has an impact on the temperature readings of the coal mass and air passing through them. The results above indicate that temperatures decrease from the combustion chamber into the two cyclones as determined at points TE 37 to TE 38.

4.4.3.3 Circulating flue gas temperature

The circulating gas temperature readings is shown in Table 4.26.

Table 4.26 Circulating flue gas temperature

	Cooling unit	Cooling	additional cooling	Before filter	After filter
Coal type / Thermo-element	TE 39 (°C)	TE 40 (°C)	TE 41 (°C)	TE 42 (°C)	TE 43 (°C)
RUS	711	256	169	159	134
SA I	719	268	171	153	131
SA II	722	276	180	163	136
SA Discard	721	296	173	158	135

The temperatures readings of the circulating flue gas are within close range on each reading point for all the combusted coals with the major difference in point TE 40, where the cooling ranges from 256°C for the Russian coal to 296°C for the SA discard passing through all other reading points TE 41, 42 and 43, respectively.

4.4.3.4 Circulating material temperature

The circulation material temperature is presented in Table 4.27 below

Table 4. 27 Circulation material temperature

	Circulating material fall temperature	Circulating material before cooling with water	Circulating material	Mid-temperature of circulation material	Circulation heating area	The temperature of the solid matter before the bed
	TE 60 (°C)	TE 61 (°C)	TE 62.1 (°C)	TE 62.2 (°C)	TE 62.3 (°C)	TE 65 (°C)
RUS	755	723	617	534	519	633
SA I	770	788	799	800	810	784
SA II	779	811	811	8133	825	801
SA Discard	779	824	835	837	839	818

One of the advantages of CFB is the circulation of material in the bed for optimum combustion through an increase in the contact of the particles, which are subject to circulation over and over again. Monitoring of the temperatures for the circulation material is fundamental practice in order to establish the combustion efficiency.

The temperature readings for the coals under investigation remained similar for SA coals and differed for the Russian coal in the different sections. The Russian coal **decreased** from 755°C to 533°C, whilst the South African coals **increased** from 769/779 °C to 799°C/836°C. The highest increase in temperatures was found in the SA Discard (839°C) and SA II (824°C). The opposing trends of increase and decrease, and the 200°C difference in temperature, are of significance, and can be related once more to the combustibility of the different coals under review and their petrographic type and grade. The Russian coals appears to provide significant heat early on and then reduces in temperature, whereas the South Africa coal exhibited the opposite trend, namely, delayed ignition, leading to higher temperatures in the upper parts and circulating regions of the CFBC.

With the exception of the SA Discard sample, the dust temperature readings for the other three coals were similar. The SA discard exhibited a 14 to 16°C higher temperature reading. This would be due to its very high inertinite content (some known to burn at almost 1800 °C) and the high ash content, which would retain the heat.

4.4.4 Ash deposit temperature

The temperatures taken in the ash deposits of each coal are shown in Table 4.28 below. The sampling points were between the two cyclones and after the second cyclone as explained in section 3.5.4.

Table 4.28 Ash deposit temperature

	Temperature of mass deposit	Temperature of mass deposit	Temperature of mass deposit	Temperature of mass deposit (back)
	TE 90.1 (°C)	TE 90.2 (°C)	TE 91.1 (°C)	TE 91.2 (°C)
RUS	494	456	496	455
SA I	499	450	494	444
SA II	497	448	495	446
SA Discard	500	468	497	497

The deposit temperatures readings for all coals tested at the specific sampling points are more or less similar, which shows consistency in the tests conducted to keep the temperature in the sampling points close to 500°C, as detailed in section 3.5.4. The consistent temperatures recorded show that all the coals tested impacted the probes in a similar way therefore the deposit has a similar impact on heat transfer.

4.4.5 Pressure and pressure drop

The pressure reading in the different sections and the pressure differential (pressure drop) are shown in the Tables 4.29 and 4.30.

Table 4. 29 Pressure drop in the riser

	Primary gas pressure below the grate	Riser Sample port 0 - 1 differential pressure	Riser Sample port 1 /1-2 pressure differential	Riser Sample port 1 /2-2 pressure differential	riser Sample port 1/3-2 pressure difference	Riser Sample port 2-3 pressure differential	Riser Sample port 3-4 pressure differential	Riser Sample port 4-5 pressure differential	Riser Sample port 5-6 pressure differential	Riser Sample port 6-7 pressure differential
Coal type / Pressure drop	P 21 (Pa)	PD 30 (Pa)	PD 31 (Pa)	PD 32 (Pa)	PD 33 (Pa)	PD 34 (Pa)	PD 35 (Pa)	PD 36 (Pa)	PD 37 (Pa)	PD 38 (Pa)
RUS	2770	1219	1337	1216	53	20	3	3	4.	8
SA I	3159	1075	1267	819	-4	55	83	27	78	47
SA II	3497	1880	1570	1046	-6	1	-3.	45	106	60
SA Discard	3473	1901	1850	1399	-5	1	-1	73	81	14

The pressure drop values given in Table 4.29 above show two sets of values for the pressure drop in the riser. It is very high in reading points PD 30 to PD 32, and very low in points PD 33 to PD 38. The first section falls under zone one of the testing equipment, which is often referred to as dense bed, and the other reading points are found in the other zones of the testing equipment.

The pressure drop in the riser in the dense bed appears to be adequate to prevent the back shifting of particles or defluidisation as highlighted by Basu[34]. Some non-uniform airflow distribution at the level of the grid may actually be advantageous in enhancing lateral solid distribution through the creation of a solid-circulation vortex.

SA discard exhibited higher pressure drop 1901 Pa compared to SA I, SA II and Russian coal with pressure drop of 1267, 1879 and 1337 Pa, respectively. These differences are likely to be due to the particle densities and morphologies, where SA discard is close to rock structure as per proximate and ultimate analysis.

The riser height is 8 m, which is relatively high for a pilot plant. Based upon the author's personal observations, this appears to allow adequate time to the solids to be laterally mixed over the riser height. These observations are in agreement with the literature concerning the potential of sinter formation due to non-uniform fluidisation, which is said to be relatively low in a CFB, because the high sheer force in the high-velocity CFB riser tends to break up any sintered mass, if formed [34].

The riser pressure drop varies from low value 819 Pa for SA I to 1900 Pa for SA discard in Table 4.29 following a similar trend studied by Guo et al. [109], where they recorded a pressure drop range from 352 Pa to 2878 Pa. No obvious changes can be found in the flow rate profiles.

The pressure drop range in our case (819-1900 Pa) is lower than the ones studied by Guo et al. (352-2878 Pa), but very close to those reported by Yates [110], who gave a detailed report quoting findings by other authors on the effect of temperature and pressure on gas-solid fluidisation.

The current engineering practice for air-distributor plates in CFB boilers calls for the use of a high-pressure drop grid to provide uniform fluidisation. Because of this, the fan power consumption of a typical CFB boiler is about 2.3% compared to only 0.75% for a PC boiler. This represents a minor energy differential between these two coal-fired processes [28].

Table 4.30 Additional Recorded pressure readings (Furnace, cyclones, filter and circulating material return pipe)

	Furnace pressure	Primary cyclone differential pressure	Secondary cyclone differential pressure	The filter differential pressure	Circulation material return pipe pressure differential
Coal type / Pressure	P 39 (Pa)	PD 40 (Pa)	PD 41 (Pa)	PD 42 (Pa)	PD 60 (Pa)
RUS	1	150	200	121	49
SA I	0	255	210	196	414
SA II	1	265	222	263	179
SA Discard	0	1358	275	134	155

Table 4.30 shows that SA discard exhibited higher differential pressure than the other coals in both cyclones (primary and secondary) whilst the Russian coal maintained a lower differential pressure in both cyclones in addition the differential pressure reading point at the filter and return pipe for material circulation.

4.5 Combustion properties and parameters affecting efficiency

Combustion efficiency is the ability of a combustor to burn carbon and it is calculated by taking into consideration heat losses in stack and moisture losses with the use either of the higher heating value (HHV) or lower heating value (LHV). For circulating fluidised bed combustion (CFBC), efficiency values are generally higher (up to >99%) relative to bubbling fluidised bed combustors BFBC. The reasons for better combustion efficiency in CFBC boilers would appear to lie in the better mixing of bed materials. The smaller size of fuel particles, the tall furnace and large internal solid recirculation design of circulating fluidised bed (CFB) plant and to a

great or lesser extent on the physical and chemical characteristics of the fuel being used as well as on the operating condition in the furnace. Factors affecting the combustion efficiency can therefore be classified into three categories:

- Fuel characteristics
- Operational parameters
- Design parameters

These factors will be expanded in sections 4.5.2 and 4.5.3

4.5.1 Combustion temperature profiles of the four coals under review

Figure 4.1 below presents the temperature profiles in the CFBC test facility for the four coals under review. The distance from the grate is measured in metres.

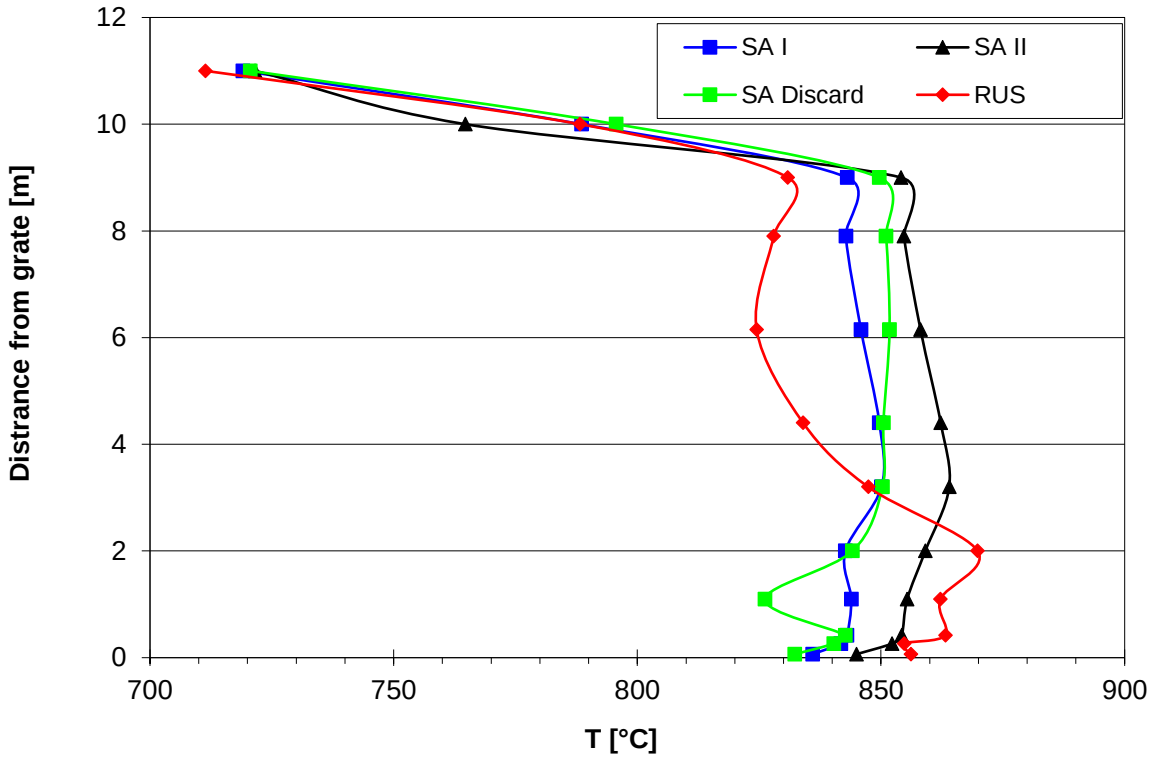

Figure 4. 1 Temperature profiles

The combustion temperatures of all coals tested follow a parallel pathway, especially for the SA coals where the maximum temperature is in the region of 830-870°C, which is in

accordance with the operating temperature of CFB as reported in the literature. The temperature in CFB is purposely controlled to these ranges of temperatures to optimise sulphur capture, and has to do with the design of the heat transfer surfaces. The combustion temperature is within a similar range for all the coals in the 0-8 m region distance from the grate, which constitutes the height of the riser of the testing rig. As discussed in section 4.4.2, the behaviour of the different coals under investigation as shown in Figure 4.1 above exhibited quick ignition in the case of the Russian coal, followed by the two SA coals, SA I and SA II. The temperature profile of the SA discard coal, on the other hand, initially showed an initial drop in temperature with slow ignition. This behaviour reflects the petrographic composition of the coals, with the sample possessing the highest **vitrite** content (the Russian coal) exhibiting the quickest ignition with rapid increase in temperature. The sample with the highest **minerite** (rock) content and the lowest vitrite content, the discard coal, initially drops in temperature, followed by a rapid rise in temperature as the delayed ignition takes place. Thereafter, the temperature profiles of all three SA coals including the discard then follow a parallel path combusting in a similar temperature range of 840-860°C (with SA II the higher temperature of the three), whilst the Russian coal completed its combustion profile in significantly lower temperature ranges, 830-840°C.

In addition to petrographic composition, the quick ignition of the Russian coal also reflects various other parameters such as this sample's high volatile matter content (%) compared to the SA II coal and discard of 36.3% and 17.18%, respectively, or by the volatile/fixed carbon ratio of 0.96 and 1.12 for the Russian coal and SA discard, respectively. Coal devolatilisation and ignition is a fundamental step in the coal combustion.

The quick ignition of the Russian coal could be explained by various parameters like its high volatiles contents of 36.3% compared to the SA II and SA discard of 28.1% and 17.18% respectively. Or by the volatile / fixed carbon ratio of 0.96 and 1.12 for the Russian coal and SA discard, respectively. Behaviour in agreement with petrographic analysis is shown in section 4.2.3.4. Coal devolatilisation and ignition is a fundamental step in the coal combustion followed by the coal particles fracturing which depends on the coal type. Many studies are available in the literature about coal devolatilisation in the fluidised bed combustion, and little has been reported on the ignition of volatiles and coal/char. The combustion of volatiles in the

fluidised bed contributes to the ignition of the coal when it occurs in zone one between 0 to 2 m distance from the grate. The combustion often continues in the freeboard section of the fluidised bed. There is a clear distinction between SA discard and the Russian coal suggests that the volatiles combustion happened in this zone, and therefore, a difference in the ignition caused these observations.

Prins et al. [111] reported that the volatile burn out time occur by oxidising conditions and depends of on the fluidised bed temperature, fluidising velocity and the coal particle size and the type of coal. The latter parameter is applicable to this study and all the other operating parameters are more similar for all the coals tested. This parameter is in agreement with the results of Riaza et al. [112], who studied the ignition temperature of different coals in oxy-fuel conditions and concluded that the temperatures of the bituminous coal particles were lower than those of the anthracitic coals, similar to SA coal discard and Russian coal, respectively.

This difference in ignition and combustion temperature in the 0-2 m from the grate is happening in zone one of the testing facility, as shown in sections 3.4 and 3.5. In this zone primary air is introduced where the flow rate of the air for the Russian coal test was marginally higher as shown in Table 4.27 of (606 Versus 588 Nl/min), in addition to the secondary air, which was also marginally higher (362 versus 349 Nl/min). One other factor which could have an impact on these combustion temperature differences is the huge gap between the pressure drop recorded in this zone, as shown in Table 4.28. The Russian coal had a pressure drop of 1219 Pa compared to the SA discard coal with a pressure drop of 1901 Pa. The differences for all the parameters stated above have an impact on the rest of the findings in the sections below.

The differences in the combustion temperatures of the coals tested as shown in the Figure 4.1 above, coupled with the apparent distinction in the ignition phase. In addition to the amount of CO formed as detailed in section 4.6.4, it is proven that a quick ignition of good quality coal does not equate to better performance or higher combustion efficiency of the Russian coal in CFB. This result is the complete opposite for the SA coal discard, with relatively lower temperature in Zone One, where it was found that lower ignition yielded a relatively high combustion efficiency, with lower CO formed, hence there can be seen to be a good performance of low grade coal in CFB.

4.5.2 Combustion efficiency

This section presents the results of the combustion efficiency of the coals as fired in the CFB. Figures 4.2 and 4.3 represent the combustion efficiencies obtained. i.e. All four coals exhibit 98 to 99% combustion efficiency. The scale for the y-axis is expanded to differentiate between all the coals tested.

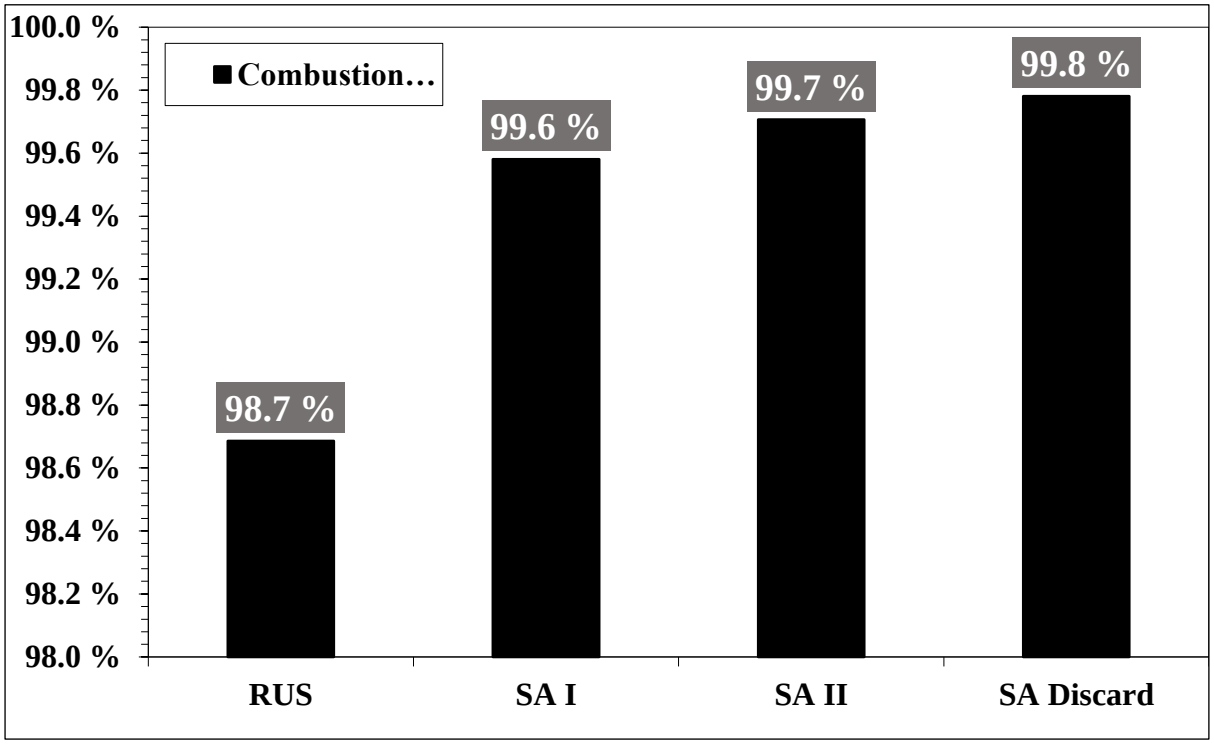

Figure 4. 2 Combustion efficiency

The long residence time in the furnace resulting from collection/recirculation of solid particulate via the cyclone, plus the vigorous solids/gas contact in the furnace caused by the fluidisation airflow, appear to have resulted in high combustion efficiencies, even with normally difficult to burn fuels. The efficiency reached of 98-99% carbon burnout has been achieved. The very high internal and external re-circulating rates of solids result in relatively uniform temperatures throughout the combustor with the average temperatures taken from table 4.22 of 848°C, 843°C, 856°C and 843°C for Russian, SA I, SA II and SA discard, respectively.

It may be noted that from Figure 4.2 that the combustion efficiency of the Russian coal is marginally lower than all the SA coals tested. The Russian coal was regarded as being of better quality than all the SA coals tested, which represents a contradiction in the combustion

efficiency expectation. Although this 1% difference may fall within the bounds of analytical error, it has an impact on the results of the section that follows.

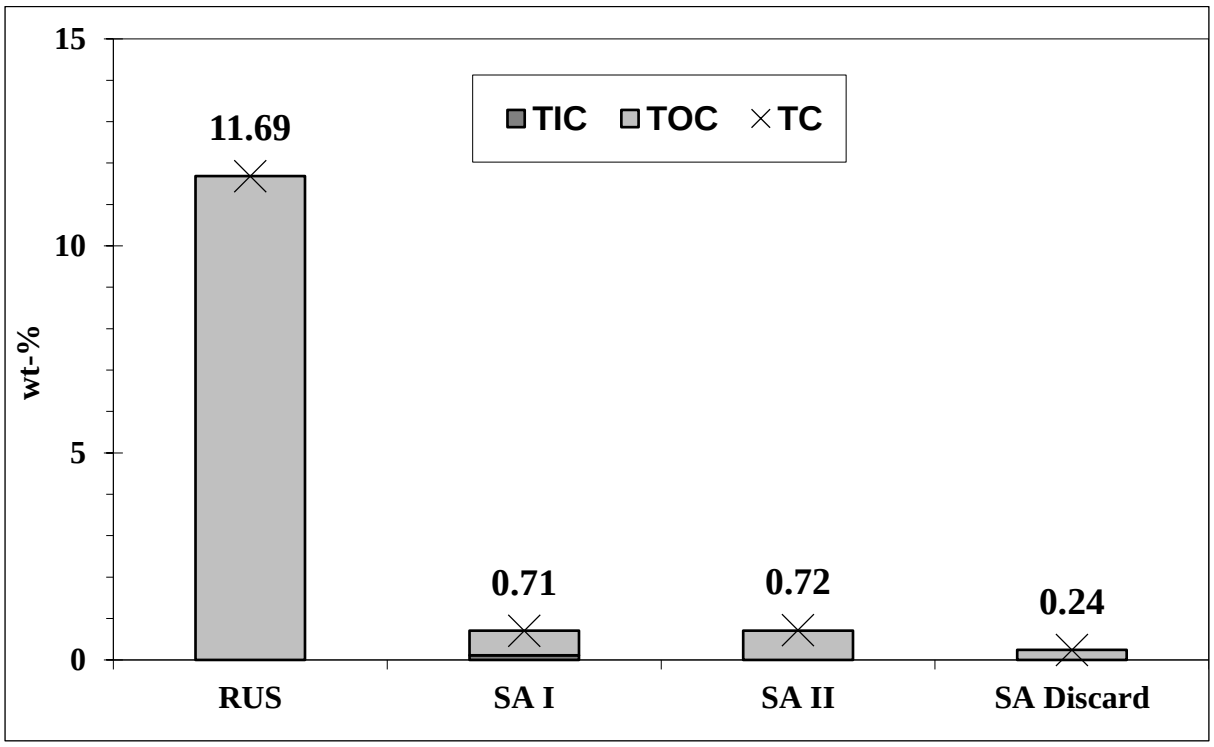

Figure 4. 3 Ratios of unburnt organic and inorganic carbon in the discharge

The incombustible ratios of organic and inorganic carbon in the discharge followed the same pattern as the combustion efficiency in Figure 4.3, where Russian coal manifested the highest incombustible ratio for the total organic carbon (TOC). This observation could be due to the same phenomena as highlighted above, or due to other elements content in the coal itself. One of the major element is the organic sulphur content in the coals as indicated in tables 4.10, 4.13. 4.16 and 4.19, respectively. The organic sulphur content as per CHEMSCAN and CQA of 81.41 for the Russian coal was far higher when compared to the SA discard of 13.86.

The link between the incombustible ratios of organic and inorganic carbon with the organic sulphur content is in agreement with the study conducted by Watanabe et al. [113], where the authors studied the ratio of combustible and incombustible sulphur and chlorine in different materials of municipal solid waste.

4.5.2.1 Impact of coals mineralogy

As per results in section 4.1.4, where a detailed mineralogical study was given for the four coals fired in CFB, all parameters highlighted above played a major role in both the combustion efficiency and incombustible organic ratios as shown in Figure 4.2 and 4.3, respectively.

The ratio of the unburnt organic carbon of Russian coal was seen as an unpredicted result in light of the coal quality of low-ash content. This is an observation, which leads us to seek an explanation in other parameters.

4.5.2.2 Impact of coals macerals

The petrographic analysis of macerals is used worldwide to predict properties of carbonisation processes. The influence of macerals on combustion processes was reported as early as 1968 [114, 115]. Unburnt carbon in ash was found to be largely the result of incompletely burnt inertinite materials on a chain grade and on PC units.

The experimental results indicate that the three SA coals studied did not display different behaviour during combustion unlike the Russian coal. This was attributed to differences in maceral composition and rank as measured by vitrinite reflectance. Vitrinite-rich and liptinite-rich coals.

Despite high vitrinite (91%) and low inertinite content (11%), the Russian coal combustion efficiency was marginally lower than of SA coal discard, which has a much lower vitrinite content of 29% and a higher inertinite content of 65 percent. This is in agreement with the research done by a Canadian study using a pilot plant boiler, where the author found that unburnt carbon and combustion efficiency were inversely related to the inertinite content of the coal. This study was reported Sanyal [115, 116], in which various studies were reported related to maceral content impact on combustion efficiency, ash formation and weight loss by various authors on different coals, including South African coal. This phenomena is an agreement with the observation made by Falcon [50], who discussed some particular coals from Southern Hemisphere (Gondwana coals), noting that certain group within the inertinite are semi-reactive. These constituents can make up to 60% of the inertinite groups and they may represent a very important part of the organic matter. She further highlight the parameters influencing the combustion efficiency in the form of organic and inorganic composition of the coal, its rank or degree of maturity, porosity, exposed surface area, moisture content, degree of weathering or

heat-effect, size of particle, state of oxidation, and characteristic initial or ignition temperature, and peak combustion temperature. With regard to the latter, the peak temperature achieved for the Russian coal is partially lower, relative to the other coals tested.

In term of reference purposes only despite technology differences, Oboirien [117] concluded in his study on the gasification of some SA coals, noting that the loss of coal reactivity was obtained from vitrinite-rich coals due to a higher degree of structural transformation of carbon in the coal. Inertinite-rich coals experienced a lower reactivity and lower degree of structural transformation, even with longer residence time. The structural transformation of the macerals is due to realignment of the carbon molecules leading to substantial swelling (enhanced plasticity) in some reactive macerals.

Another factor for the difference in the combustion efficiency of the coals tested could be due to the existence of high aromaticity and strong cross linkages, which exist within the inertinite macerals.

4.5.3 Fuel Ash content versus circulation rate

The circulation rate is the return of unburnt particles by gravity into the bed after the cyclone where flue gas and particles are separated. This is expressed in kg per hour. The details of the circulation rate calculation is given in Appendix E.

Figure 4.4 represents Fuel ash content versus particles circulation rate.

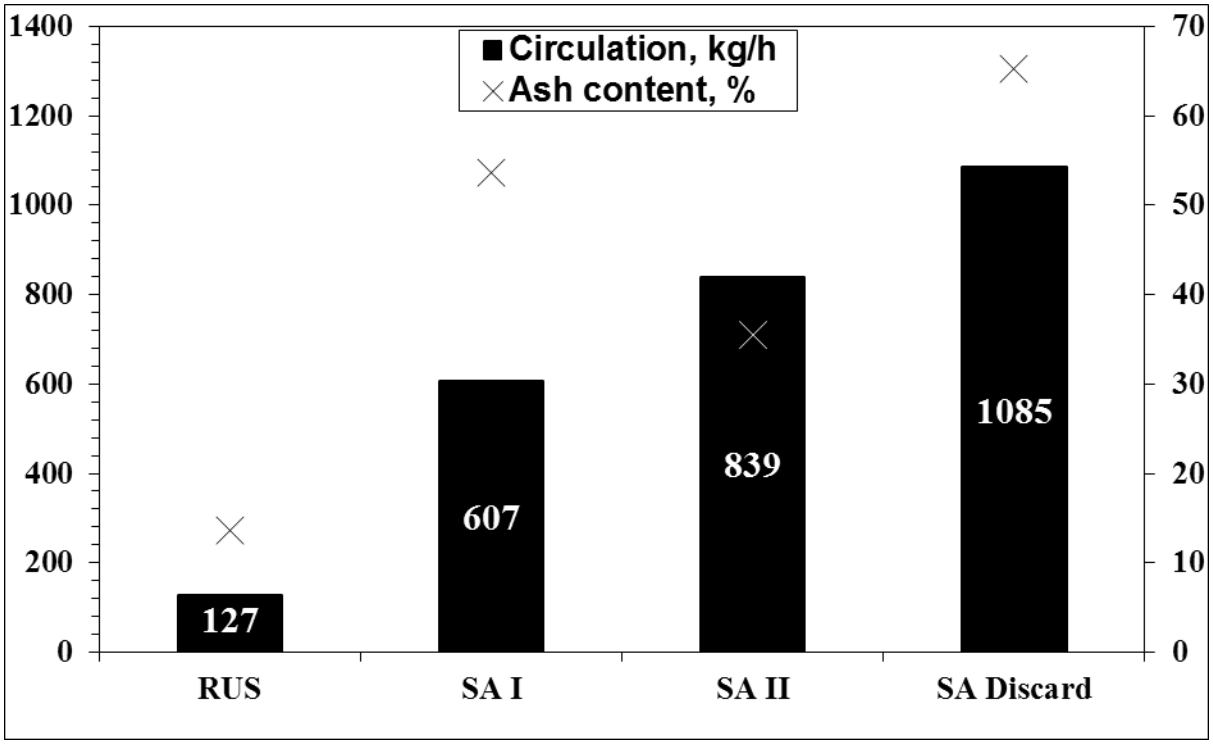

Figure 4. 4 Fuel ash content versus particles circulation rate

The circulation rate is very high for all SA coals including the SA discard compared to the Russian coal. The high circulation rate in the SA coals has the advantage of extending the particles residence time especially the unburnt ones. The low circulation rate of the Russian coal means that Russian coal particles burnt quickly, as per both Figure 4.1 and Figure 4.4. Quick ignition and low circulation played a part on the combustion efficiency of the Russian coal, as detailed in sections above.

As highlighted in Appendix F, combustion efficiency is linked to the ratio of the percentage from fuel carbon to fly ash, which is detailed in the following section dealing with ash formation and its composition (bottom ash and fly ash).

It is observed from the data collected, as shown in Figure 4.4, that the circulation rate is proportional to the ash content and unburnt carbon particles in the coals fed back into the boiler, with the exception for SA II. The Russian coal with the lowest ash content has the lowest circulation rate, and marginally lowest combustion efficiency, as explained in the previous sections.

4.5.4 Ash impact

4.5.4.1 Ash formation

The ash and spent sorbents released in the furnace were extracted partially from the bed and partially from the flue gas. The split of coal ash depends on the nature of ashes, their attrition behaviour in the bed, and the cyclone performance. Coal ash could reside in the coal matrix in two forms, extraneous or intrinsic.

The intrinsic ash is extremely fine and is dispersed throughout the coal matrix. The extraneous ash includes the rock or discrete ash particles embedded in the coal structure. When coal is consumed or fragments, the discrete ash particles are exposed and dislodged from the burning face of the char. The intrinsic ash, being fine, is progressively released as the coal burns and usually escapes the furnace to be collected in the bag-house. The extraneous ash, being large, generally concentrates near the bottom of the furnace and is extracted as bed drain.

The split is also governed by the performance of the cyclone or any other gas-solid separation device used.

The general rule calls for a 20 to 80% split of the boiler ash, i.e. 20% to coarse ash (bed drain) and 80% fly ash of the solid waste pass through the bed drain. Boilers firing high-ash coal without WIT sorbent injection have higher bed drain. For lignite and subbituminous coals, the amount of ash retained in the bed as bottom ash is substantially smaller. About 30 to 80% passes through the bag-house [34].

The following section deals with ash formation in the CFB, with parameters ranging from fuel carbon to fly ash, ash formation ratios between fly ash and bottom ash in addition of the circulation rates as a function of ash content. Ash formation is an important parameter in any combustion process. This study focused on the section highlighted above, excluding ash characterisation, which does not fall under the scope of this study.

Figure 4.5, 4.6 and 4.7 represent ash formation ratio, ash forms distribution, ash formation mechanism of bituminous coal combustion in CFB, respectively.

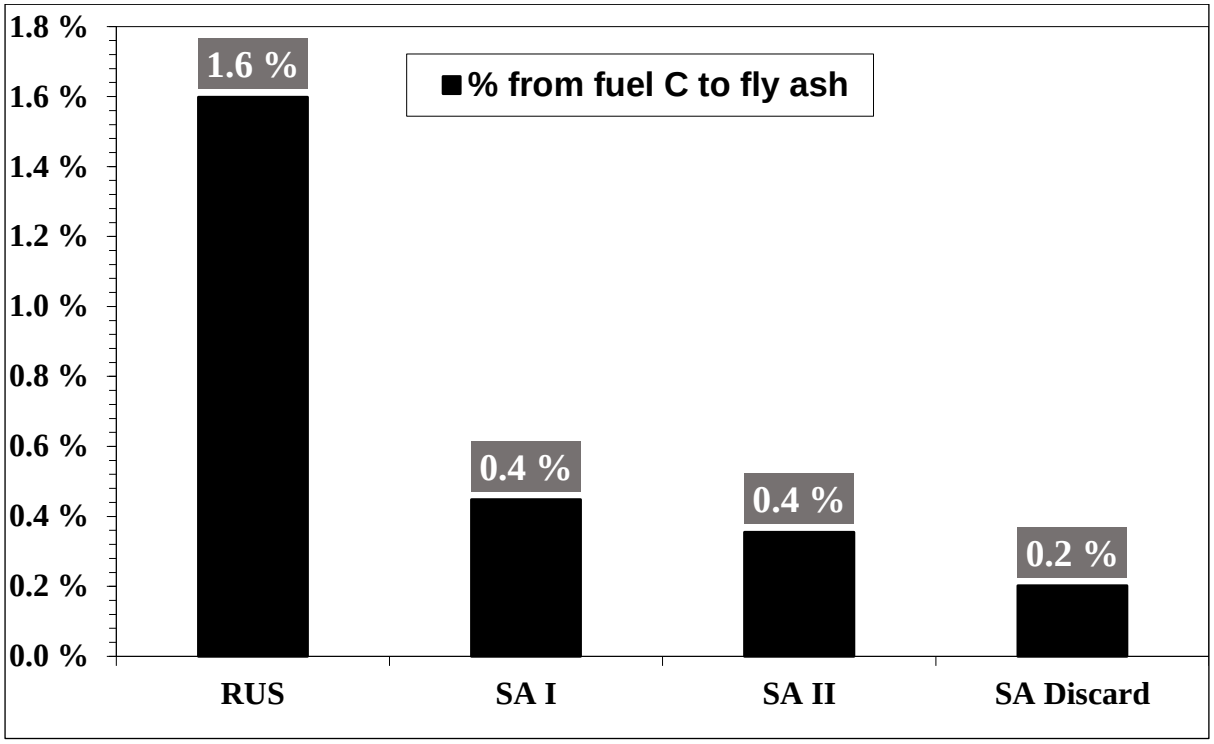

Figure 4.5 Ash formation ratios

The ratios from fuel carbon to fly ash is the proportion of carbon in fly ash over total carbon content in the fed fuel as detailed in Appendix F. The ratios from fuel carbon to fly ash of the SA coals as shown in Figure 4.5. The values fall in narrow low ranges (0.2-0.4 %), unlike the Russian coal, which reached 1.6 percent. These values are in agreement with the difference obtained in the combustion efficiency section above.

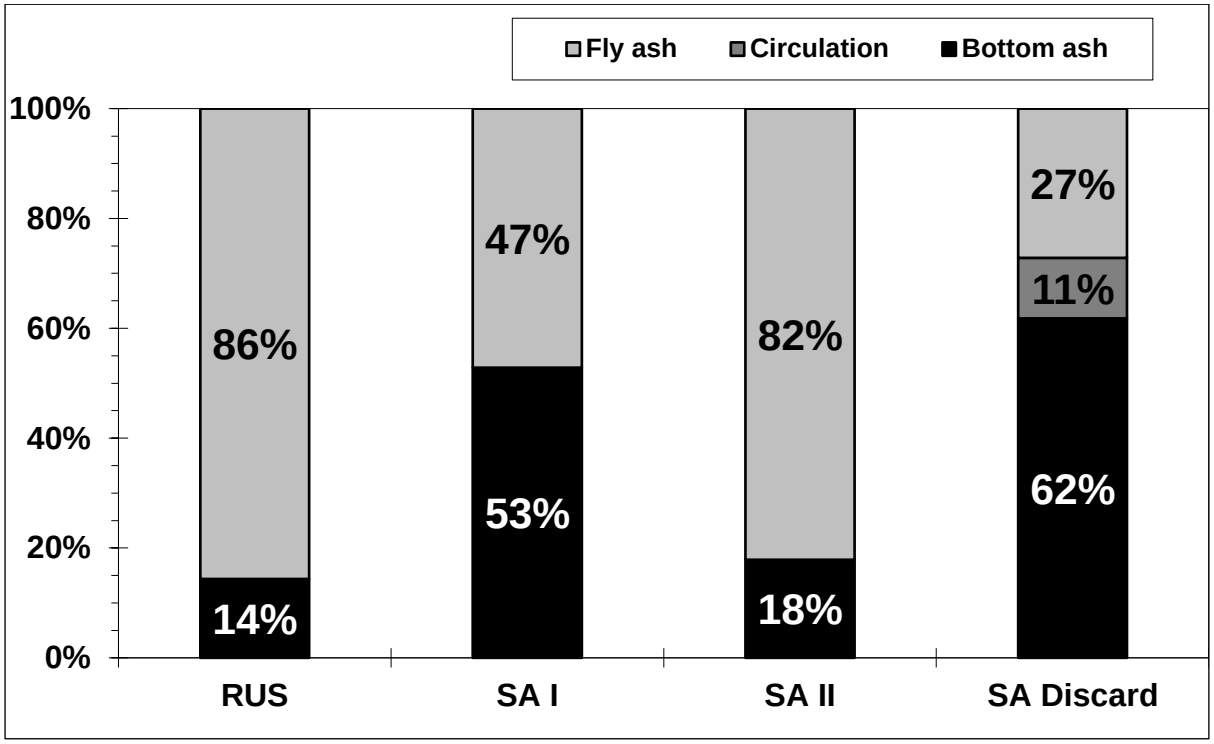

Figure 4. 6 Ash forms distribution

The ash split between fly ash and bottom ash as shown in Figure 4.6 presented a different behaviour of the four coals tested. SA coal II and the Russian coal have similar ratios between them in both fly ash and bottom ash, with high proportions of fly ash. Despite the two coals being different in proximate analyses, both are characterised by finely distributed clay contents and low proportions of high ash and minerites (rock) particles. This results in low proportions of bottom ash for both SA coal II and Russian coal. Such ash contents are in agreement with the literature, as detailed by Basu [34]. The proportion of bottom ash is very high for both SA I and SA discard. This is due to the high ash and minerite (rock) contents of those coals, i.e. 54 and 65 % ash contents and 68% and 95% carbominerite and minerite combined, respectively. Redemann et al. [118] has also attributed the ash distribution in fluidised bed technology not only to the ash formation characteristics of the fuel, but also to other solids fed into the combustion chamber, e.g. additional inert material, recycled ash or sorbent material, which can impact significantly, depending on sorbents types. For no agglomerating fuels, the mineral inclusions contribute significantly to the bottom ash [34]. All such materials can be retained when recycled through the classification and comminution processes occurring in the CFB combustion system.

The mechanism of ash formation in CFB as detailed by T Lind[105], in Figure 4.7 below which provides the concepts of formation at the various stages.

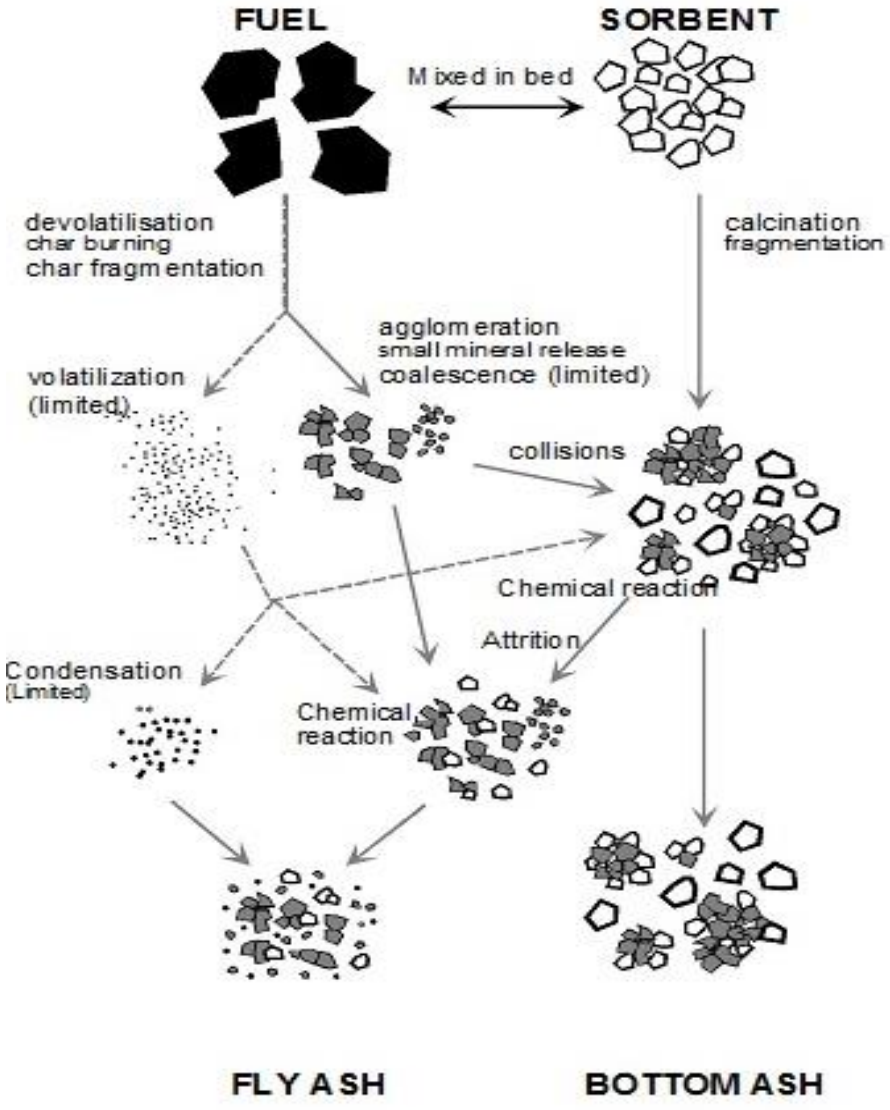

Figure 4. 7 Ash formation mechanism of bituminous coal combustion in CFB [105]

Lind [105] attributed the bottom ash formation mechanism to the agglomeration of the coal minerals, as well as some unfragmented sorbent. The fly ash have two particle modes, coarse and fine fly ash particles. The coarse fly ash was formed by fragmentation of sorbent in the bed and residual ash particles. His research proved that a major fraction of the sorbent, approximately 80 %, ended up in the fly ash, while only 20% was removed from the furnace in the bottom ash, these observations can change depending on sorbent properties, e.g. limestone hardness and friability. Residual ash particles were formed inside and on the surface

of the char particles by agglomeration of a few mineral particles originally contained in the coal. In the South African coals, the very presence of particles of rock (minerite) in the feed would lead to the natural accumulation of such particles in the coarse ash fraction. Such material is not often encountered in coals of Europe and the USA.

4.5.4.2 Effect of volatiles content on Ash formation

The impact of the volatile content in the fuel on the ash formation is shown in Figure 4.8 below.

The dry ash free or the volatiles ash free as often expressed is calculated as follows:

$$Vashf = Vol\ content/(100 - Ash\ content) \quad 4.1$$

Vashf: volatile ash free

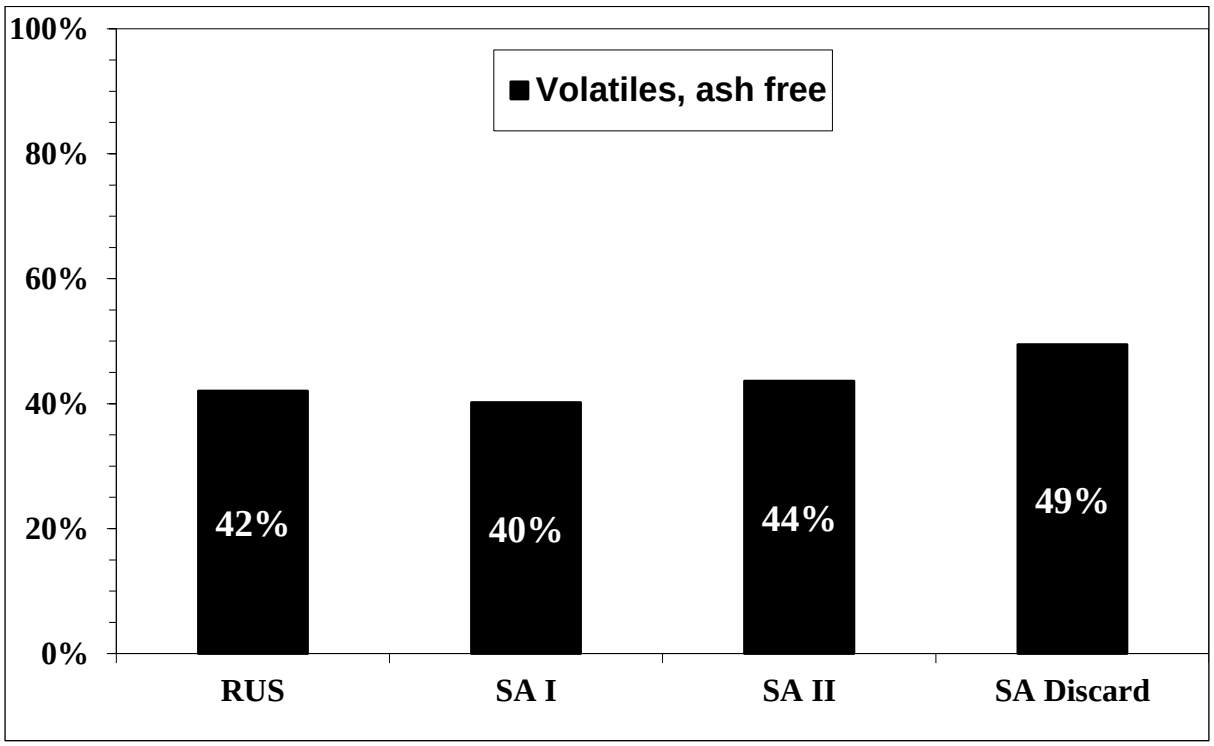

Figure 4. 8 Impact volatiles on ash formation

As explained by Lind [76] the ash formation goes through few stages and the devolatisation stage is the first stage during combustion, followed by char fragmentation. The volatile content

in the initial fuel has an impact on the combustion efficiency, and lesser influence on the ash formation mechanism as shown in Figure 4.8, where the volatiles, ash free for the coals tested, were in close range, which is in agreement with Lind's [105] findings on ash formation.

4.6 Emission Impact

4.6.1 Background

The major air pollutants released from the combustion of fossil fuels and biomass are SOx, NOx, and particulate matter, including emissions of particulate matter with aerodynamic diameters less than 10μm, i.e. PM10. Other substances, such as heavy metals, HF, HCl, unburned hydrocarbons, non-methane volatile organic compounds (NMVOCs) and dioxins are emitted in smaller quantities. In addition to NOx, nitrous oxide N_2O features prominently in the combustion of fossil fuel in CFB due to the low temperatures in the region of 800-900 °C.

The emission of SOx, NOx, N_2O, particulate matter and greenhouse gases (CO, CO_2) has been the subject of many studies providing details on the formation, release, ways of minimisation, capture and sequestration in the case of CO_2 in addition to various modelling tools and software used. Such models have normally been applied to coal-fired PC combustion. CFB however, operates at different temperature regimes and is used to combust not only coal but also biomass, bark, wastes, and other materials. Modelling in these cases is extremely complex.

This section deals with emission impact and greenhouse gas formation. An overview of all emission trends is presented in Appendix A. The main results recorded on a stable period are used in the sections below. The detailed study of each selected component as related to the results obtained in the CFFB tests in this investigation. These results are compared to previous work done on coal and other materials during combustion in CFBC boilers.

4.6.2 NOx and N_2O

CFB combustion is known for its environmental benefits due to its inherently low NOx emissions without selective catalytic reduction, because of the relatively low combustion temperature and inherent dynamic characteristics. Such factors include higher bed height, lower fluidising velocity and higher carbon load in the bed, all of which enhance the NOx reduction in the dense bed compared to the conditions prevailing in an atmospheric PC. These

factors have a different effect on the emission of N_2O, which is higher in CFB due to the low combustion temperature. Emissions of N_2O from fluidised beds are much higher than from other combustion systems.

The recorded emission of NOx (NO & NO_2) and N_2O in the current series of CFB tests is illustrated in Figure 4.9 below:

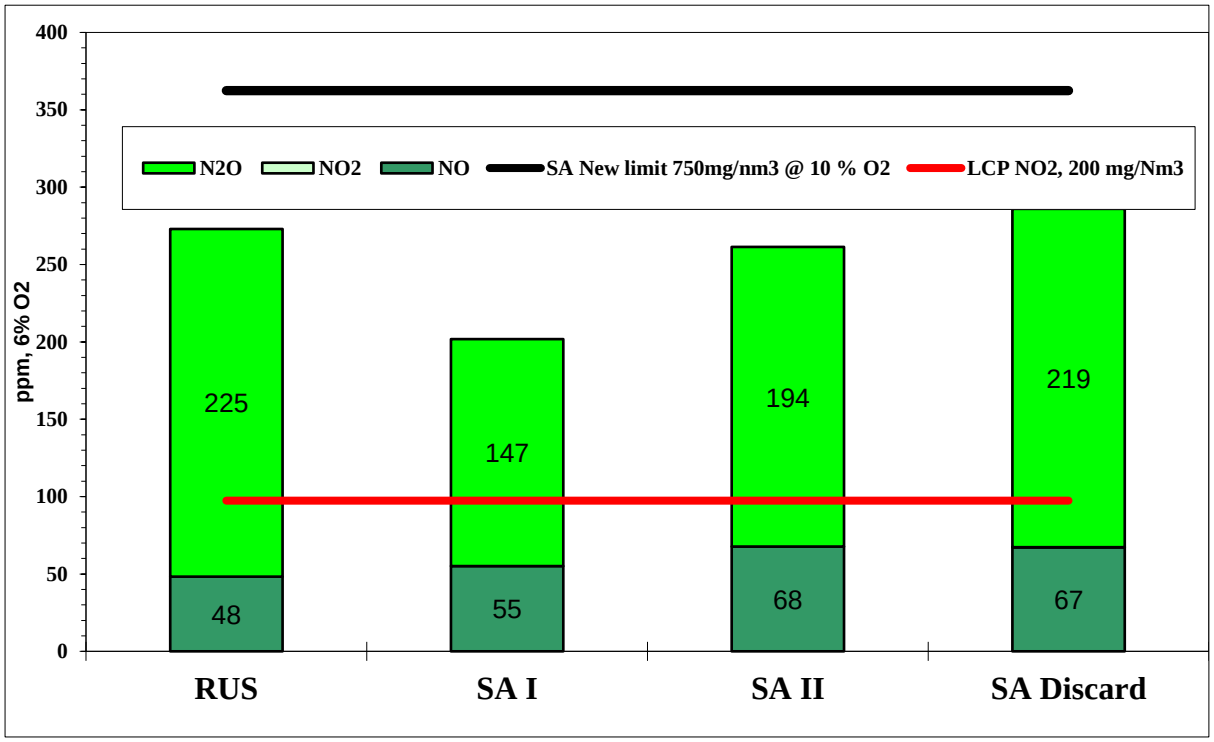

Figure 4. 9 NOx and N2O Emission

The values of NOx (48-68 ppm) and N_2O (147-225 ppm) emission of the coals tested are in agreement with data obtained by various authors especially Svoboda [79], Diego et al. [39], and Zhao et al. [119]. These authors studied the effect of various parameters on the emission of NOx and N_2O, attributing parameters such as temperature, circulation rate pressure drop, and distance from the wall to the emission of NOx and N_2O.

According to the new European standards, the emission values of NOx achieved in the current tests are below the limit of the pilot plant range, which is 300 ppm for plant with generating capacity below 100 MWth. In the same context, the new limit for large combustion plant (LCP), The European Large Combustion Plant directives is in the range of 200 mg/Nm^3. In Figure 4.13 above, this value limit is shown with a red line. The limit is in the range of 97 ppm

after conversion. The conversion procedure and all other calculations are shown in Appendix F. A comparison of the emissions recorded for NOx, N_2O and SOx against both the international and the SA standard is given in section 4.4.7. The emission of NO and NO_2 is recorded separately but, for discussion purposes, the two gases are referred collectively as NOx, as is often reported in the literature. In the current test, the emission of NO_2 is negligible compared to NO. Factors affecting the formation of NOx and N_2O in addition to the mechanism are detailed in the following sections.

4.6.2.1 Background of NOx, N_2O formation

The emissions of NOx and N_2O from CFB are highly dependent on a number of operating conditions. Figure 4.10 shows a simplified scheme for the conversion of fuel-nitrogen in CFB.

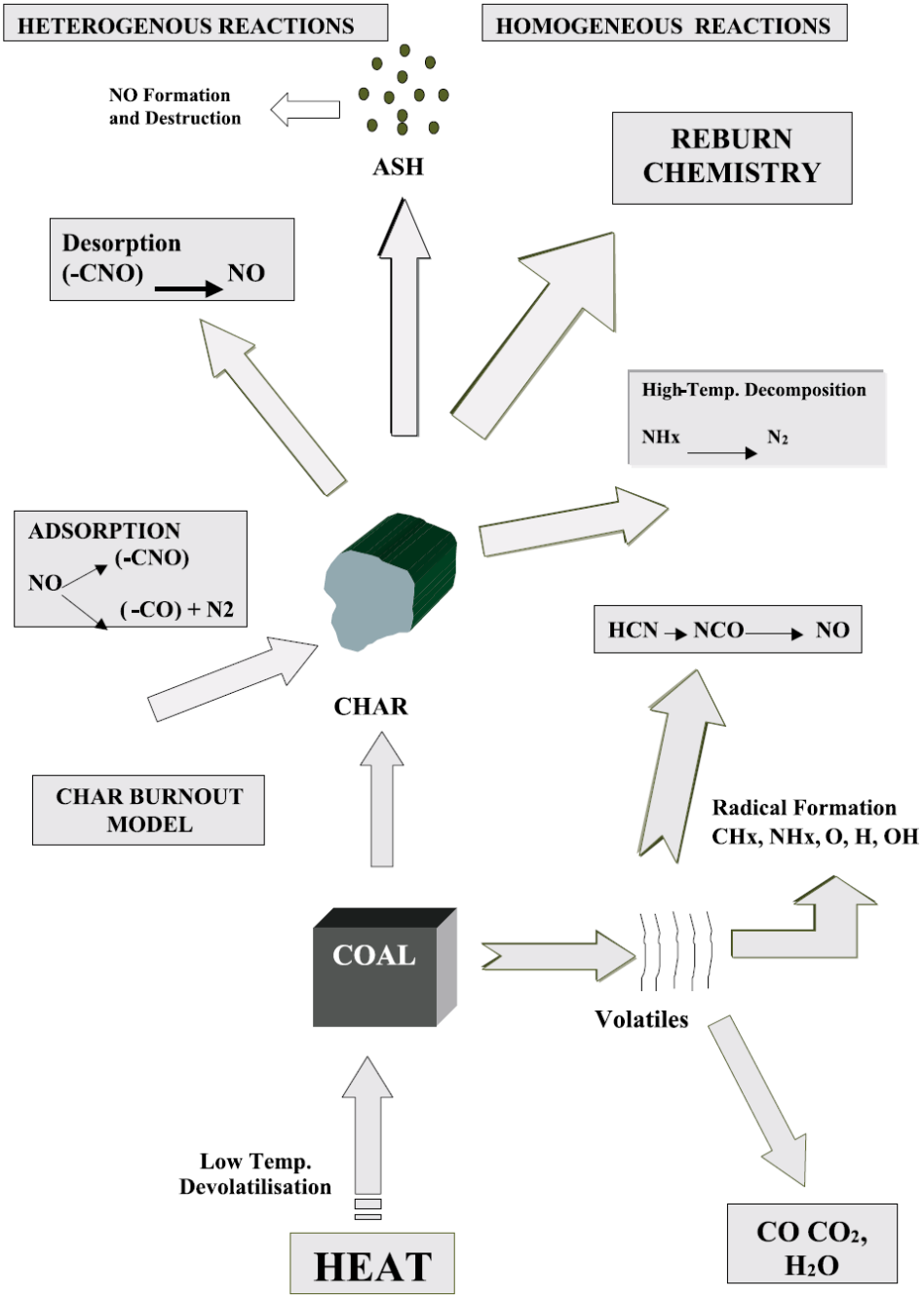

Figure 4. 10 Coal combustion steps with NOx reactions pathways [120].

The mechanism of NOx formation as highlighted in Figure 4.10 above has three major steps, namely: devolatilisation, char burnout, adsorption combined with desorption. The pathways favour mainly the formation of NO, which is confirmed by the data obtained in Figure 4.9 for the coals tested in CFB.

These pathway mechanisms focused on the NOx formation. Figure 4.11 will address the formation of N_2O.

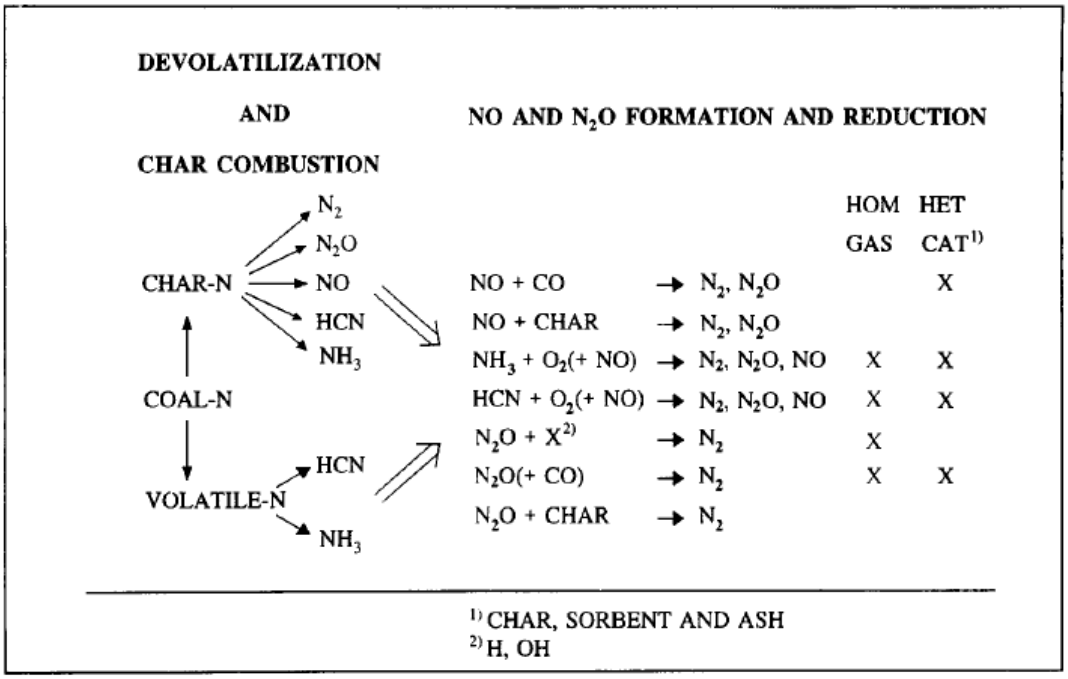

Figure 4. 11 Simplified reaction scheme for formation and reduction of NO and N2O [121].

The mechanism of NOx and N_2O formation in Figure 4.11 confirms the steps highlighted in Figure 4.10. The pathways of N_2O formation are manifested at the char combustion stage as shown by the various reactions. These reactions therefore take place at relatively low temperatures in the region of 800-900ºC, where the formation of N_2O is very prominent. Such formation of N_2O would be low at higher temperatures as such conditions would facilitate the decomposition of N_2O rather than its formation, as confirmed in literature. The formation of NOx and N_2O is accompanied by the formation of other nitrogen products such as HCN and NH_3 as shown in figures 4.9, 4.10 and 4.11. Tourunen et al. [107] studied the formation and decomposition of NOx, N_2O, HCN and NH_3 in different regions of the beds as functions of temperature, oxygen concentration and char inventory. They confirmed that there is a linear correlation in the formation of NOx as a function of temperature which is linked to the char inventory [107].

4.6.2.2 Factors affecting NOx and N_2O formation

The formation and decomposition of NOx and N_2O depends on various operating parameters such as temperature, pressure, (SO_2, O_2, CO_2) concentrations, and fuel types.

The combustion temperature in this study as shown in Figure 4.1 followed a pattern in the range of 830-870^oC therefore the effect of NOx formation would have been the same for all coals. The same could not be said about the pressure and pressure drop which has an impact on circulation rate (which in turn had an impact on N_2O) formation, As shown in Table 4.29. The Russian and SA I coal both have lower pressures drop compared to the other two coals, and this lead to relatively lower NOx formed compared to the other two coals, as shown in Figure 4.9.

The effects of O_2, CO_2 and the ratio of limestone to sulphur (Ca/S) have also been shown to have a direct impact on the formation of NOx and N_2O, as confirmed by Svoboda [79], ,Zhao [119], and Diogo [39]. The impact of Ca/S ratio is detailed in the SOx formation section.

The adopted oxygen content of 6% in this study is in line with literature as highlighted by Svoboda [79] in his investigation on two different coals using the oxygen content of 3.1, 6.1 and 9.6%, respectively. He concluded that the higher oxygen concentrations, higher fluidised bed and higher freeboard temperatures lead to higher NOx emission concentrations.

4.6.2.3 Ratio of Nitrogen content in fuel converted to NOx & N_2O.

In fluidised bed coal combustion, the major part of NO*x* emissions arise from fuel-bound nitrogen released during different stages of coal combustion while in PC combustion the major portions come from air N_2.

The effect of nitrogen content in the feed fuel on NOx and N_2O formation cannot be studied in isolation without including all the operating parameters as detailed in the previous sections. It was found that oxygen partial pressure and total pressure exerted opposite effects on fuel-N conversion to NOx, i.e. the NOx emissions increased with increasing oxygen partial pressure as per results in Table 4.29. NOx emission was lower for the Russian coal. Concerning N_2O emissions, oxygen partial pressure and total operating pressure were shown to have only minor influences on the fuel-N conversion to N_2O [79]. Temperature had the opposite effect on the

formation of NOx and N_2O, where the increase in temperature favoured the formation of NOx and decrease the formation of N_2O.

The nitrogen content in the Russian coal was the highest among the coals tested (i.e. 2.17 %) but there was little increase in the N_2O formed compared to the other coals. In addition to the nitrogen content and operating parameters, the formation of O, H and OH, CO and CO_2 radicals are also said to have an impact on NOx and N_2O formation. Calculating and predicting the amount of N in fuel converted into NOx and N_2O is complicated as confirmed by Martti et al. [122], who established highly complicated models of calculation of the conversion of Nitrogen in fuel to NO, NO_2, N_2O and NxOy, respectively. These investigations established that the impact of fuel-N content is weak vis à vis the formation of NOx and N_2O, compared to the effect of the operating parameters.

One of the additional parameters for the formation of NOx is the effect of limestone in the combustion bed in the course of SO_2 reduction. A study undertaken by Amand [123] showed an increase of NOx formation due to the catalytic effect of limestone while oxidising ammonia species to NO. The following section will address the emission of SOx where the impact of limestone will feature prominently.

4.6.3 SOx

One of the most attractive features of bubbling or circulating fluidised bed combustion (FBC) is the potential to use a low-cost sorbent, such as limestone, to capture sulphur within the fluidised bed. After being injected, either with coal particles or separately, into the riser of a coal-fired atmospheric circulating fluidised bed combustion (CFBC) system, limestone particles are quickly heated up and calcine to form the calcium oxide and to develop pores [124].

$$CaCO_3 \longrightarrow CaO+CO_2 \text{ -183 kJ/mol} \qquad (4.2)$$

The sulphur dioxide formed from the oxidation of coal sulphur in the combustion gases penetrates the pores and reacts with the calcium oxide to form the calcium sulphate:

$$CaO + SO_2 + 1/2\ O_2 \longrightarrow CaSO_4 \text{ -486 kj/mol} \qquad (4.3)$$

This can be removed with the ash. In the reducing regions of a combustor, calcium oxide combines with hydrogen sulphide (H_2S), derived from coal-sulphur, to form calcium sulphide according to the following reaction.

$$CaO+H_2S \longrightarrow CaS+H_2O \quad (4.4)$$

Calcium sulphide can subsequently be oxidised to calcium sulphate in the oxidising regions of the combustor.

$$CaS+ 2O_2 \longrightarrow CaSO_4 \quad (4.5)$$

However, at temperatures above 850^{o}C, the following solid phase reaction becomes important:

$$CaS+ 3CaSO_4 \longrightarrow 4\ CaO +4\ SO_2 \quad (4.6)$$

The sulphur capture performance of a CFBC system by limestone addition depends mainly on the limestone properties and on the CFBC system's operating conditions. The combustor temperature and the intensity of air staging, which is commonly used for the control of NO*x* emission from CFBC systems, are the operating conditions, which have the greatest impact on sulphur capture performance by limestone addition. In addition to its main role for the abatement of SO_2 emissions, limestone addition has also been found to have an influence on other gaseous emissions, namely nitrogen oxides NO*x*, nitrous oxide (N_2O) and carbon monoxide (CO) [49, 124-126].

$$CaSO_4 + CO \longrightarrow CaO +4\ SO_2 + CO_2 \quad (4.7)$$

In the current study, the emission and formation of SO_2 studied as part of the behaviour of the SA coals in CFB. Some of the operating and fuel parameters as highlighted above were investigated and are presented below.

4.6.3.1 SOx formation

The emission of SOx (SO_2) formed (with and without limestone addition) during the combustion of the SA coals and Russian coal are presented in Figure 4.12 below.

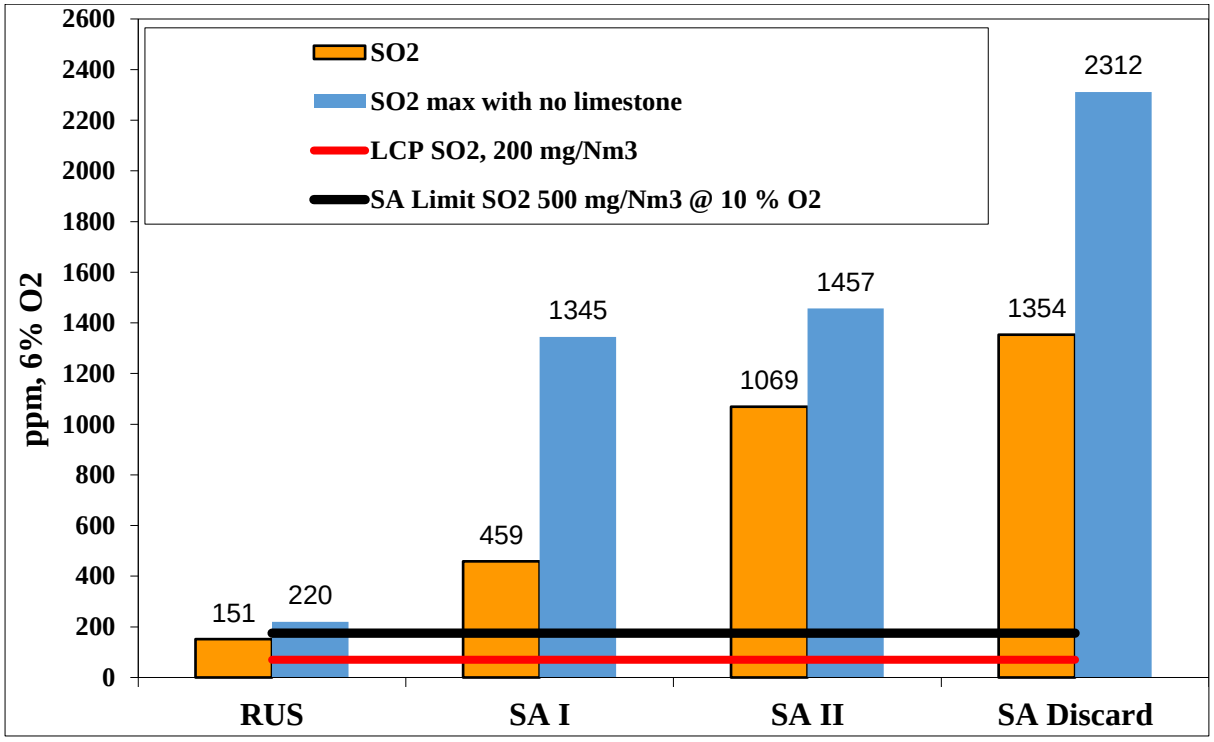

Figure 4.12 SO_2 Formation with or without limestone addition

The emission of SO_2 from the coals tested showed an uneven pattern in which the Russian coal emission was low (151 ppm and 220 ppm as the max quantity without limestone addition) compared to the SA coals ((459, 1345), (1069, 1457), and (1354, 2312) for SA I, SA II and SA Discard respectively). The emission and capture of SO_2 depends on various factors, as detailed in literature in the form of:

- Bed temperature (the combustion temperature are in the region of 820-850°C, which constitute optimum condition for sulphur capture as confirmed by Anders Lyngfelt [127].
- Particle residence time (little variance in particle residence time).
- Air staging and reducing condition (this is an important parameter not only for SOx capture but for N_2O, as well as explained in section 4.6.2. In our case we have similar operating parameters and little differences in air flow rates and pressure drop as per section 4.4.5.).
- Sulphur content in the initial fuel (different sulphur content of all fuels as per section 4.1.2; ratios of Sulphur in fuel converted into SOx is covered in section 4.6.3.3 below.
- Sorbent properties and reactivity (not the subject of this study, use of appropriate literature).

- CaS formation: depends on sorbent addition
- Ca/S ratio (the subject of the next section)

4.6.3.2 Impact of Ratio of Ca/S on SOx emission

The impact of limestone addition in specific Ca/S ratios as well as SO_2 conversion are shown in Figure 4.13 below.

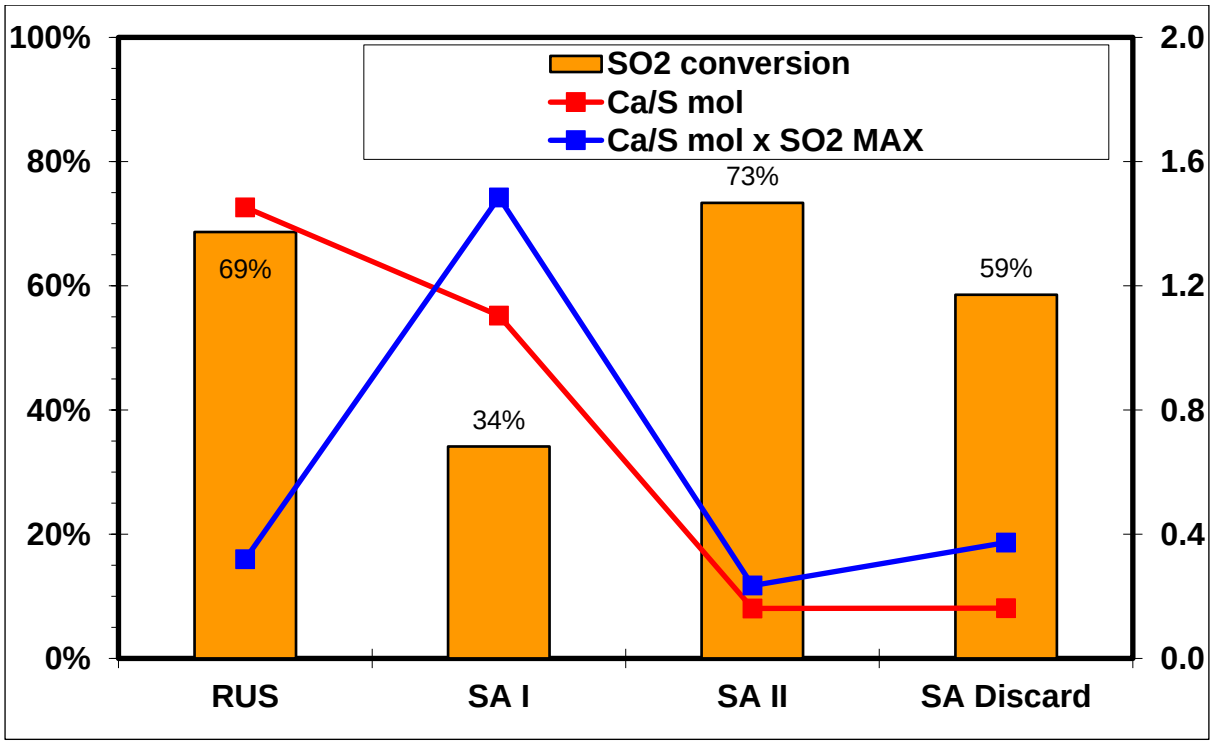

Figure 4.13 Ca/S ratio impact on SO_2 conversion

The data from both Figure 4.12 and 4.13 gave a clear indication about the SO_2 conversion ratio calculated as the proportion of SO_2 formed with lime stone addition over the SO_2 max (with no limestone addition), as shown in Figure 4.12. These conversion ratios exhibited three ranges: the first one relatively high (73% and 69%) for SA II and Russian coal, respectively. The second one is medium range of 59% conversion rate for the SA discard and the third one relatively low for SA I at 34% conversion. These ranges are due to many parameters especially the Ca/S ratio, which has a significant impact on SO_2 emission. This is especially the case for SA II and SA discard, where the ratio is 0.2 compared to the Russian coal, and SA I, with Ca/S ratio of 1.5 and 1.2, respectively. These observations are an agreement with Liu [124], who studied the impact of Ca/S ratio and its addition in different points along the fluidised bed, at

the bottom of the riser and the other above the secondary air injection ports. His study not only confirmed that the increase in Ca/S ratio yields a decrease in SO_2 emission, but also that it has a direct influence on N_2O, NOx and CO emission.

The Ca/S and Ca/SO_2 maximum as shown in Figure 4.13 above vary in parallel pattern where an increase of Ca/S ratio reduces the SO_2 emission and has a direct impact on SO_2 conversion expressed in percentage. The SO_2 conversion is the proportion of SO_2 released as a function of SO_2 maximum.

4.6.3.3 Ratio of Sulphur content in fuel converted to SOx

The total sulphur content in the fuels used, as highlighted in Table 4.3 is 0.3, 0.84, 1.43 and 1.35 percentages for Russian coal, SAI, SA II and SA discard, respectively. The combination of the sulphur content and Ca/S ratio used have a considerable impact on the emission of SO_2, as demonstrated in Figure 4.12 and 4.13, where a low emission of SO_2 for both Russian coal and SA I compared to SA II and SA coal discard.

The emission of SO_2 values obtained are compared to the standard emission limits as shown in section 4.6.6 below. These results show that the coals under review produce emission of SO_2 of 151 ppm and 459 ppm for the Russian coal and SA I, respectively. These values are in line with the current and future emission limits for both South Africa and international standard. As for SA II and SA discard emission, this could change with an increase of Ca/S ratio, as discussed above.

4.6.4 CO and CO_2

Carbon dioxide from burning fossil fuel is said to be the major contributor to the greenhouse gas inventory in the atmosphere, which has become an important environmental topic. This section is a brief overview of the emission of CO and CO_2, emission results of the coals tested are shown in Figure 4.14.

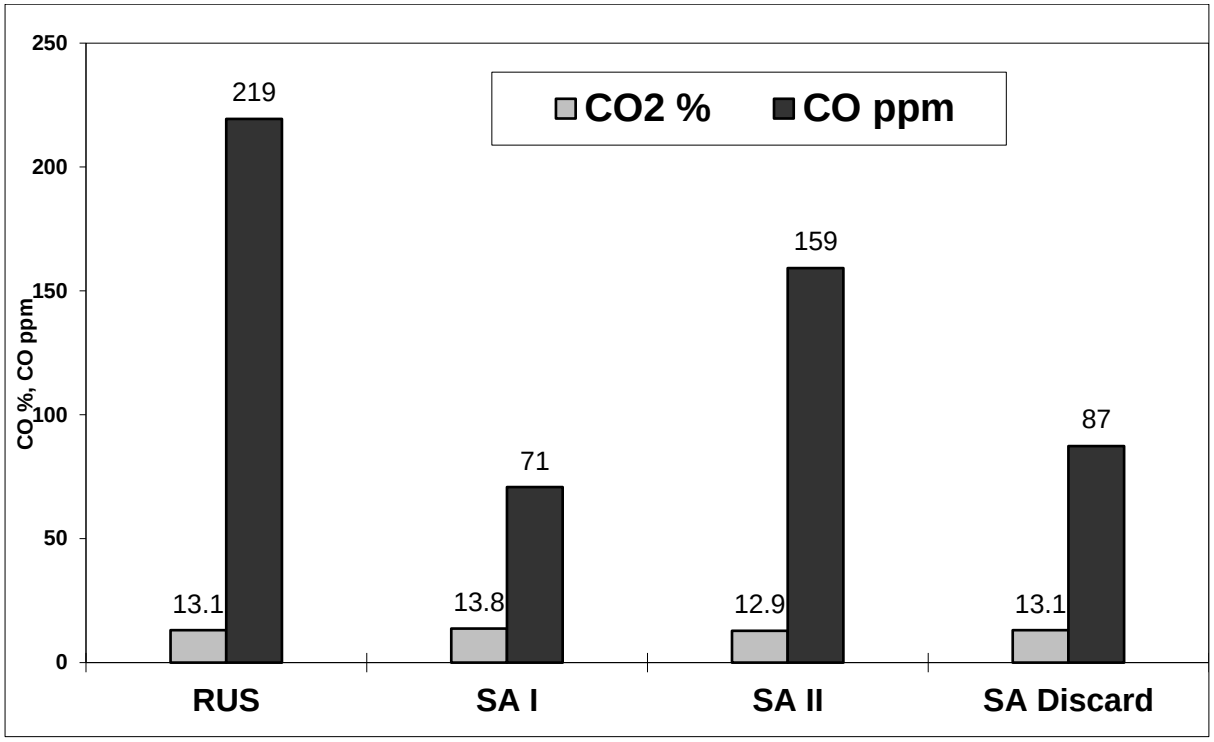

Figure 4. 14 CO/ CO_2 formation

The emission of CO_2 is similar for the coals tested (13-14 %), the same could not be said about the emission of CO. The Russian coal produced the highest CO (219 ppm) compared to the other three coals, 71 ppm, 159 ppm and 87 ppm for SA I, SA II and SA discard, respectively. This is an indication of the occurrence of incomplete combustion for the Russian coal, despite having marginally higher flow rate of both primary and secondary air as shown in Table 4.22. CO formation has a direct impact on the combustion efficiency as discussed in sections 4.5.1, 4.5.2 and 4.5.3.

The major contributing factor of the low CO_2 emissions recorded may be due to the addition of limestone in the bed, the primary objective of this being SO_2 emission reduction, but which also seems to play a role in the reduction of both N_2O and CO_2, as demonstrated by Liu [124]. Other authors attribute the reduction of CO_2 to the presence of CaO, a by-product in SO_2 reduction through the following path:

$$CaO + CO_2 \longrightarrow CaCO_3 \qquad (4.8)$$

There are various studies which dealt with the impact of CaO on CO_2 capture, as illustrated by Lupanez et al. [128], Shimizu et al. [129], Abanades [130] and Rodrigueza et al. [131]. These studies focused on CO_2 capture either in the post combustion stage or the use of twin fluidised

beds. The above authors concluded that the efficiency of CO_2 capture depended on sorbent concentration and degradation, i.e. carbonation–calcination systems, which are influenced by CaO/CO_2 molar ratio and sorbent deactivation ($CaSO_4$ generation and CaO cyclic deactivation). High CaO/CO_2 molar ratios improve the carbonation conversion. The effect of CaO/CO_2 is more significant than the O_2/CO_2 in the combustion process.

Rodrigueza et al. [131] concluded that the effect of operating parameters such as temperature, gas velocity and solid circulation rate can be understood through the link of these variables with the inventory of active CaO in the riser. Such parameters are believed to have contributed to the low CO_2 emissions in the coals under review, due to the presence of CaO in the riser.

4.6.5 VOCs and trace elements emission

Volatile organic compounds (VOCs) release into the atmosphere during the combustion of fossil fuel are the subject of various studies with a view to minimising its emissions and/or abatement techniques. Furthermore, during combustion fossil fuels also release trace elements.

A trace element is defined as an element occurring in very low proportions (< 100ppmw). Recently, trace elements have drawn more and more interest from scientists because of the concern for their toxicological and environmental effects. Heavy metals, another more common term for these elements, also impacts on the ecosystem as well as human health [132].

The concern about the fate of trace elements (TEs) during coal combustion (i.e. partitioning, environmental impacts, emission control, etc.) is a relatively new subject.

One of the major harmful trace elements is mercury. The composition of a coal has a major impact on the quantity and form of Hg in the flue gas and, as a result, on the ability of air pollution control devices (APCDs) to remove Hg from flue gas. [133].

In the current investigation, the trace elements of concern including Hg, Br, F and Cl are notably low, whereas the Hg is high in proportion in the Russian coal as per the coals analysis shown in Table 4.4 in section 4.1.

The emission of VOCs is not prominent in CFB, where not all systems are equipped to record acids in the form of HCl, NH_3, HF and HBr. The recording of these VOCs and trace elements from the coals being tested are shown in Table 4.31.

Table 4. 31 VOCs and Trace element emission

	NH_3 (ppm)	HCl (ppm)	HF (ppm)	HCN (ppm)	HBr (ppm)	Ethylene (ppm)	Acetylene (ppm)	Benzene (ppm)
RUS	7	32	4	19	0	0	0	0
SA I	2	3	1	9	0	1	0	1
SA II	1	6	17	8	0	0	0	0
SA Discard	0	5	23	9	0	0	0	0

Here it will be noted that the emissions of Br, Cl and F as herein recorded in Table 4.30 occur in the form of HBr, HF and HCl, respectively, whilst Hg emission occurs in the form of Hg^0 and oxidised form as Hg^{2+} as per the literature [134]. The latter was not recorded in the FTIR analysis.

Russian coal had a higher HCl and HCN emission compared to the SA coals, despite having more or less the same chlorine content in the initial coals as per Table 4.4. SA II and SA Discard had higher emission of HF. There are no significant emissions of HBr or VOCs products. Low emission of NH_3 was observed, which could be due to the role of in-bed scrubbing in absorbing mines.

The emission of Hg can be estimated by calculation using Pacyna et al. [88] and Streets et al. [135] estimation calculation values of 0.1-0.3 g/tonne and 0.1-0.22 g/tonne, respectively. Their estimation factors were calculated on coals, with Mercury contents of 0.05-0.52 percent. However, all three SA coals were found to have extremely low mercury contents (below 0.01%) compared to the Russian coal (0.08%). The emission of Mercury in SA coals tested is therefore negligible whilst the emission from Russian coal is estimated at 0.786 mg of Mercury, which would be released into stack gas, fly ash, and bottom ash. From the above estimated values, it was deduced that the emission of mercury is negligible for all three coals tested.

4.6.6 Summary of Emission results

The release of SOx, NOx, N_2O, CO, CO_2 and other pollutants from the combustion of the SA and Russian coals in CFB can be compared, since all fuels were burned under similar experimental conditions in some aspects such air velocity, air to fuel ratio, range primary, secondary air, and temperature range. In this section, maximum emission values are shown in Table 4.30 below, including the current and the amended South African air quality standards [14, 72] and as per and international standards [7, 70].

The comparison between emissions from the various coals were conducted in two scenarios based on the limits and standards linked to O_2 of 6% and 10%, respectively. The international limit are set at 6% O_2 content whilst the SA limit is at 10% O_2.

The new emission limit for the international standard is set according to plant sizes and total power output, the larger the plant, the lower the limit. Since the current tests were conducted in a pilot plant with energy output below 100 MW the comparisons are taken at that level. Even though South Africa limits allow for pilot plants below 50 MW to have uncapped emission.

The emission summary and comparison of the results with both the SA and international standards (European standards) are shown in Tables 4.33 and 4.34 below.

Table 4. 32 Overall Emission versus International standard @ 6% O2

	SOx mg/m^3n	NOx mg/m^3n	N_2O mg/m^3n	CO mg/m^3n	CO_2 mg/m^3n
Russ	432	99	441	274	26
SA I	1311	113	288	89	27
SA II	3054	139	380	199	25
SA Discard	3869	138	429	109	26
Limit existing plant	400-2000	500-600		40-250	
Limit New plant	200-850	200-400			

Table 4. 33 Overall emission versus current and new standard SA Standard @ 10% O2

	SOx mg/m^3 n	NOx mg/m^3n	N_2O mg/m^3n	CO mg/m^3n	CO_2 mg/m^3 n
Russ	317	72	303	201	19
SA I	960	82	196	65	20
SA II	2234	103	261	146	18
SA Discard	2831	101	291	80	19
Limit existing plant	3500	1100			
Limit New plant	500	750			

The emission summaries, as depicted in Tables 4.32 and 4.33, show that the emission on NOx and CO are below the limits for both current and new limits set at 6% and 10% O_2 respectively. The SOx emissions were higher than the limits due to the low Ca/S ratio as explained in section 4.6.3.2. SA coals including discard had a lower Ca/S ratio compared to the Russian coal. Liu [124] confirms that an increase of Ca/s ratio will impact in SO_2 emission reduction.

4.7 Potential of Coal Discard Utilisation

4.7.1 Background

The main objective of the research is the study of the behaviour of selected SA coals in CFB and one of the coals tested is discard coal, which is classified as an opportunity fuel for use in CFB where fuel flexibility is one of the major advantages of the technology. This section deals with the potential and technical basis for utilising coal beneficiation discards for electricity generation in South Africa, by applying circulating fluidised bed boilers.

The following data were extrapolated using the 2001 inventory conducted by the Department of Minerals and Energy (DME) [17]. The aim was to obtain new estimates of discard material over a 10-year period since 2001 to 2011. Rough estimates of the total tonnage from the literature in 2011 revealed that there is close to a theoretical value of 1.5 billion tons of discard present in South Africa, where some could have been reclaimed one way or another. This has been produced at a rate of between 54 million tonnes to 60 million tonnes per year over 10 years. This production rate and the difference between the 2001 tonnage (1.1 billion) and the tonnage estimate in 2011 (1.5 billion) was used as the basis for the calculation of new estimates of the discard inventory in 2011 [136].

4.7.2 Discard tonnage and active sites

An extract from the survey conducted by the DME in 2001 shows the following results, namely, the number dumps versus the tonnages of active and defunct sites, respectively [17]. The inactive dumping sites are referred to as defunct site. Figure 4.15 below is an extract of the coal discard state in 2001 for both active and inactive sites.

Tonnage Estimates in year 2001 (DME Survey)

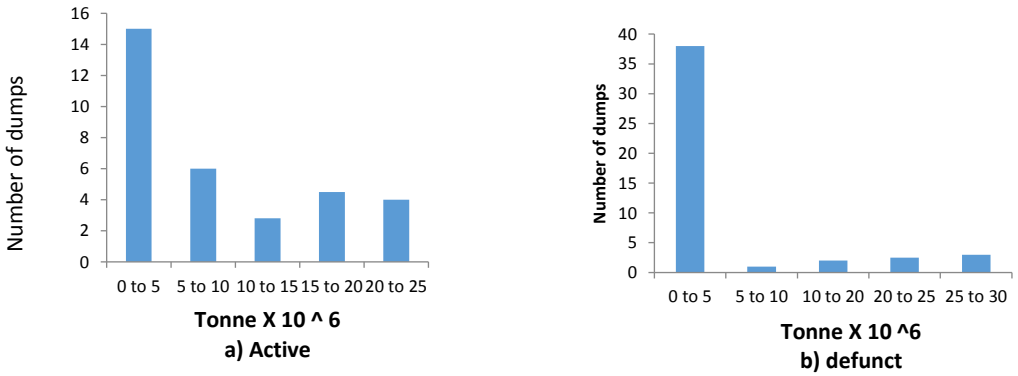

Figure 4. 15 Discard dump tonnages from the 2001 survey, a) active sites, b) defunct sites, source DME report 2001

Tonnage Estimates in year 2011 (Present study)

Using the 2001 data as baseline for the coal discard accumulation over a period of ten years 2001 to 2011. The estimation for the active sites was based on the assumption that the degree of activity of 100 %, 80% and 50%, respectively.

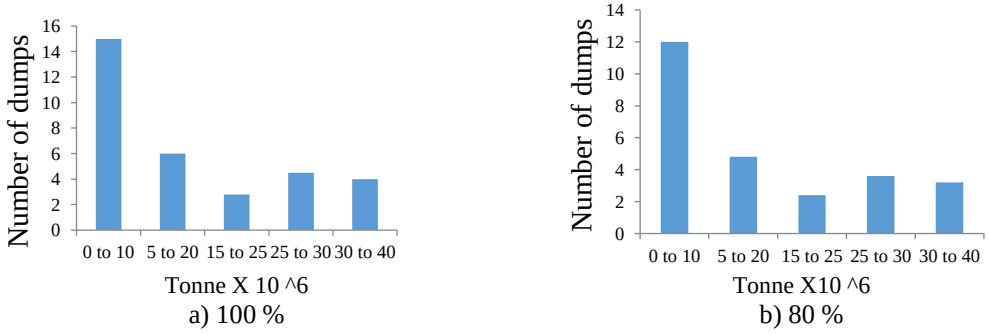

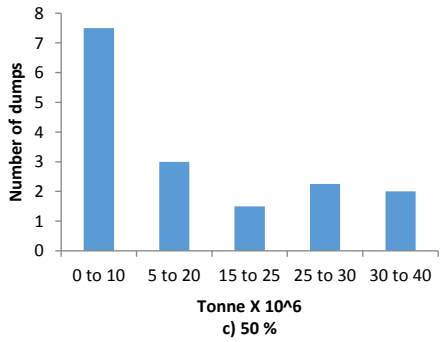

Figure 4.16 Estimate of discard dump tonnages by activity percentages, a) 100%, b) 80%, c) 50% active sites) in 2011.

From Figure 4.16 it can be seen that the number of active dumps would have decreased in some tonnages ranges like (0 to 10 million tonnes) category from 16 dumps in 2001 (Figure 4.15 a) to 7 (Figure 4.16 b) and 12 (Figure 4.16 c) dumps for the 50% and 80% active sites in 2011, respectively. The reduction in number of active sites cant' be seen as reduction in accumulation of coal discard.

It can be noticed from Figure 4.16 that there is an increase in the amount of coal discard accumulated with the apparition of a new category in the tonnage ranges of 25-30 and 30-40 million tonnes. There are at least three to four dumps of this category for each of the site activity percentages.

The inactive discard dump sites would now fall into the category of defunct (inactive) dumps which have ceased increasing in tonnage, but which still form a significant part of the overall inventory of discard coal.

Figure 4.17 shows the estimate of the number of inactive (defunct) dumps and their tonnage in 2011, assuming that only 80% and 50% of the dumps which were active in 2001 were still being utilised in 2011.

From this figure, it can be seen that the number of active dumps contributing to discard production would have decreased from 32 dumps in Figure A to 26 dumps in Figure B. If the number of active sites has reduced by 50% from the 2001 survey, the estimate of active sites

in 2011 is represented by Figure C. This would result in the estimated tonnage from active sites for 2011 being 10% to 20 % lower.

The inactive discard dumpsites would now fall into the category of defunct (inactive) dumps that have ceased increasing in tonnage, but which still form a significant part of the overall inventory of discard coal.

The following figure shows the estimate of the number of inactive (defunct) dumps and their tonnage in 2011, assuming that only (80% and 50%) of the dumps active in 2001 are still active in 2011.

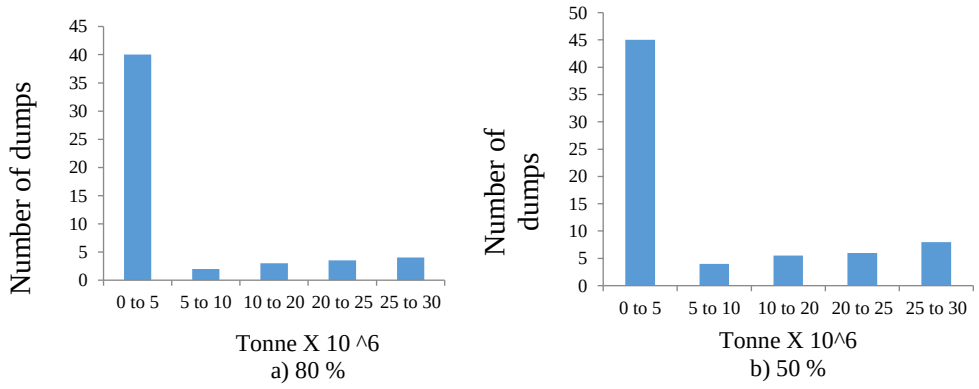

Figure 4.17 : Estimate of discard tonnage inactive (defunct) dumps in 2011

Based on the activity ratio of 80% and 50% respectively, this will lead to an increase of the number of defunct sites compared to the 2001 survey, the inactivity is due to some of the collieries closing down completely, or scaled down their operations over the ten-year period. Nevertheless, the coal discard accumulation continued to increase in active sites in addition to the defunct sites.

4.7.3 Age of the coal discard and area covered

It should be noted that the age of the coal discard material is important, as discard undergoes weathering over a number of years when its exposed to the elements. For this reason, there is likely to be a percentage of coal discard that would have undergone significant weathering and will probably be of a poor quality for beneficiation and use in normal PC plants.

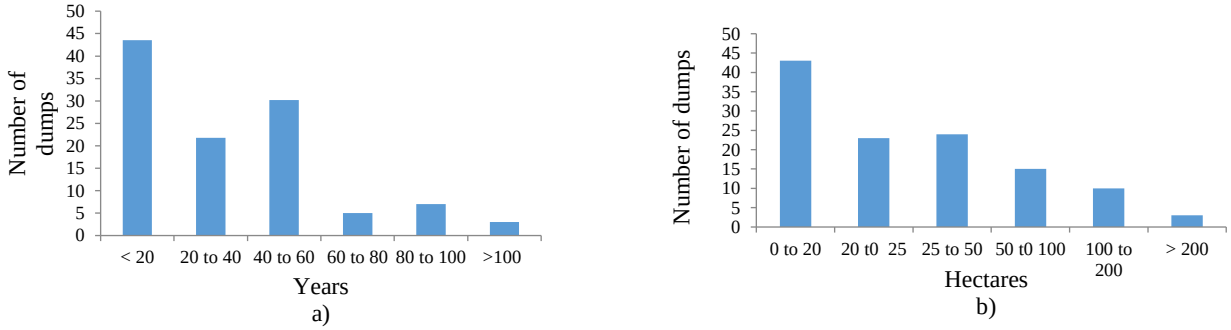

Figure 4. 18 Estimate of the age and area covered by coal discard in 2011: (a) age of coal discard, (b) area covered by coal discard

Figure 4.18 indicates that the highest number of dumps occupy between 0 to 20 hectares of land. Not only do these dumps occupy land that could be rehabilitated for other useful purposes, but also these discard dumps contribute to pollution in these areas i.e. spontaneous combustion and ground water contamination. This is undesirable.

4.7.4 Discard Properties

The potential beneficiation of discard material towards power generation depends on the properties of the discard material, in particular the calorific value, volatile matter and ash content of the material. These specifications are important in determining the combustibility of the material and the possible technologies that could be employed to beneficiate the coal discard.

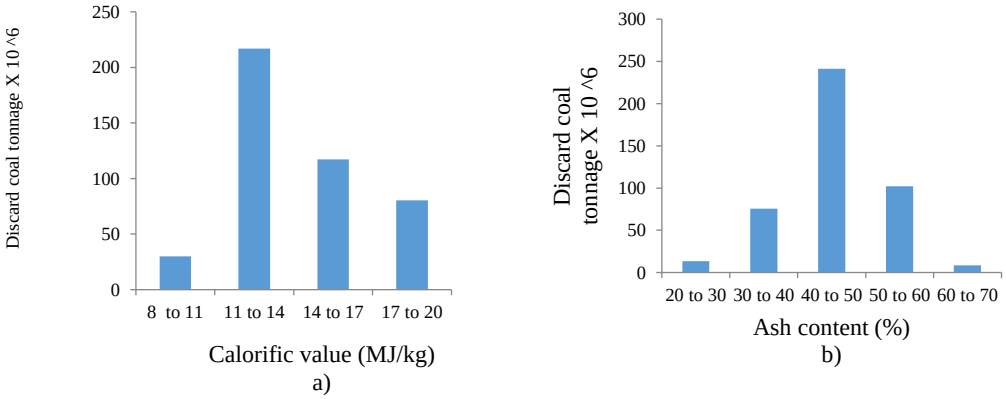

Figure 4. 19 Estimate of the calorific value and ash contents in 2011 of coal discard in 2011

The discard coal produced has a calorific value ranges from 8-20 MJ/kg with 11-14 MJ/kg as the highest category in tonnage of over 200 million tonnes, as shown in Figure 4.19. This calorific value range is close to the poor quality coal currently being used by Lethabo, one of Eskom's power stations. This burns poor quality coal with a calorific value between 14 and 16 Mj/kg, but is the only one of the 14 stations to do so at this time.

In terms of ash content, the highest tonnage in the discard reports indicate ash contents of 40% to 50% ash, which could be beneficiated. A further significant tonnage has coals that have ash contents that fall within 20% to 30%, which is reported to be acceptable and within the combustible range of most power station coal feedstock.

4.7.5 Coal discard accumulation summary

The estimate of the amount of coal discard in 2011 (Figure 4.16) appears to be quite significant in comparison with the amount of 2001 survey (Figure 4.15). As expected the amount of discard material has continued to increase over the 10 years period. From Figure 4.16 it can be seen that the number of dumps which produced discard between 0 and 5 tonnes now produces approximately between 0 to 10 tonnes, as these active sites further increases in the tonnage can be projected. It's also important to note that some of the dumps that were active in 2001 could now be defunct therefore reducing the tonnage estimate for active sites Figure 4.17, 4.18, as this accounts for the possible decrease in the amount of active sites due to some collieries closing etc. It should be noted that the now inactive (defunct) number of dumps would increase Figure 4.18 and 4.19, when compared to the number of defunct dumps in 2001. Figure 4.15 therefore still contributes to the overall discard inventory. It can be deduced from the above data that discard continues to increase at a rate of 60-70 million tonnes per annum as confirmed by literature [137].

4.7.6 Feasibility analysis of electricity generation from coal discard

Discard coal beneficiation and potential of its usage for electricity generation in South Africa using CFB technology carries few challenges, which could be nullified by some of the technology's benefits, as discussed in 2.2.5, and 2.4. The installation of such technology has challenges including but not limited to the following:

- Lack of technological developments;
- Initial capital cost;
- Composition of the discard material;
- Environmental concerns; and
- Location of the discard.

These challenges will add to the new proposed plant's costs in terms of the following items:

- Research of development and capacity building;
- Licence independent power producers especially mining companies accumulating coal discard;
- Coal discard beneficiation and involving small SMME;
- Environmental aspect assessment and monitoring; and
- Proposed plant to be localised around coal discard stockpiles.

The feasibility study was carried out using one of Eskom's largest power stations (Lethabo power station) in the Vaal Triangle. Lethabo is one of the few plants in South Africa, which burn poor quality coal close to discard, with a calorific value of 14.MJ/kg and ash 38-45% content, which suggests that most other power stations are currently unable to beneficiate the remainder of the potentially combustible discard in the region of about 1.5 billion tonnes as discussed previously. This plant can generate up to 3600 MW at full capacity with its six units with generating capacity of 600 MW each, burning close to 50 000 tonnes/day of coal. Considering Lethabo power station buys raw coal at a cost of R200-R300 per tonne, these amounts to approximately 240-360 million Rand per year for the purchase of coal. It is relevant to note that good quality coal is diminishing and existing reserves are limited. Only poorer grade coals are likely to be available in the future.

This feasibility study for a CFBC plant focuses on a large-scale plant with the same generation capacity as the chosen plant as reference, and will draw data from the previous studies on the subjects in the last few years. Namely, work published by North at al [137], Hall et al. 2011[95] and Aziz et al. [96].The study will also make reference to the work of Kavidas et al. [38] and Koornneef [41], as well as other authors, for comparative purposes between CFB and PC.

Table 4.34 below highlight typical plant(s) proposal versus one of Eskom's plant (Lethabo power plant) general information, primary costs, other additional cost and observations about both the proposal and the references.

Table 4.34 Typical power plant based on CFB technology versus one of the current's power producer's plants (Lethabo power station).

Item	Lethabo power station	New plant proposal	Observation
Coal firing plant type	PC	CFB	
Consumption (tonne per day)	50000	78545-50823	Depends on the calorific value and ash content
Capacity (MW)	6 units X 600 =3600	8 units X 450 =3600	Plant capacity depends on the coal location
Coal cost (Rand/ tonne)	230	100	Current fuel cost was taken from Eskom website. Discard coal cost is an estimate for site clearing up, beneficiation, potential charge from the site owner.
Fuel annual coal cost (Million Rand)	276	78-50	Coal discard cost is less than the third of power plant coal used currently.
Sorbent cost R/(tonne)	None	450 [137]	Sorbent cost excluding transport.
Efficiency (%)	35-38	40-42	Subcritical to ultra-subcritical CFB.
Capacity factor (%)	85-95 %	85-95	90% used as a base line.
Coal heating value (MJ/kg)	14-16 MJ/kg	11-17	The largest quantity of discard coals as per survey and estimates from this work.
Ash content (%)	30-40	30-65	CFB has the abilty to burn high ash coal.
Ca/S ratio (kg/kg)	None	2-5	This is subjected to optimisation after process testing.
SOx reduction	none	Within the emission standard limits	In bed
NOx reduction	SCR	Low emission due to the low combustion temperature	In bed, no SCR required due to the low combustion temperature.
CO_2 capture and storage	No Removal unit installed	Provision for oxy-fuel	Energy penalty and increase of capital cost for PC.

		combustion and CCS	
Ash disposal	Electric Precipitator/ bag filter	Electric Precipitator/bag filter	Similar technology
Plant life span (years)	30*	40-50 years	Depends on the stockpile if plant is set out at mine mouth

*Remaining life span time, the plant has been in operation for more than 25 years.

As can be seen from Table 4.34 above, there are various parameters to consider for electricity generation, regardless of the technology deployed. The total cost of electricity generation (COE) has three components, the capital and investment cost (C&I), the operating and maintenance cost (O&M), and the cost of the fuel (F).

O&M cost covers the following:

- Sorbent cost and transport;
- Labour;
- Water;
- Ash disposal cost; and
- Plant maintenance.

C&I cost covers the following:

- Engineering, procurement, and construction (EPC);
- Capital cost; and
- Financing cost.

Fuel (F) cost covers

- Fuel cost;
- Fuel transport; and
- Fuel preparation including coal washing and sized reduction.

The cost of electricity is evaluated with the following formula [41]:

$$\mathrm{COE} = \frac{(\mathrm{C\&I})+(\mathrm{O\&M})+\mathrm{F}}{\text{Anual electricty generation}} \qquad 4.9$$

The distribution of COE for both CFB and PC, as highlighted by Koorneef [41], who compiled the data shown in Table 4.35 below using various sources.

Table 4. 35 Breakdown of COE for coal fired power plants [41]

Description	Fuel %	C&I %	O&M %
Coal-fired power plants (no technology specified)	41	32	27
Coal-fired power plants (pulverised coal)	29	52	19
100MWe net CFB retrofit	26	61	13
Coal fired FBC	31	50	19

As can be seen from Table 4.34 and 4.35 above, various parameters went into consideration for the cost of the proposed CFB plant. Using discard coal is favourable due to the fact the cost of fuel is very low, 26% in theory, and much less in practice, less than 80 million rand per annum compared to 276 million rand paid currently for electricity generation for the Lethabo Power Plant. From Equation 4.9, the reduction of fuel cost and the reduced cost of O&M around 13% for CFB technology, compared to 19% for PC technology, these parameters will have an impact on COE for the CFB proposed plant.

C&I for the PC plant is lower than CFB plant, but that will change with the installation of FGD plant and fitting CO_2 capture technology. Major challenges with the carbon capture system are that it requires additional power and reduces the efficiency of the plant by about 9-13%, with an energy penalty of the PC plants of 8-9% [138].

The international energy agency IEA [139] introduced a new factor for cost of electricity generation, namely, the notion of levelised cost of electricity (LCOE).

The LCOE is calculated using COE above with addition of other factors like the discount rate and decommissioning cost expressed by the following factors:

Electricity n : The amount of electricity produced in year "n"

$(1+r)^{-n}$: The discount factor for year "n"

Investment n : Investment costs in year "n"

O&M n : Operations and maintenance costs in year "n"

Fuel n : Fuel costs in year "n"

Carbon n : Carbon costs in year "n"

Decommissioning n : Decommissioning cost in year "n"

$$LCOE = \sum_{n=1}^{n} \frac{n((Investment\ n + O\&M\ n + Fuel\ n + carbon\ n + decommissioning\ n) * (1+r)^{-n})}{\sum(Electricity\ n * (1+r)^{-n}))} \quad 4.10$$

Equation 4.10 is more comprehensive than Equation 4.9, by the inclusion of the decommissioning cost and the discount rates. Nevertheless, both equations 4.9 and 4.10 confirm that the proposed CFB with coal discard as fuel has an advantage over the use of the current PC technology, especially with today's climates and sensitivity towards emission of harmful gases, as well as the motivation curb global warming. The cost of the sorbent deployed in the CFB is a fraction of the FGD installation and operation cost needed for PC boiler, which could increase the cost of electricity generation by 7% per kW, as confirmed by Utt and Gigllio [54]. In addition to other costs including fuel size, reduction to 75 micron and the PC pulverisers requires significant maintenance expenses. These costs are virtually nullified in CFB as the coal is crushed to 12-6 mm. Even though CFB boiler equipment is designed for relatively lower flue gas velocities, the heat transfer coefficient of the CFB furnace is nearly double that of PC, which makes the furnace compact [42]. In summary the COE and LCOE of CFB are lower than of PC due to the additional cost in both C&I and O&M, in practice predicting plant cost for either technologies is very challenging due to the market instability and cost volatility.

CHAPTER FIVE:

CONCLUSION AND RECOMMENDATIONS

5.1 Conclusion

This research undertook an investigation of the combustibility of two South African coals, one South African discard coal and one Russian coal, in a pilot scale CFBC boiler. The coals, coarse (bed) and fly ash, as well as gaseous emissions were analysed, and their impacts on the combustion processes determined. The outcome of the study yielded valuable information concerning the behaviour of the selected SA coals in a CFBC pilot scale unit, this proving the major advantages of CFB technology. Based upon the results obtained in this research, the following conclusions are drawn:

1. With regard to combustion efficiency, all four coals exhibited high efficiencies, 98 to 99%, with the Russian coal marginally lower or within the experimental error. The Russian coal was characterised by being low in ash and high in the reactive maceral vitrinite. The two South African coals possessed high ash contents (35 to 45%), one with relatively high vitrinite and the other very low vitrinite, whilst the South African discard possessed an ash content of 65-70% and extremely low reactive vitrinite content. This implies that all SA coals tested irrespective of grade, with wide ash contents and different maceral compositions, combusted performed well in the CFBC boiler.

2. With regard to ash behaviour in the boiler, investigations were undertaken on the ash and spent sorbents released in the furnace, which were extracted partially from the bed and partially from the flue gas. The results indicated that:
   - Coals that possessed high proportions of minerite and extrinsic mineral/stone forms produced high quantities of ash in the bed and those with high proportions of fine intrinsic mineral distribution (mostly kaolinite) in the coals produced higher concentrations of fly ash. i.e. the SA I and SA Discard produced high proportions of coarse ash in the bed (53% and 62% for SA I and SA Discard, respectively), whereas the Russian coal and SAII produced higher proportions of fly ash (86% and 82%, respectively).
   - SA coal II and the Russian coal have similar ratios between them in both fly ash and bottom ash, with high proportions of fly ash. Despite the two coals being different in

proximate analyses, both are characterised by finely distributed clay contents and low proportions of high ash and minerites (rock) particles. This results in low proportions of bottom ash for both SA coal II and Russian coal.

- In the South African coals, the very presence of particles of rock (minerite) in the feed would lead to the natural accumulation of such particles in the coarse ash fraction. Such material is not often encountered in the coals of Europe and the USA.
- It is proposed that the ash distribution in the test CFBC was attributed not only to the ash formation characteristics of the fuel but also to other solids fed into the combustion chamber, e.g. additional inert material, recycled ash or sorbent material. All such materials are retained when recycled through the classification and comminution processes occurring in the CFB combustion system.
- The volatile content in the initial fuel has an impact on the combustion efficiency and lesser influence on the ash formation where the volatiles – determined ash free – are closely similar for all the coal tested.

3. In terms of NOx emissions, all coals tested showed that their NOx and N_2O emission meet the minimum requirements for plants as set out by the European and SA standards. The values of NOx (48-68 ppm) and N_2O (147-225 ppm) emission of the coals tested i.e. <300 ppm for plant with generating capacity below 100 MW. These results are in agreement with data from literature.

4. The emission of SOx (SO_2) from the coals tested showed an uneven pattern, in which the Russian coal emission was low (151 ppm) compared to the SA coals (459, 1069 and 1354 for SA I, SA II and SA Discard, respectively). SO_2 emitted from the South African coals was higher than the national permitted standard, due to the low Ca/S ratio used. This was especially the case for SA discard. The emission and capture of SO_2 depends on various factors as detailed in literature like the sulphur content in the initial coal, which also has an impact on the Ca/S Ratio that can be used.

5. CO_2 emissions from the coals under review were found to be the same for all the coals tested. In the emission of CO the Russian coal produced the highest CO (219 ppm) compared to the other three coals, 71 ppm, 159 ppm and 87 ppm for SA I, SA II and SA

discard, respectively. This is an indication of the occurrence of incomplete combustion for the Russian coal, which has a direct impact on the combustion efficiency.

6. The emission of Hg can be estimated by calculation using literature, all three SA coals were found to have extremely low mercury contents (below 0.01%) compared to the Russian coal (0.08%). The emission of Mercury in SA coals tested is therefore negligible, whilst the emission from Russian coal is estimated at 0.786 mg of Mercury, which would be released into stack gas, fly ash, and bottom ash. From the above estimated values it was deduced that the emission of mercury is negligible for all three SA coals tested.

7. Vast reserves of discard coal containing from 2MJ/kg to 14 MJ/kg in calorific value have accumulated in South Africa since the last inventory of 2001, i.e. close to 1.5 billion tonnes are in existence. It is apparent that one of the looming challenges regarding discard coal is putting this ever-accumulating material to use. From the combustion results obtained in this research, it is proposed that such materials can be combusted in a CFBC boiler, and that it produces the same efficiency as other coals from South Africa and a clean coal from Europe. Ash distribution within the boiler was found to change in proportion, bed ash to fly ash, subject to the quality of the coal used. This is also likely to change the proportions of sulphur-absorbing sorbents in future.

8. The tests results gave an indication that SA coals may be well suited for CFBC.
   In summary, the research undertaken in this thesis has illustrated that CFBC can utilise a wide range of coal qualities efficiently and for the most part environmentally acceptably. Based upon these results, it is anticipated that the adoption of CFBC technology in South Africa would be of inestimable value with the following overall benefits:
   - Provision of additional power to the national grid or for ‘own use or sale’ by independent power producers;
   - Utilisation of coal discards for which there is little or no other use and which, if used in CFBC, would lead to the prevention of considerable environmental problems;

- Reduction gas emissions including all forms of NOx and SOx through in-bed scrubbing (SOx) and low temperature control (forms of NOx); and
- The potential for CFBC units to be located strategically where source feed materials occur, such as large discard sites or new collieries in new coalfields. This has great benefit when compared to the fixed locations of large scale (4 000+MW) pf power stations such as is the case in South Africa at present.

Though there is a need for research, development and demonstration to progress to higher steam conditions in CFB over time, there are no obvious barriers to CFBC other than the size of the market.

5.2 Recommendations

Based upon the research undertaken to date, the following recommendations are put forward to advance the case for CFB adoption in South Africa:

1. Investigations into the use of sorbents is vital; dolomite as a sorbent is especially important as this is widely abundant in South Africa.

2. A thorough characterisation study should be conducted on all sorbents to be tested, i.e. both limestone and dolomite using relevant forms of analysis including the following [132]:

- XRF
- XRD
- SEM

3. It is necessary to carry out tests without limestone addition to investigate the inherent sulphur capture by minerals in coals. A high inherent sulphur capture reduces the amount of limestone required to bring SO_2 concentration in the flue gas below the compliance limit.

4. Ca/S Ratio process optimisation needs to be studied and it impact on other greenhouse gases reduction

5. Characterisation and impact of ash on the full combustion process in the CFBC should be undertaken, with specific reference to the following [130]:

- Ash mineralogy (use of different analytical techniques and analytical equipment);
- Ash usage in other industries;
- Impact of ash on combustion efficiency of coals blends; and
- Impact of ash on boiler efficiency.

6. Process modelling and optimisation (use of modelling software) should be considered, with the modelling of all critical and non-critical operating parameters. Kinetics modelling using some of the models as detailed in Appendix A is recommended.

7. Further research with tests in a CFBC pilot scale facility repeating the methods applied in this study should be undertaken in order to obtain a larger and more comprehensive dataset and more detailed cost/price data. Such research could yield a better estimation of the process cost for CFBC implementation purposes.

8. A comparative technical and economic analysis should be undertaken to explore the option of using oxy fuel in CFBC technology. In Oxy fuel (the combustion chamber is highly enriched in CO_2 which means that the combustion process takes place in an O_2/CO_2 environment [140]) as a technology of choice for power generation in South Africa, also with a variety of coal types as a feed.

APPENDICES

Appendix A: FTIR

This appendix presents some theoretical background about the testing methods and provide some of the experimental results in the form of graphs using the recorded results from an excel spreadsheet.

Appendix A 1: FTIR Background

FTIR stands for Fourier Transform Infra-Red. FTIR Spectroscopy is a technique based on the determination of the interaction between an IR radiation and a sample that can be solid, liquid or gaseous.

The working principle in the case of gas detection is based on few steps as follow [141]:

1. The Source: The infrared energy is emitted from a glowing source. This beam passes through an aperture which controls the amount of energy presented to the sample (and, ultimately, to the detector).

2. The Interferometer: The beam enters the interferometer where the "spectral encoding" takes place. The resulting interferogram signal then exits the interferometer. Different FT-IR spectrometers use different interferometers.

3. The Sample: The beam enters the sample compartment where it is transmitted through or reflected off of the surface of the sample, depending on the type of analysis being accomplished. This is where specific frequencies of energy, which are uniquely characteristic of the sample, are absorbed.

4. The Detector: The beam finally passes to the detector for final measurement. The detectors used are specially designed to measure the special interferogram signal. The main difficulty in performing Fourier spectroscopy depends upon the correct realization of the interferogram.

5. The Computer: The computer controls optical components, collects and stores data, carries out calculations on data, and displays spectra. Because of the direct interfacing of the computer to the spectrometer, spectra can be arithmetically manipulated in an inventive way such that, for example, interfering absorbances can be eliminated by subtracting out from composite spectra the absorption bands due to interfering components.

The five steps are highlighted in the figure below:

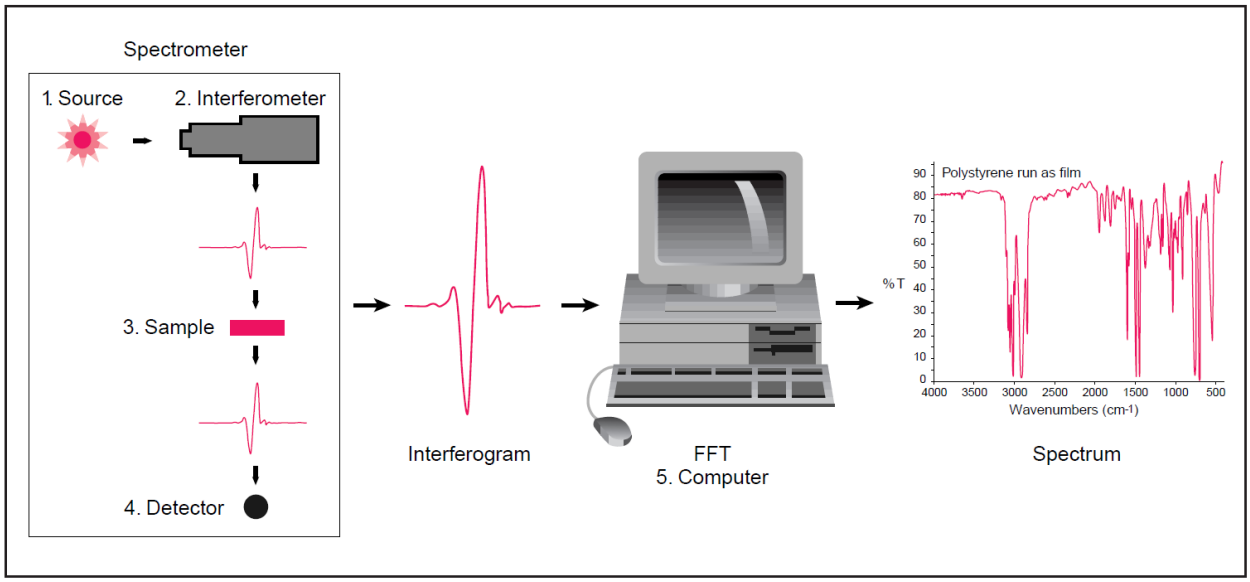

Appendix A 1: FTIR working principle [142]

The major advantages of the FTIR technique in environmental studies are [143]:

- Real time data collection and reporting;
- Excellent sample-to-sample reproducibility;
- Enhanced frequency accuracy;
- High signal to noise ratio;
- Superior sensitivity, analytical performance; and
- The measurement is very rapid so that a large number of samples can be analysed.

Appendix A 2: FTIR Experimental results

The FTIR was used to measure the emission trends of the following components:

CO, NO, CO_2, SO_2, NO_2, N_2O, H_2O, CH_4, Ethylene (C_2H_4), Acetylene, (C_2H_2) Benzene (C_6H_6), NH_3, HCl. HCN, HF and HBr. The results of the coals tested in this investigation are shown in the appendices below. The coals were fired in different time sequences allowing for cooling times in between operations, each combustion test per coal type lasted for about three hours.

Full operations schedule per each sample was done as follow:

Russian coal: 12:00-8:00

SA I: 12:00-20:00

SA II: 0.00-8:00

SA Discard: 12:00-20:00

The figures A2 to A15 below show the trends of the emission only. The results shown in the following sections were extracted from the trends figures and the computed data spreadsheet.

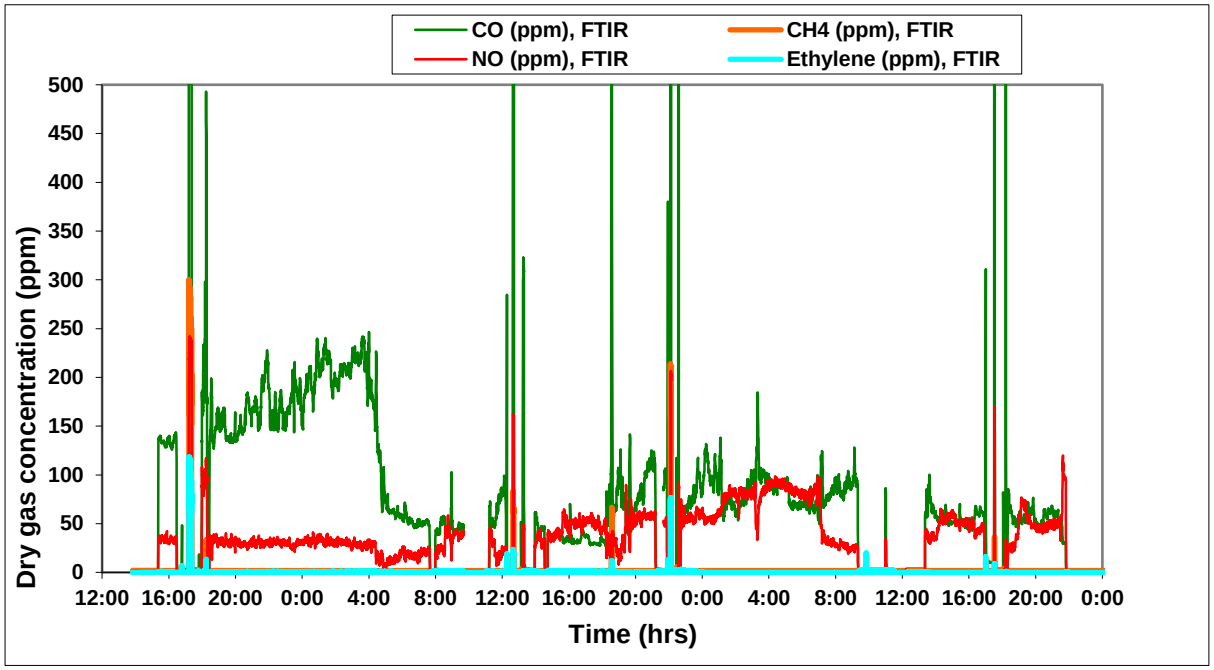

Russian coal: *12:00-8:00;* ***SA I:*** *12:00-20:00;* ***SA II:*** *0.00-8:00;* ***SA Discard:*** *12:00-20:00*

Appendix A2: Emission trends one (CO, NO, CH_4 and C_2H_6)

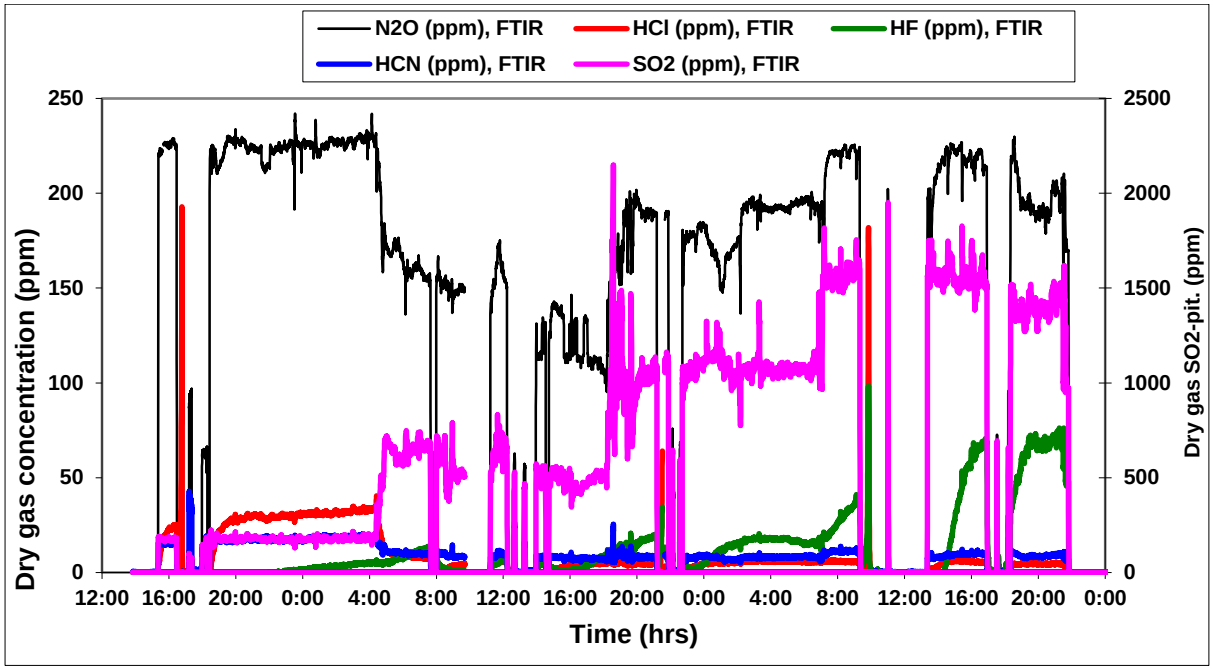

Russian coal: *12:00-8:00;* ***SA I:*** *12:00-20:00;* ***SA II:*** *0.00-8:00;* ***SA Discard:*** *12:00-20:00*

Appendix A3: Emission trend two (N2O, SO2, HCN, HCl and HF)

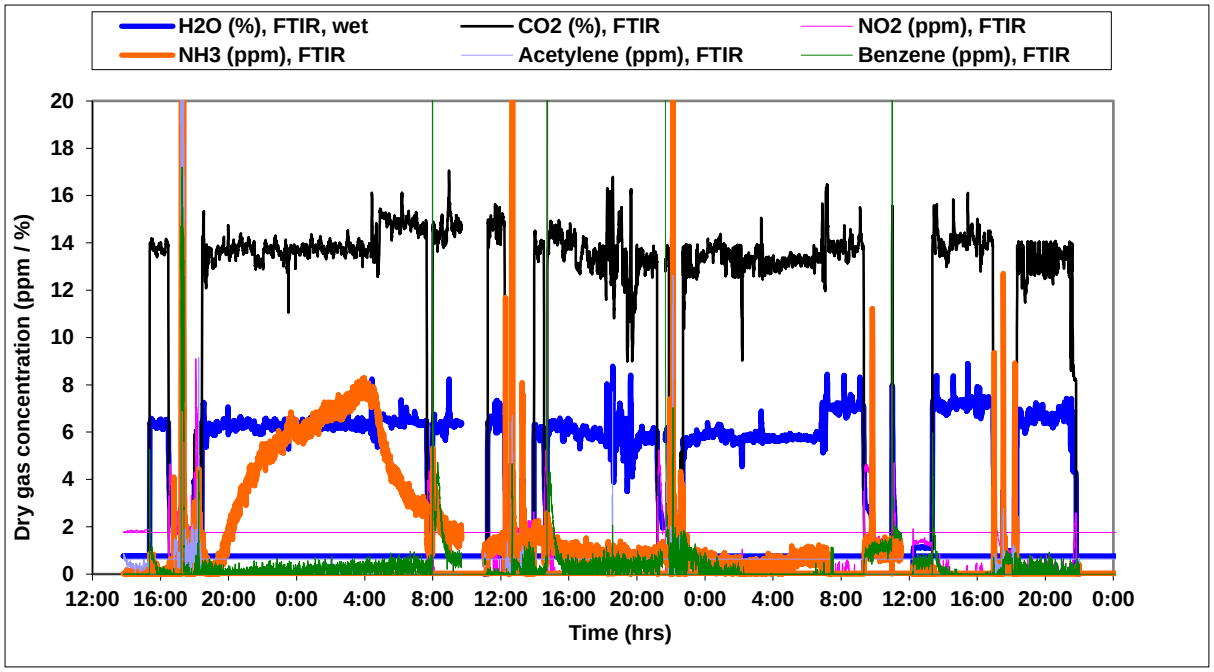

Russian coal: *12:00-8:00;* ***SA I:*** *12:00-20:00;* ***SA II:*** *0.00-8:00;* ***SA Discard:*** *12:00-20:00*

Appendix A4: Emission trend three (CO_2, NO_2, NH_3, H_2O, C_6H_6 and Acetylene)

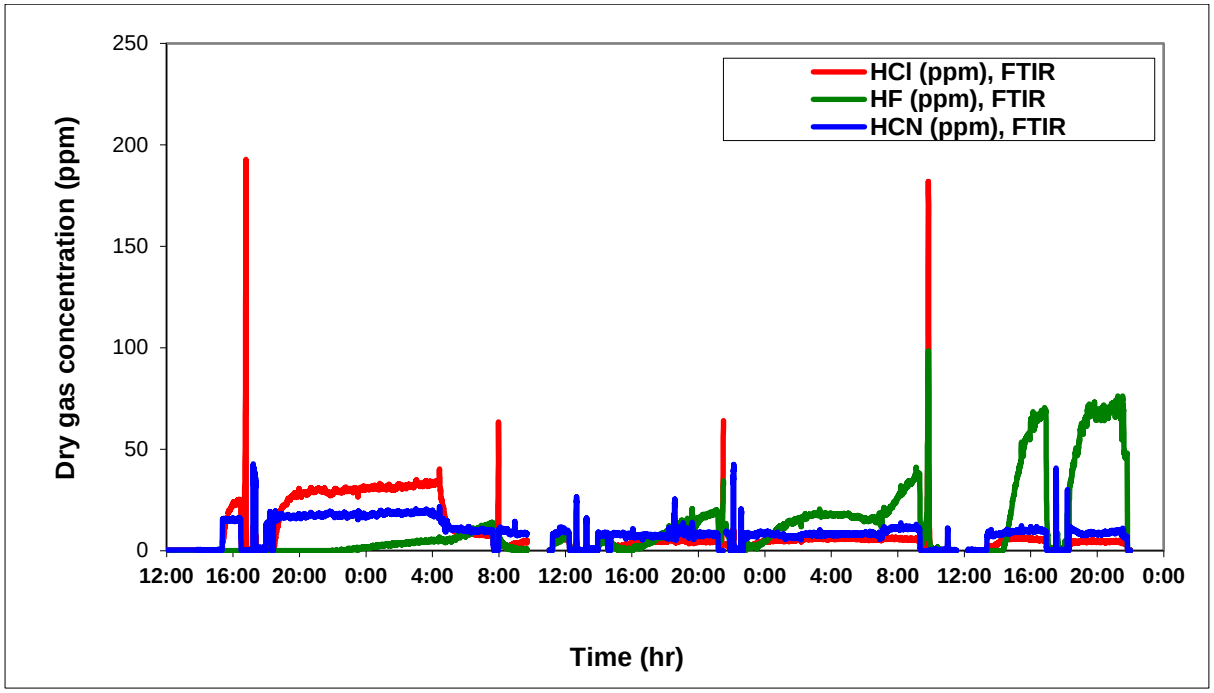

Russian coal: *12:00-8:00;* ***SA I:*** *12:00-20:00;* ***SA II:*** *0.00-8:00;* ***SA Discard:*** *12:00-20:00*

Appendix A5: HCl, HF, and HCN FTIR results (ppm)

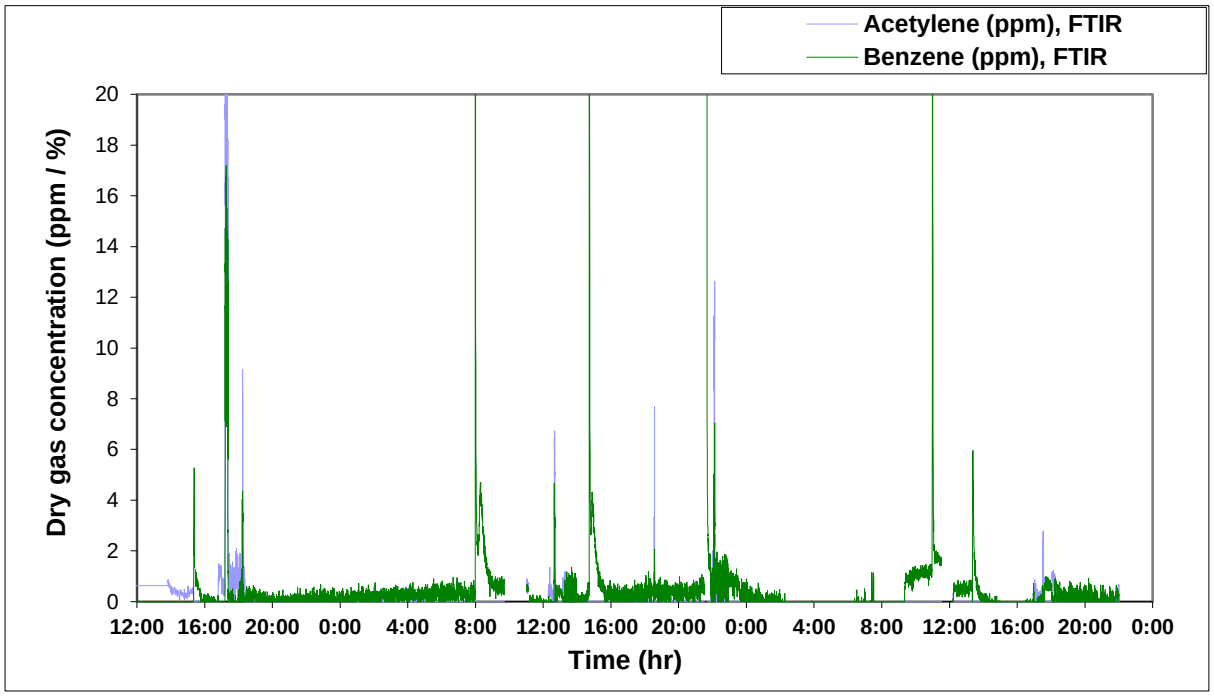

Russian coal: *12:00-8:00;* ***SA I:*** *12:00-20:00;* ***SA II:*** *0.00-8:00;* ***SA Discard:*** *12:00-20:00*

Appendix A6 Acetylene and Benzene FTIR results (ppm)

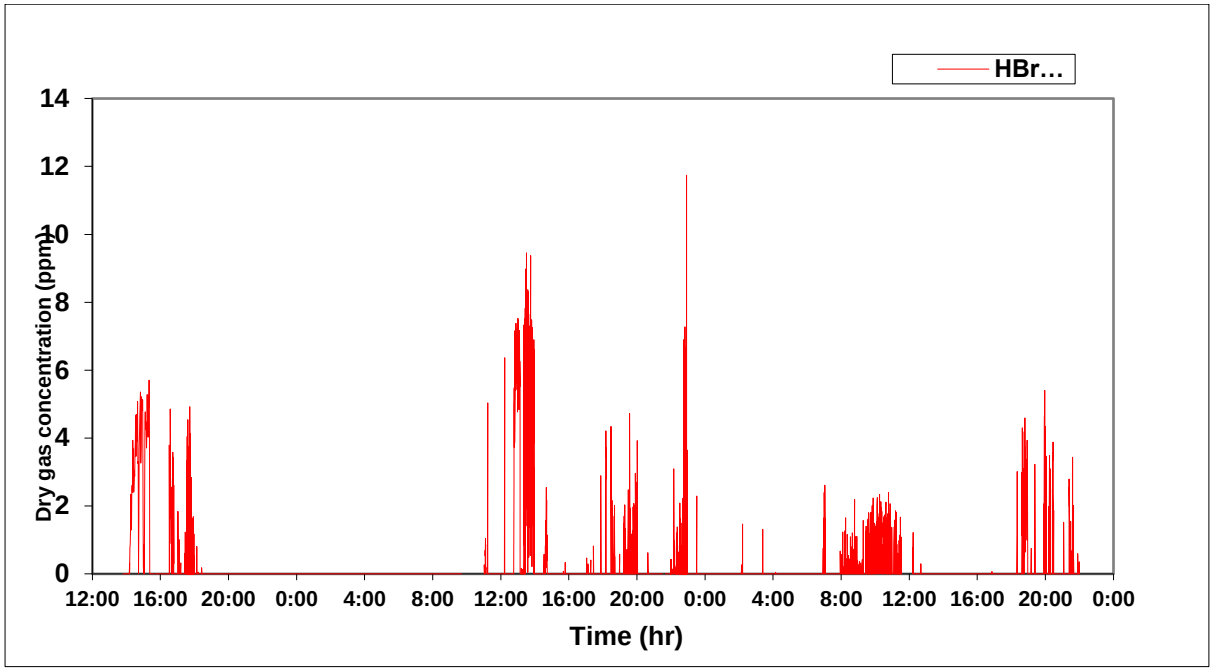

Russian coal: *12:00-8:00;* ***SA I:*** *12:00-20:00;* ***SA II:*** *0.00-8:00;* ***SA Discard:*** *12:00-20:00*

Appendix A7: Emission trends four (HBr)

The following figures are for individual entities

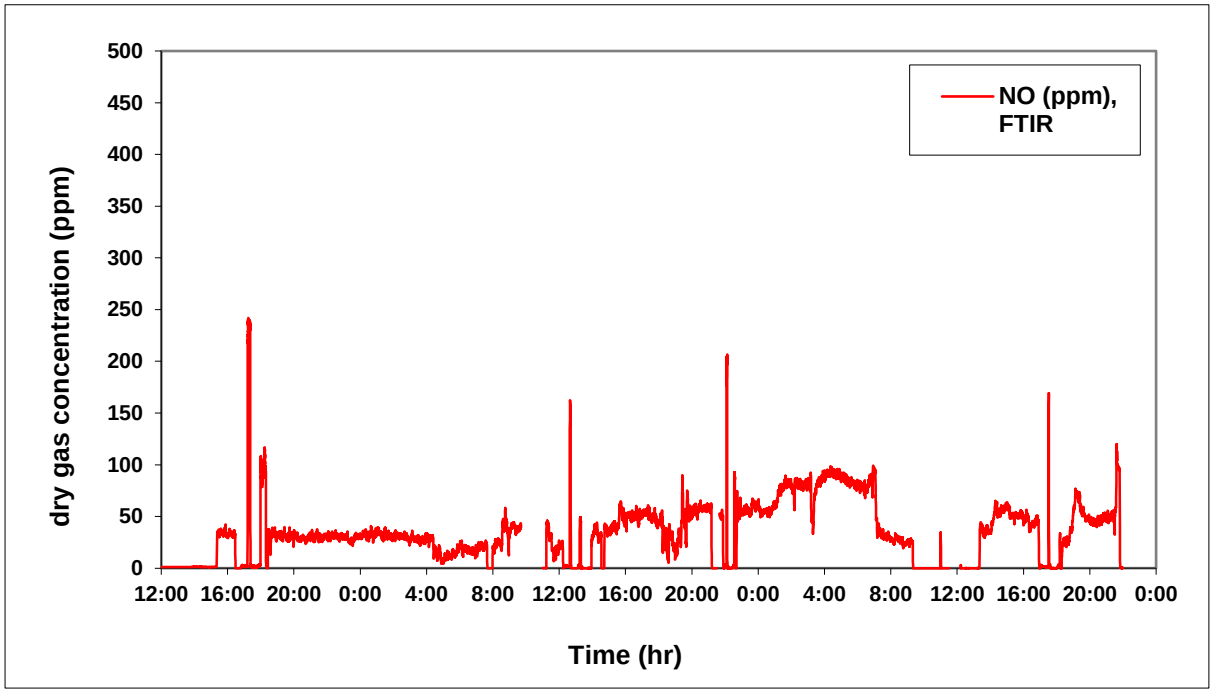

Russian coal: *12:00-8:00;* ***SA I:*** *12:00-20:00;* ***SA II:*** *0.00-8:00;* ***SA Discard:*** *12:00-20:00*

Appendix A8: NO FTIR results (ppm)

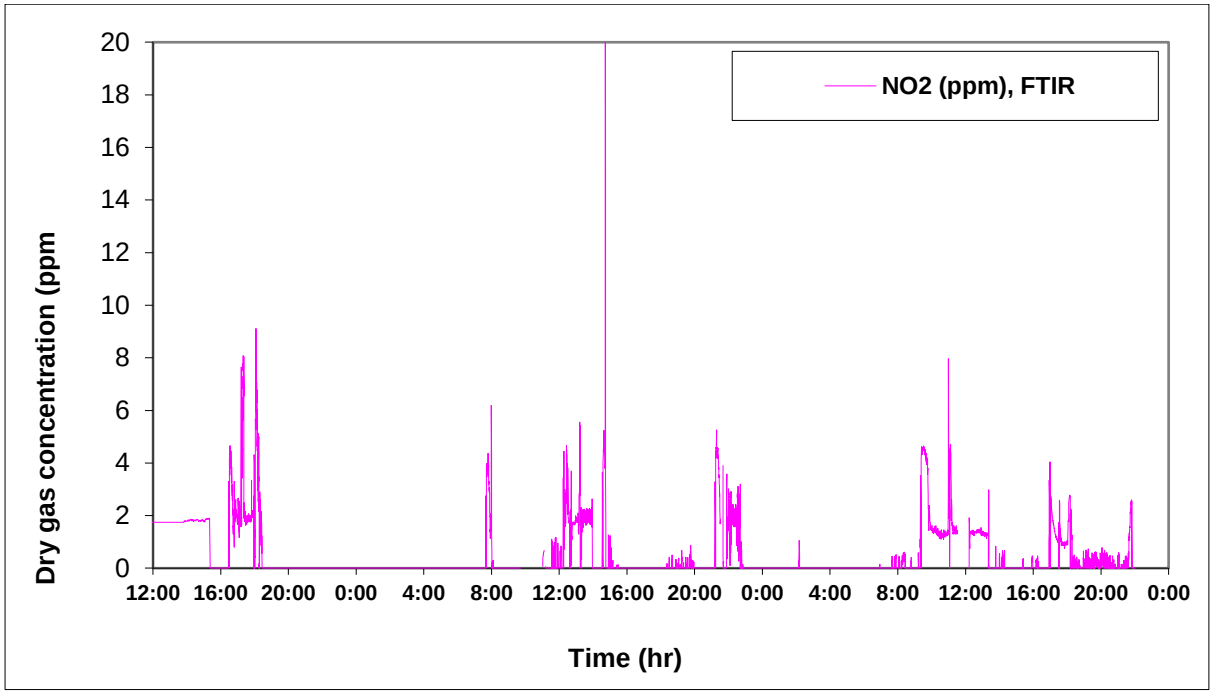

Russian coal: *12:00-8:00;* ***SA I:*** *12:00-20:00;* ***SA II:*** *0.00-8:00;* ***SA Discard:*** *12:00-20:00*

Appendix A9: NO_2 FTIR results (ppm)

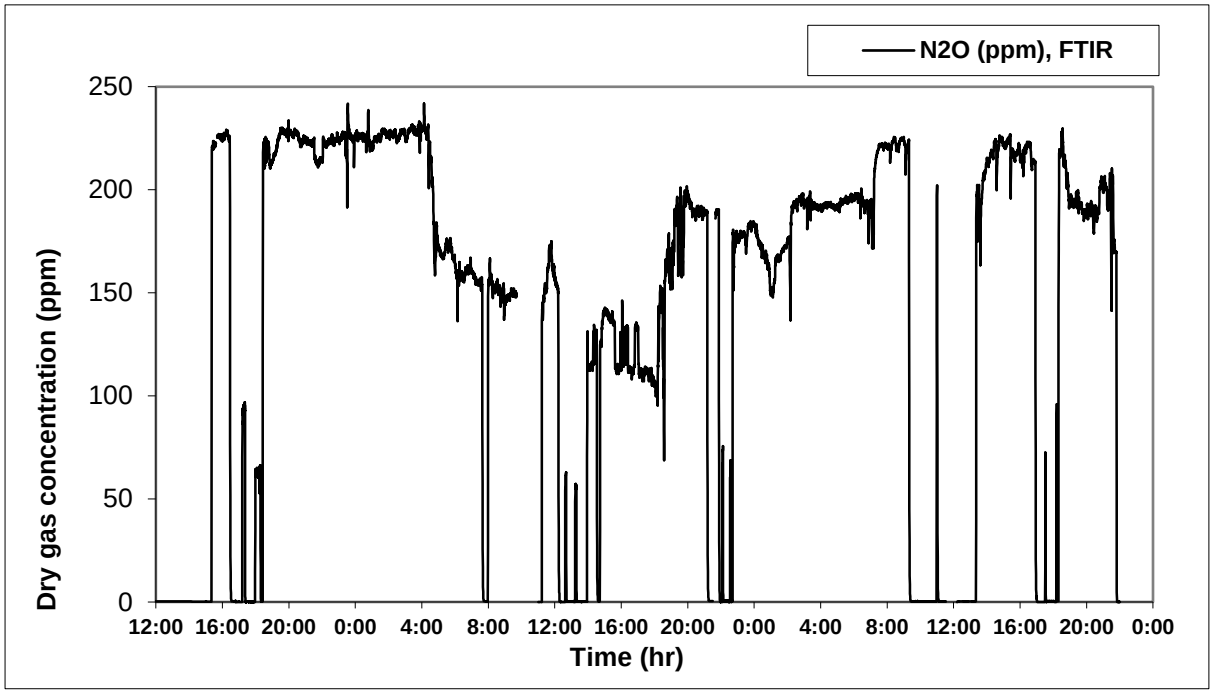

Russian coal: *12:00-8:00;* ***SA I:*** *12:00-20:00;* ***SA II:*** *0.00-8:00;* ***SA Discard:*** *12:00-20:00*

Appendix A10: N_2O FTIR results (ppm)

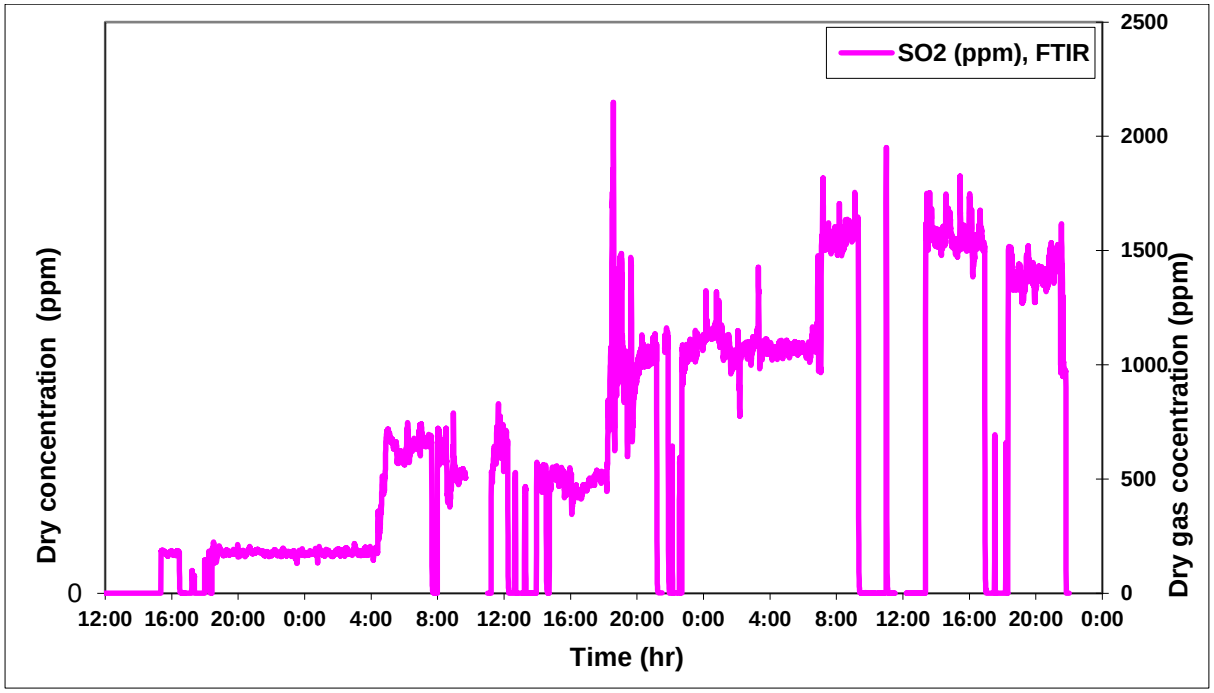

Russian coal: *12:00-8:00;* ***SA I:*** *12:00-20:00;* ***SA II:*** *0.00-8:00;* ***SA Discard:*** *12:00-20:00*

Appendix A11: SO_2 FTIR results (ppm)

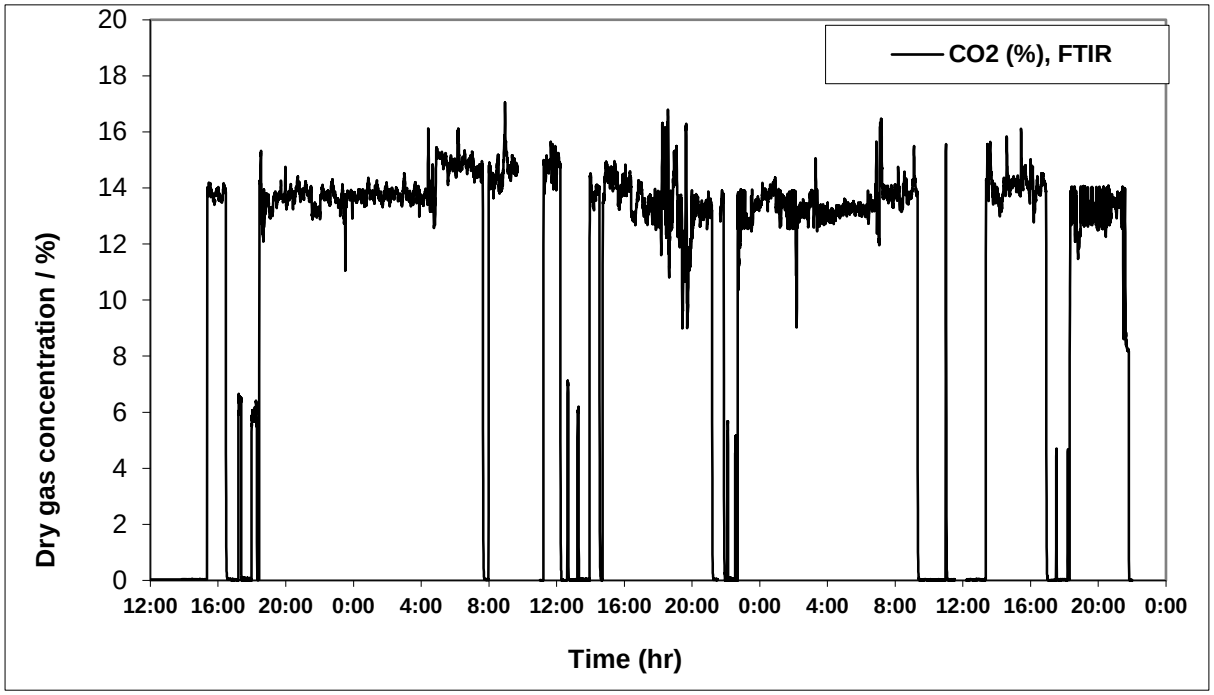

Russian coal: *12:00-8:00;* ***SA I:*** *12:00-20:00;* ***SA II:*** *0.00-8:00;* ***SA Discard:*** *12:00-20:00*

Appendix A12: CO_2 FTIR results (%)

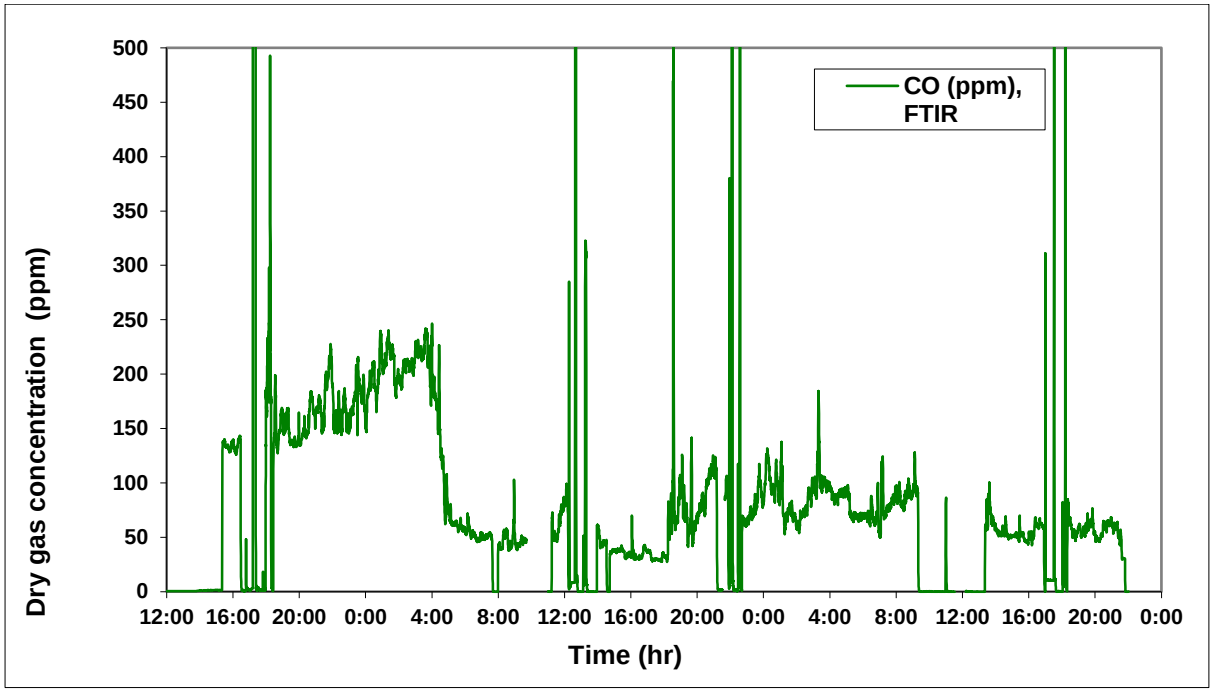

Russian coal: *12:00-8:00;* ***SA I:*** *12:00-20:00;* ***SA II:*** *0.00-8:00;* ***SA Discard:*** *12:00-20:00*

Appendix A13: CO FTIR results (ppm)

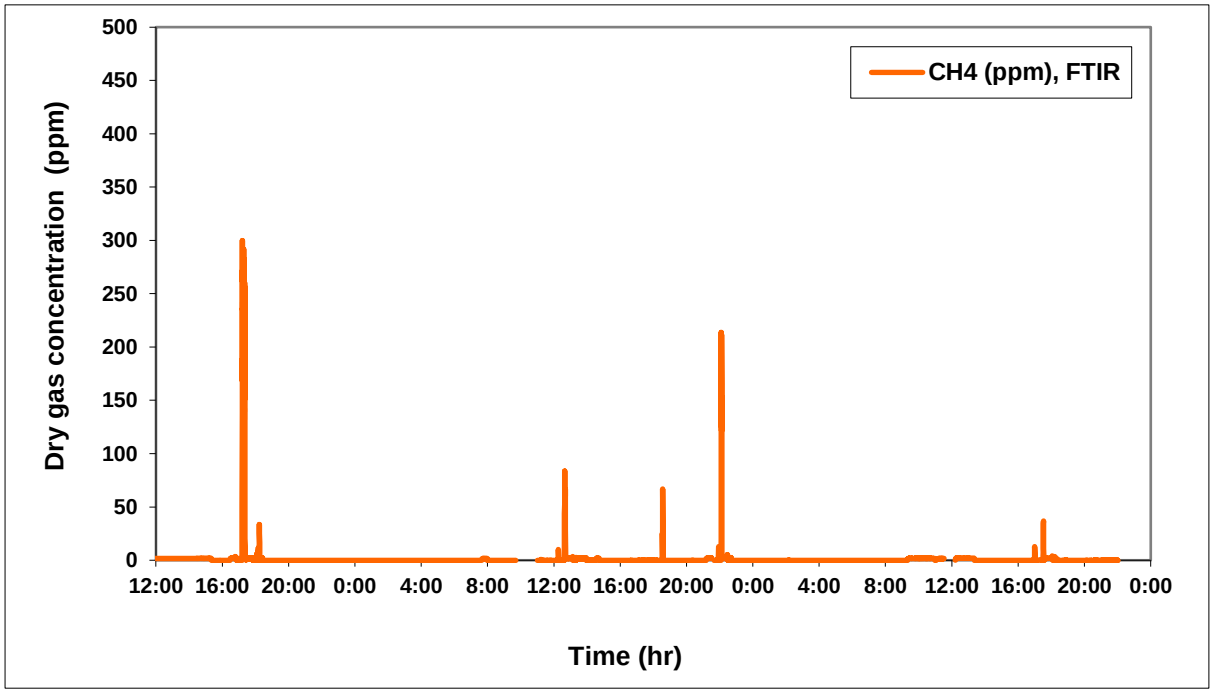

Russian coal: *12:00-8:00;* ***SA I:*** *12:00-20:00;* ***SA II:*** *0.00-8:00;* ***SA Discard:*** *12:00-20:00*

Appendix A14: CH_4 FTIR results (ppm)

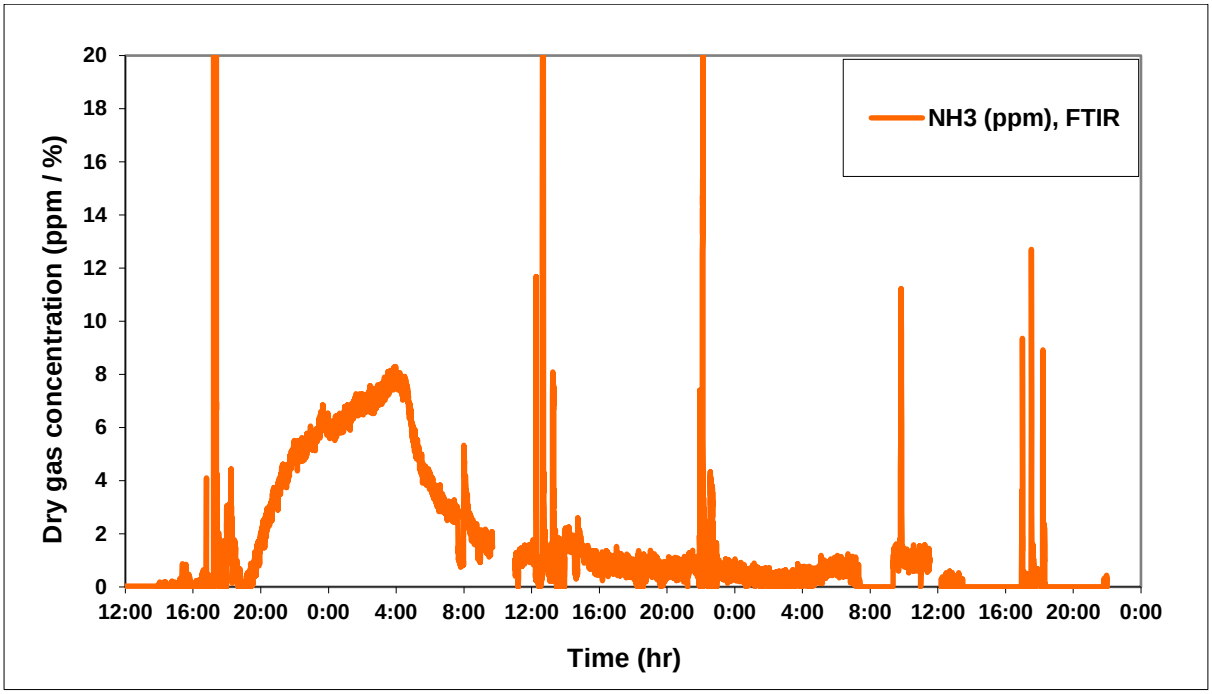

Appendix A15: NH_3 FTIR results (ppm)

Appendix B:
Emission Tables Summary

This appendix presents an extract of the major emission results

Appendix B1 Emission results wet basis

	H_2O (%)	O_2 (%)	CO_2 (%)	CO (ppm)	CH_4 (ppm)	N_2O (ppm)	NO (ppm)	NO_2 (ppm)	SO_2 (ppm)
Russian	6	5	14	213	0	227	30	0	180
SA I	6	5	15	48	0	149	36	0	531
SA II	6	5	13	83	0	193	85	0	1068
SA Discard	7	5	14	56	0	214	49	0	1572

Appendix B1 continued

	NH3 (ppm)	HCl (ppm)	HF (ppm)	Ethylene (ppm)	Acetylene (ppm)	Benzene (ppm)	HCN (ppm)	HBr (ppm)
Russian	7	32	4	0	0	0	19	0.0
SA I	2	3	1	1	0	1	9	0.0
SA II	1	6	17	0	0	0	8	0.0
SA Discard	0	5	23	0	0	0	9	0.0

Appendix B2 Emission results on wet basis @ 6 % O_2

	CO_2 (%)	CO (ppm)	CH_4 (ppm)	N_2O (ppm)	NO (ppm)	NO_2 (ppm)	SO_2 (ppm)
Russian	13	198	0	211	28	0	167
SA I	13	44	0	137	33	0	488
SA II	12	79	0	182	80	0	1007
SA Discard	13	53	0	203	46	0	1488

Appendix B2 continued

	NH_3 (ppm)	HCl (ppm)	HF (ppm)	Ethylene (ppm)	Acetylene (ppm)	Benzene (ppm)	HCN (ppm)	HBr (ppm)
Russian	6	30	3	0	0	0	17	0.0
SA I	2	3	1	1	0	1	8	0.0
SA II	0	6	16	0	0	0	8	0.0
SA Discard	0	5	22	0	0	0	9	0.0

Appendix B3 Emission results on dry basis @ 6 % O_2

	CO_2 (%)	CO (ppm)	CH_4 (ppm)	N_2O (ppm)	NO (ppm)	NO_2 (ppm)	SO_2 (ppm)
Russian	14	211	0	225	30	0	179
SA I	14	47	0	147	35	0	521
SA II	13	83	0	194	85	0	1069
SA Discard	14	57	0	219	50	0	1603

Appendix B3 continued

	NH_3 (ppm)	HCl (ppm)	HF (ppm)	Ethylene (ppm)	Acetylene (ppm)	Benzene (ppm)	HCN (ppm)	HBr (ppm)
Russian	7	32	4	0	0	0	19	0.0
SA I	2	3	1	1	0	1	9	0.0
SA II	1	6	17	0	0	0	8	0.0
SA Discard	0	5	24	0	0	0	9	0.0

Appendix C:
Petrography analysis

Appendix C1 Maceral analysis (percent by volume, mineral matter- free basis)

	VITRINITE			LIPTINITE			INERTINITE									RANK REFLECTANCE	
Sample	VIT %	PV %	TV %	S/R/C %	ALG %	TOTL %	RSF %	ISF %	F/SEC %	MIC %	R %	I %	TOT I %	HEAT ALTERED %	TOTAL REACTIVES %	Rr %	σ
SA I	17	1	18	5	0	5	11	22	6	2	11	25	77	< 1	45	0.60	0.099
SA II	74	4	78	5	0	5	3	5	3	1	1	4	17	0	87	0.68	0.058
SA Discard	27	2	29	6	0	6	12	22	7	1	7	16	65	0	54	0.68	0.079
Russian	83	3	86	3	0	3	1	3	3	1	1	2	11	0	91	0.60	0.060

Appendix C2 Carbominerite and minerite analyses (percent by volume)

	CARBOMINERITE ANALYSIS				MINERITE ANALYSIS			
	CARB-ARGILITE /SILICITE COAL MACERALS PLUS CLAYS/QUARTZ	CARBO - PYRITE COAL MACERALS PLUS PYRITE	CARB-ANKERITE COAL MACERALS PLUS CARBONATES	TOTAL CARBO-MINERITE * MACERAL/ MINERAL ASSOCIATIONS	CLAY/QUARTZ GROUPS MINERALS	PYRITE MINERALS	CARBONATE GROUP MINERALS	TOTAL MINERITE MINERAL RICH PARTICLES
SA I	41	4	1	46	20	1	1	22
SA II	21	2	1	24	10	2	2	14
SA Discard	10	1	1	12	79	2	2	83
Russ	2	< 1	1	3	4	< 1	1	5

Appendix C3: Explanation of abbreviations and terms

Maceral analysis *(% by volume, mineral matter-free basis)* - see Appendix D1

VIT	:	Vitrinite
PV	:	Pseudovitrinite
TV	:	Total vitrinite
S/R/C	:	Sporinite/resinite/cutinite
ALG	:	Alginite
TOT L	:	Total liptinite (formerly referred to as exinite)
RSF	:	Reactive semifusinite
ISF	:	Inert semifusinite
F/SEC	:	Fusinite/secretinite
MIC	:	Micrinite
R INT	:	Reactive inertodetrinite
I INT	:	Inert inertodetrinite
TOT I	:	Total inertinite

Reactive Macerals	:	Vitrinite + liptinite + RSF + reactive inertodetrinite

REFLECTANCE MEASUREMENTS - see Appendix D1 and Table 4.5

Rr %	:	Random reflectance of vitrinite, oil immersion
σ	:	Standard deviation

Microlithotype analysis *(% by volume, mineral matter basis)* - see Table 4.7 and Table 4.9

VITRITE	:	Vitrinite > 95 %	)
LIPTITE	:	Liptinite > 95 %	) ***Monomacerals***
INERTITE	:	Inertinite > 95 %	)
CLARITE	:	Vitrinite + Liptinite > 95 %	)
DURITE	:	Inertinite + Liptinite > 95 %	) ***Intermediates***
VITRINERTITE	:	Vitrinite + Inertinite > 95 %	)
TRIMACERITE	:	Vitrinite, Inertinite, Liptinite > 5 %	)
CARBOMINERITE	:	Total inorganic/organic microlithotypes	
MINERITE	:	> 60 Vol % minerals	

Carbominerite analysis *(% by volume)* - see appendix D2 and Table 4.9

CARBARGILITE	:	Coal + 20 to 60 Vol % clay minerals
CARBOSILICITE	:	Coal + 20 to 60 Vol % quartz minerals
CARBOPYRITE	:	Coal + 5 to 20 Vol % sulphides
CARBANKERITE	:	Coal + 20 to 60 Vol % carbonates
CARBOMINERITE	:	Total inorganic/organic microlithotypes

Appendix C4: Theoretical standard deviation and repeatability limit of the percentage of a component, based on counts of 500 points

Volume %	**Standard Deviation**	**Coefficient of Variation**	**Repeatability limit**
5	1.0	20	2.8
20	1.8	9	5.1
50	2.2	4.4	6.3
80	1.8	2.3	5.1
95	1.0	1.1	2.8

For example, if the volume percentage of vitrinite in a sample is 80%, then the analyst can expect to obtain two results differing by less than 5.1 percentage points (e.g. 78% and 83%) in 19 cases out of 20 [101].

Appendix D:
Quantitative evaluation of minerals by scanning electron microscopy (QEMSCAN)

Appendix D1: Technology background

QEMSCAN was developed by CSIRO, Australia for originally determining the mineral proportions and characteristics of base metal and precious mineral samples. Analysing coal, clinkers, fouling deposits and fly ash, is a comparatively new application for QEMSCAN.

QEMSCAN: is a fully-automated micro-analysis system that enables quantitative chemical analysis of materials and generation of high-resolution mineral maps and images as well as porosity structure. It uses a scanning electron microscopy platform (SEM) with an electron beam source in combination with four energy-dispersive X-ray spectrometers (EDS).

The measured backscattered electron and electron-induced secondary X-ray emission spectra are used to classify sample mineralogy. A variety of quantitative information can be obtained including distribution, composition, and angularity of minerals, and the fabric, distribution, texture and porosity of materials.

There are three general types of measurement, those using the linear intercept and those based on particle mapping[144].

Bulk Mineral Analysis (BMA) is performed using the linear intercept method, and is used to provide statistically abundant data for mineral identification, speciation, distribution and quantification.

Particle mapping modes, including Particle Mineral Analysis (PMA), Specific Mineral Search (SMS) analysis and Trace Mineral Search (TMS) analysis, provide information on spatial relationships of minerals, including liberation and association data and provide a visual representation of mineral textures.

The Field Scan (FS) mode of measurement maps a rock or core chunks sample that has been mounted in the polished section. It collects a chemical spectrum at a set interval within the field of view. Each field of view is then processed offline to produce a low resolution digital map of the field of view [145].

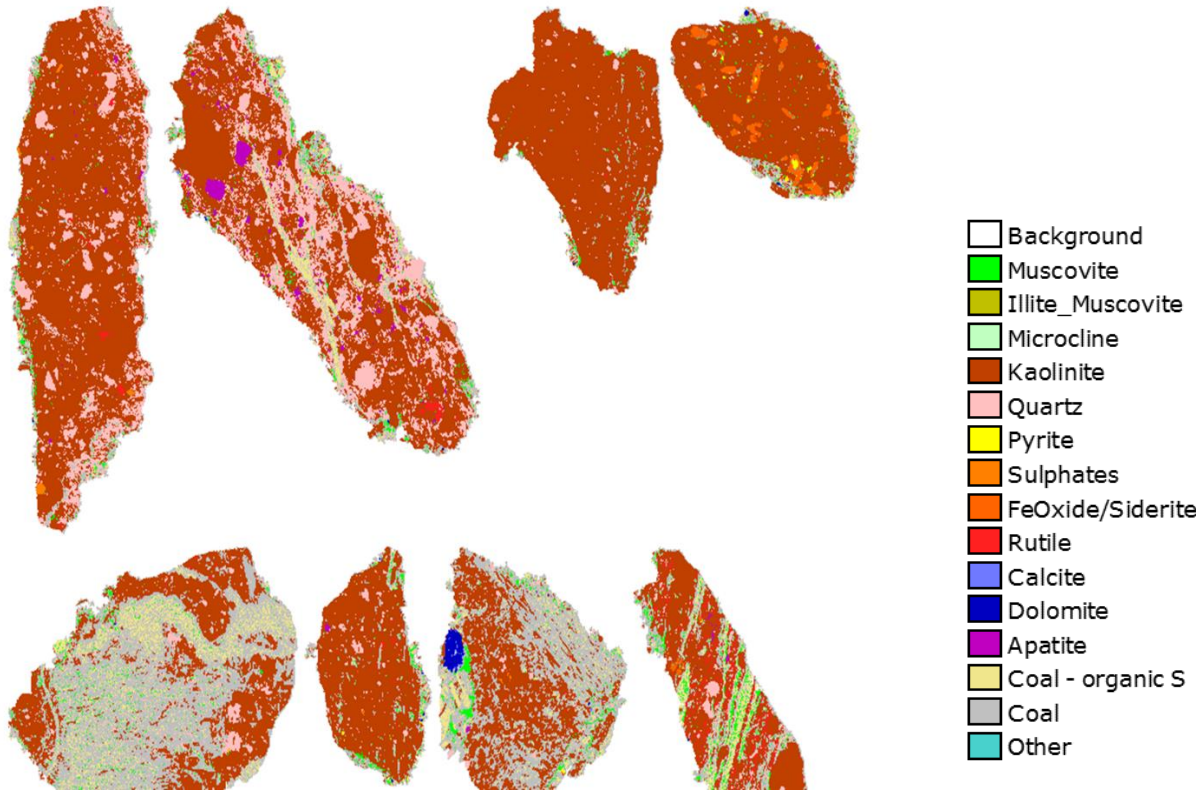

Appendix D2: SA I Selected kaolinite (brown) bearing particles [104]

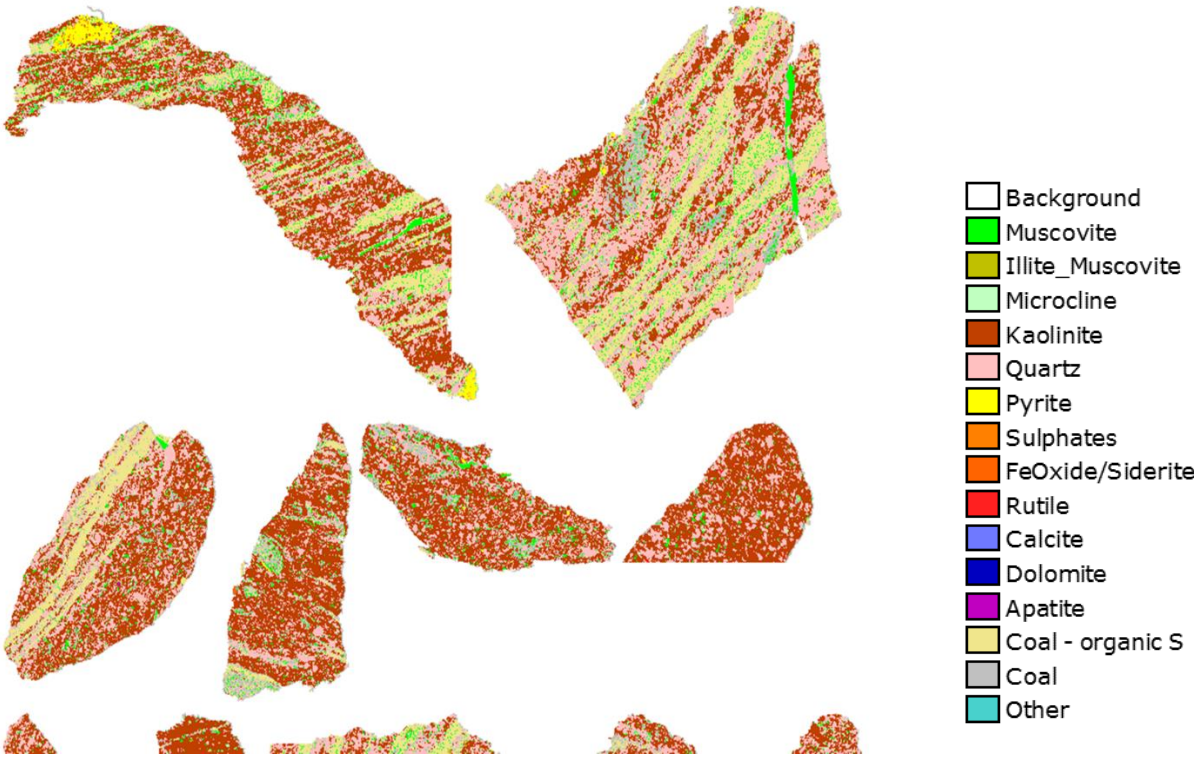

Appendix D3: SA II Selected kaolinite (brown) bearing particles

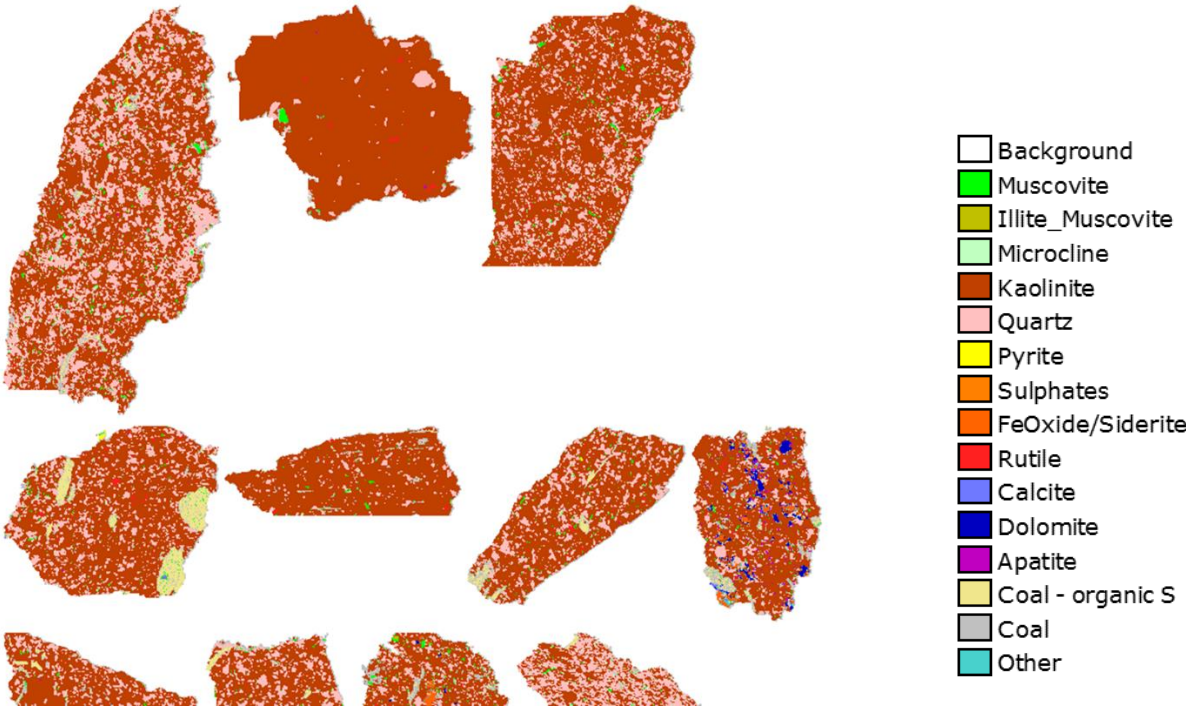

Appendix D4: SA Discard selected kaolinite (brown) bearing particles

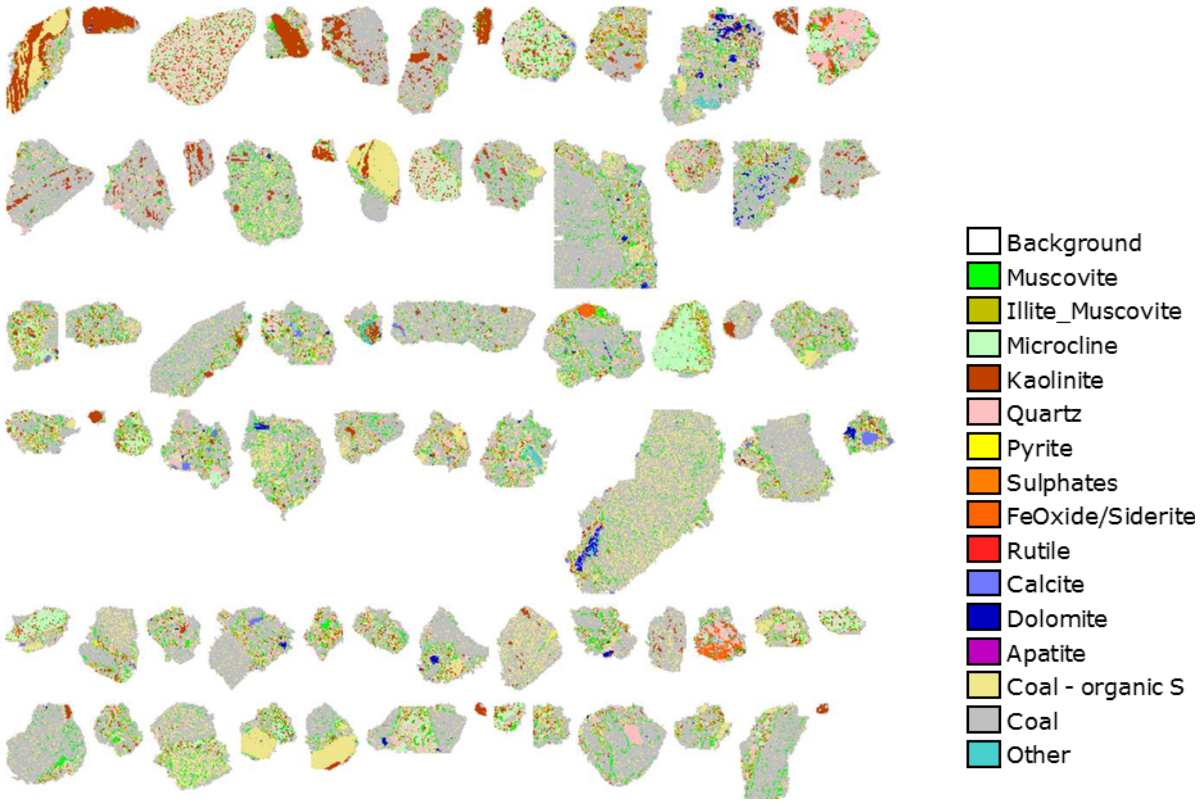

Appendix D5: Russian coal selected kaolinite (brown) bearing particles

Appendix E:
Calculations

This appendix highlight the major calculation methods used in the thesis.

Abbreviations used:

C: Carbon

LHV: Lower heating value (MJ/kg), measured during coal analysis

LHV real: Lower heating value (MJ/kg) done by calculation

1. Combustion Efficiency

The combustion efficiency is estimated (as percentage of the LHV), the heat losses owing to incomplete combustion (accounting the CO emission) and unburned carbon losses [34, 146].

The unburned carbon loss formula (F.1) given by Basu[34] below:

$$Unburned\ carbon\ loss\ (U_{cl}) = \frac{X_c * W_a * 32790}{HHV} * 100 \qquad \text{E.1}$$

Where Xc is the fractional carbon (not as carbonate) in the solid waste, and Wa is the ash per unit mass of the fuel feed.

HHV is the highest heating value of the fuel.

Higher Heating Value (HHV)

The Higher Heating Value (HHV) is the total amount of heat in a sample of fuel - including the energy in the water vapour that is created during the combustion process.

Lower Heating Value (LHV)

The Lower Heating Value (LHV) is the amount of heat in a sample of fuel **minus** the energy in the combustion water vapour. The Lower Heating Value is always **less** than the Higher Heating Value for a fuel.

The combustion efficiency in this study is calculated using the following formulas:

$$Combustion\ Efficiency\ (CE)\ (\%) = \frac{LHV\ real}{LHV} * 100 \quad \text{E.2}$$

$$LHV\ real\ (\frac{MJ}{kg}) = LHV\ -(measured)\frac{\%\ from\ fuel\ Carbon\ to\ fly\ ash * Carbon\ in\ Fuel}{100 * 32.7} \quad \text{E.3}$$

$$CE(\%) = \frac{LHV\ -(measured)\frac{\%\ from\ fuel\ Carbon\ to\ fly\ ash * Carbon\ in\ Fuel}{100 * 32.7}}{LHV} * 100 \quad \text{E.4}$$

$$CE(\%) = 1 - (measured)\frac{\%\ from\ fuel\ Carbon\ to\ fly\ ash * Carbon\ in\ Fuel}{100 * 32.7 * LHV} * 100 \quad \text{E.5}$$

The combustion efficiency is calculated in the form of:

$$CE = 1 - T \quad \text{E.6}$$

Where T is a term which is calculated by different formulas according to the literature using various factors like heat losses approach, ash approach or like in this study it is in the following form:

$$T = \frac{\%\ from\ fuel\ Carbon\ to\ fly\ ash * Carbon\ in\ Fuel}{100 * 32.7 * LHV} * 100 \quad \text{E.7}$$

T encompasses both the ash content and carbon content in the fuel and the changes of their content before and after combustion (unburnt carbon), close to the formulas E8 [147] and E9 [148] from the literature. In these formulas, the term T is characterised by the computation of the heat losses in the stack for Formula F8 and by the heat released in different parts for the Formula E9, respectively.

$$(CE)(\%) = 1 - \frac{Stack\ heat\ losses}{Fuel\ heating\ value} * 100 \quad \text{E.8}$$

Where the stack heat losses are the total of losses due to dry gas, moisture from burning, moisture in the fuel and from the heat losses from the formation of carbon.

$$(CE)(\%) = 1 - \frac{Q_{Unburnt\ carbon} + Q_{Ash} + Q_{Unburnt\ CO} + Q_{Flue\ gases} + Q_{Wall}}{Fuel\ heating\ value\ (LHV)} * 100 \quad \text{E.9}$$

The following is a glossary of terms:

$Q_{\text{unburnt carbon}}$: the loss due to the unburnt carbon contained in the discharged mass.

Q_{Ash} : the loss due to the ash discharging from the bed.

$Q_{\text{unburnt CO}}$: the heat loss due to the unburnt CO in the flue gas.

$Q_{\text{Flue gases}}$: the heat losses due to the flue gases

Q_{Wall} : the heat loss due to the bed to wall heat transfer.

LHV : fuel lower heating value

Fly ash

$$from\ fuel\ carbon\ to\ fly\ ash\ (\%) = \frac{Carbon\ in\ fly\ ash}{Total\ carbon\ content\ in\ fuel} \quad \text{E.10}$$

$$Carbon\ in\ Fly\ Ash\ (\%) = \frac{TOC}{real\ fly\ ash\ (\%) * 100} \quad \text{E.11}$$

$$Real\ Fly\ Ash\ \% = Fly\ ash\ \% * Ash\ content\ in\ the\ fuel \quad \text{E.12}$$

$$Fly\ Ash\ (\%) = \frac{Weight\ of\ fly\ ash\ recorded}{weight\ of\ Ash\ fed\ in} \quad \text{E.13}$$

2. Carbon

Total Carbon in the discharge (TC)

$$TC\ (weight\ \%) = \frac{Carbon\ (g)}{W\ (g)} * 100 \quad \text{E.14}$$

W: weight of discharge (g)

TOC (weight%) = total organic Carbon in the discharge

TIC: Total Inorganic Carbon in the discharge

$$TOC\ (Weight\%) = TC - TIC \quad \text{E.15}$$

3. Bottom Ash

$$Bottom\ Ash\ \% = 1 - Fly\ ash \quad \text{E.16}$$

4. Volatiles Ash free

$$Volatiles\ Ash\ free\ (\%) = \frac{Volatiles\ content\ in fuel}{100 - ash\ content\ in\ fuel} \quad \text{E.17}$$

5. Material circulation rate (kg/h)

$$Circulation\ rate\ (\frac{kg}{h}) = \frac{Material\ Rotation}{1000 * \frac{3600}{Time\ interval}} \quad \text{E.18}$$

Time interval: either 5 s or 10 s

6. Percentages of primary air and secondary air

$$Primary\ Air\ (\%) = \frac{Primary\ air\ volume}{Total\ volume\ (primary\ air + secondary\ air)} \quad \text{E.19}$$

$$Secondary\ Air\ (\%) = \frac{Secondary\ air\ volume}{Total\ volume\ (primary\ air + secondary\ air)} \quad \text{E.20}$$

7. Conversions

The conversion of atmospheric Pollutant Concentrations is done in order to draw the comparison with the standard limits. Often the units used differs from one country to another.

The conversion factor depends on the temperature at which the conversion (usually about 20 to 25 degrees centigrade). At an ambient pressure of one atmosphere: the general equation, from mg/m3 to ppmv and Vis versa [149].

$$ppmv = \frac{\frac{mg}{Nm^3} * (273.15 + °\mathbf{C})}{12.187 * M} \quad \text{E.21}$$

$$\frac{mg}{Nm^3} = \frac{(ppmv)(12.187)(M)}{(273.15 + °\boldsymbol{C})} \quad \text{E.22}$$

ppmv: ppm by volume (i.e., volume of gaseous pollutant per 10^6 volumes of ambient air)

$\frac{mg}{Nm^3}$: milligrams of gaseous pollutant per cubic meter of ambient air

M: molecular weight of gaseous pollutant

$°C$: ambient air temperature in degrees Centigrade

Using ideal gas law, Volume = 22.4 l for 1 mol under standard temperature and pressure

$$(ppmv) = \frac{V\ in\ \left({}^{mg}/_{m^3}\right) * 22.4}{M} \quad \text{E.23}$$

Correction of the gas volume at 6 % or 10 % O_2

In this study, the exhaust gas contains 5 % O_2

$$Volume\ in\ ppm\ @\ (6\%\ O_2) = \frac{V(ppm) * (20.9-6)(\%)}{(20.9-5)\ (\%)} \quad \text{E.24}$$

The same for 10 % O_2 by replacing 6 with 10 in the formula

Appendix F8 Conversion table from ppm to mg/Nm^3

GAS	**Conversion from ppm to mg/Nm^3 At 0 ºC and 101.3 kPa**
CO	1ppm = 1.25 mg/Nm^3
N_2O	1ppm = 1.96 mg/Nm^3
NO	1ppm = 1.34 mg/Nm^3
NO_2	1ppm = 2.05 mg/Nm^3
SO_2	1ppm = 2.86 mg/Nm^3
NH_3	1ppm = 0.76 mg/Nm^3
HCL	1ppm = 1.63 mg/Nm^3
HF	1ppm = 0.89 mg/Nm^3

CH_4	1ppm = 0.72 mg/Nm^3

REFERENCES

1. Franco, A. and A.R. Diaz, *The future challenges for "clean coal technologies": joining efficiency increase and pollutant emission control.* Energy, 2009. **34**(3): p. 348-354.
2. E.I.A., *Annual Energy Outlook With Projections to 2030, this publication is on the WEB at: www.eia.doe.gov/oiaf/aeo/ accessed on 13/03/2016.* (2008).
3. I.E.A., *World Energy Outlook Special Report "Energy and Climate Change" this publication from www.iea.org accessed on 13/03/2016.* 2015.
4. Burnard, K. and S. Bhattacharya, *"power generation from coal Ongoing developments and outlook" www.iea.org accessed on 13/03/2016.* 2011.
5. Sanpasertparnich, T., et al., *Integration of post-combustion capture and storage into a pulverized coal-fired power plant.* International Journal of Greenhouse Gas Control, 2010. **4**(3): p. 499-510.
6. Lako, P., *"Coal fired power plants" IEA ETSAP - Technology Brief E01 – April 2010 - www.etsap.org*. 2010.
7. I.E.A., *CO2 Emissions from fuel combustion, www.iea.org accessed on 13/03/2016.* 2015.
8. I.E.A., *Africa Energy outlook, "a focus on energy prospects in sub-saharan Africa" www.iea.org, accessed on 11/03/2016.* 2014.
9. online, S.A., *"Energy in south Africa," Available at: http://www.SouthAfrica.co.za/about South Africa/environment/energy and water. (Accessed on 15 may 2012).* 2012.
10. North, B.C., *"Utilisation of low grade fuels in fluidised bed combustion", PhD thesis, University of Witwatersrand.* 2012.
11. S.A.N.E.D.I., *South African Energy Development Institute (SANEDI), Annual report, available at www.sanedi.org.za accessed on 1 August 2016.* 2013.
12. Shimizu, T. and M. Toyono, *Emissions of NO x and N 2 O during co-combustion of dried sewage sludge with coal in a circulating fluidized bed combustor*. Fuel, 2007. **86**(15): p. 2308-2315.
13. U.N.F.C.C., *Framework convention on climate change, Conference of the parties serving as the meeting of the parties to the Kyoto protocol Fifth session Copenhagen, 7–18 December 2009, FCCC/KP/CMP/2009/7 available at www.unfcc.int accessed on 13/03/2016* 2009.
14. Act, A.Q., *Government Gazette Republic of South Africa.* Cape Town, 2004. **463**(25899): p. 1-10.
15. Africa, S., *"National Response to South Africa's Electricity Shortage" available at www.gov.za accessed June 2011*. 2011.
16. Falcon, R., *Personal communication.*
17. Dupree, I., *National Inventory of Discard and Duff coal.* South African Department of minerals and Energy, Pretoria, 2001. **pp. 1 – 31**.
18. Zhu, Q. *Developments in circulating fluidised bed combustion*. 2013. IEA.
19. Hotta, A., et al. *CFB technology provides solutions to combat climate change*. in *9th International Conference on Circulating Fluidized Beds*. 2008.
20. Hotta, A. *Foster wheeler's solutions for large scale CFB boiler technology: features and operational performance of Łagisza 460 MWe CFB Boiler*. in *Proceedings of the 20th international conference on fluidized bed combustion*. 2009. Springer.

21. Hack, H., et al., *Ultra-Supercritical CFB Technology to Meet the Challenge of Climate Change.* Power-Gen International, 2008: p. 2-4.
22. Squires, A.M., *The story of fluid catalytic cracking in Circulating Fluidized Bed Technology* I, Basu, P Ed., Pergamon Press, Toronto, 1986.
23. OUTOTEC, *Roasting plants, available at www.outotec.com, accessed April 2011.*
24. Jäntti, T. and R. Parkkonen, *Lagisza 460 MWe Supercritical CFB–Design.* Start-up and Initial Operation Experience, Power Gen Asia, 2009.
25. Jäntti, T., et al., *Circulating Fluidized-bed Technology towards zero CO2 Emissions.* POWER-GEN Europe Cologne, Germany, 2006.
26. Gibilaro, L.G., *Fluidization–dynamic: The formulation and applications of a predictive theory for the fluidized state.* Firth Publication-Butterworth-Heinemann, 2001.
27. Hesketh, R.P., et al., *Fluidized bed polymer coating experiment.* Chemical Engineering Education, 2002. **36**(2): p. 138-143.
28. Yang, W.-C., *Handbook of fluidization and fluid-particle systems*. 2003: CRC press.
29. ENERGOCON, *"Principle of fluidisation" available at www.energocon.com accessed on May 2010.*
30. Barišić, V., *Catalytic Reactions of N2O and NO Over Bed Materials from Multi-fuel Circulating Fluidized Bed Combustion*. 2006: Åbo Akademi.
31. Podolski, W.F., *Pressurised FBC Technology.* Noyes Data Corporation, U.SA, 1986.
32. Coal, D.o., *Fluidised Bed Coal-Fired Boilers* A National Coal Board Report, London, Accessed 2016.
33. Geldart, D., *Types of gas fluidization.* Powder technology, 1973. **7**(5): p. 285-292.
34. Basu, P., *Combustion and gasification in fluidized beds*. 2006: CRC press.
35. wheeler, F., *Power generation.* Available on www.FW.com accessed May 2011.
36. Bariši, V., et al., *Foster Wheeler Experience in Combustion of Low-Grade High-Ash Fuels in CFBs.* Termotehnika, 2009. **35**(2): p. 133-148.
37. Zhu, H. and J. Zhu, *Comparative study of flow structures in a circulating-turbulent fluidized bed.* Chemical Engineering Science, 2008. **63**(11): p. 2920-2927.
38. Kavidass, S., G. Anderson, and G. Norton, *Why build a circulating fluidized bed boiler to generate steam and electric power.* PowerGen Asia, 2000.
39. Luis, F., et al., *Influence of operating parameters on NO x and N 2 O axial profiles in a circulating fluidized bed combustor.* Fuel, 1996. **75**(8): p. 971-978.
40. power, *http://www.power4georgians.com/coal.aspx , Accessed 10 April 2013* 2013.
41. Koornneef, J., M. Junginger, and A. Faaij, *Development of fluidized bed combustion—An overview of trends, performance and cost.* Progress in energy and combustion science, 2007. **33**(1): p. 19-55.
42. Lockwood, T., *Techno-economic analysis of PC vs CFB No 13/14 November combustion technology.* 2013.
43. Khan, A., et al., *Biomass combustion in fluidized bed boilers: potential problems and remedies.* Fuel processing technology, 2009. **90**(1): p. 21-50.
44. C.S.I.R., *www.csir.co.za/mineral/CPO-0024.PDF, Accessed 16 April 2013.* 2013.
45. CSIR, *www.csir.co.za/mineral/CPJJKO-0024.PDF, Accessed 28 August 2013.* 2013.
46. Jantti, T. and K. Nuortimo, *Circulating Fluidized Bed Technology for Large Scale Power Generation Using Coal and Petroleum Coke.* Russia Power, March, 2012: p. 5-7.
47. Engelbrecht, A., et al., *Fluidised bed gasification of South African coals–experimental results and process integration.* 2011.
48. Bruce, G., *Clean Coal Engineering Technology*. 2011, United Kingdom: Elsevier.

49. Peña, J.A.P., *Bubbling Fluidized Bed (BFB), When to use this technology?* Industrial Fluidization South Africa (IFSA) Foster Wheeler, Johannesburg, South Africa, 2011.
50. Falcon, R. and A. Ham, *The characteristics of Southern African coals.* Journal of the South African Institute of Mining and Metallurgy, 1988. **88**(5): p. 145-161.
51. HENDERSON, D., *Clean Coal Technologies. IEA Clean Coal Centre Report: CCC/74, ISBN 92-9029-389-6.* . 2003.
52. Basu, P., *Combustion of coal in circulating fluidized-bed boilers: a review.* Chemical Engineering Science, 1999. **54**(22): p. 5547-5557.
53. Goidich, S.J. and T. Hyppanen. *Foster Wheeler compact CFB boilers for utility scale*. in *16 th International Conference on Fluidized Bed Combustion*. 2001.
54. Utt, J. and R. Giglio, *Technology comparison of CFB versus pulverized fuel firing for utility power generation.* Journal of the Southern African Institute of Mining and Metallurgy, 2012. **112**(6): p. 449-454.
55. Coal, G., *http://www.utilityguide.com/1common/coal.html-Utility , cited July 2013.* 2013.
56. Lowry, H.H., *Chemistry of coal utilization: supplementary volume.* 1963.
57. Sotudeh-Gharebaagh, R., et al., *Simulation of circulating fluidized bed reactors using ASPEN PLUS.* Fuel, 1998. **77**(4): p. 327-337.
58. Förtsch, D., et al. *A kinetic model for the prediction of NO emissions from staged combustion of pulverized coal*. in *Symposium (International) on Combustion*. 1998. Elsevier.
59. PRÉVOST, X.M.A.M., M.D, DUVAL, J.A.G., *South African Minerals Industry 2005-2006, Department of Minerals and Energy report, pp 42–50.* 2005.
60. Engelbrecht, A., B. North, and B. Oboirien, *Making the most of South Africa's low-quality coal: Converting high-ash coal to fuel gas using bubbling fluidised bed gasifiers.* 2010.
61. Özkan, G. and G. Doğu, *Combustion of a high ash and sulfur containing lignite in a pilot circulating fluidized bed combustor and its pollution characteristics.* Chemical Engineering and Processing: Process Intensification, 2002. **41**(1): p. 11-15.
62. Zhai, H. and E.S. Rubin, *Performance and cost of wet and dry cooling systems for pulverized coal power plants with and without carbon capture and storage.* Energy Policy, 2010. **38**(10): p. 5653-5660.
63. Koornneef, J., et al., *Life cycle assessment of a pulverized coal power plant with post-combustion capture, transport and storage of CO 2.* International journal of greenhouse gas control, 2008. **2**(4): p. 448-467.
64. Von Fredersdorff, C. and M.A. Elliott, *Coal gasification.* Chem. Coal Util., Suppl. Vol., 1963. **1963**.
65. IEA, *http://www.iea.org/publications/freepublications/publication/name,32869,en.html Accessed 8 July 2013.* 2013.
66. coal, W., *http://www.worldcoal.org/coal-energy-access/coal-and-clean-energy/ Accessed July 9, 2013.* 2013.
67. Carpenter, A.M., *Advances in multi-pollutant control.* IEA: London, UK, 2013.
68. Kavalov, B. and S.D. Peteves, *The future of coal.* Luxembourg: Europäische, 2007.
69. Board, C.I.A., *Power generation from coal: measuring and reporting efficiency performance and CO2 emissions.* CIAB International Energy Agency, Paris, Report: OECD/IEA2010, 2010: p. 1-114.

70. Oka, S.N., *Fluidized Bed Combustion.* Marcell Dekker, New York, 2004. **pages 510,-569**.
71. EPA, *National Air toxic, www.epa.gov accessed 13 May 2013.* 2005.
72. Patel, E.M., *Practical considerations in the implementation of emission reduction solutions at Eskom's coal plant" 4th EU-SA clean coal technolgys workshop group meeting, hosted by the department of Energy (RSA) in association with SANEDI and the European Commission. 6 November.* 2011.
73. IEA, *Energy and Air Pollution.* World Energy Outlook Special Report, 2016.
74. Makansi, J., *Few new options emerge for complying with CAA Phase 2.* Power;(United States), 1994. **138**(7).
75. Qing-gang, L. and Z. Jian-guo, *Pulverized Coal Combustion and NO_x Emissions in High Temperature Air From Circulating Fluidized Bed [J]*. Proceedings of the CSEE, 2007. **32**: p. 004.
76. Mann, M.D., M.E. Collings, and P.E. Botros, *Nitrous oxide emissions in fluidized-bed combustion: fundamental chemistry and combustion testing.* Progress in energy and combustion science, 1992. **18**(5): p. 447-461.
77. Johnsson, J.E., *Formation and reduction of nitrogen oxides in fluidized-bed combustion.* Fuel, 1994. **73**(9): p. 1398-1415.
78. Xiangsong, H., et al., *N 2 O decomposition over the circulating ashes from coal-fired CFB boilers.* Chemical engineering journal, 2008. **140**(1): p. 43-51.
79. Svoboda, K. and M. Pohořelý, *Influence of operating conditions and coal properties on NO x and N 2 O emissions in pressurized fluidized bed combustion of subbituminous coals.* Fuel, 2004. **83**(7): p. 1095-1103.
80. Bonn, B., G. Pelz, and H. Baumann, *Formation and decomposition of N 2 O in fluidized bed boilers.* Fuel, 1995. **74**(2): p. 165-171.
81. Shen, B., et al., *N 2 O emission under fluidized bed combustion condition.* Fuel Processing Technology, 2003. **84**(1): p. 13-21.
82. Krzywański, J., et al., *Modelling of CO 2, CO, SO 2, O 2 and NO x emissions from the oxy-fuel combustion in a circulating fluidized bed.* Fuel Processing Technology, 2011. **92**(3): p. 590-596.
83. Sims, R.E., H.-H. Rogner, and K. Gregory, *Carbon emission and mitigation cost comparisons between fossil fuel, nuclear and renewable energy resources for electricity generation.* Energy policy, 2003. **31**(13): p. 1315-1326.
84. Kutz, M., *Environmentally conscious alternative energy production*. 2007: Wiley Online Library.
85. Hristov, J. *Fluidized Bed Combustion as a Risk-Related Technology: A Scope*. in *3rd South-East Symposium on Fluidization, Romania*. 2001.
86. Barišić, V., et al., *CFB technology provides solutions for reducing CO2 emissions.* Journal of the Southern African Institute of Mining and Metallurgy, 2009. **109**(2): p. 107-119.
87. Kurose, R., M. Ikeda, and H. Makino, *Combustion characteristics of high ash coal in a pulverized coal combustion.* Fuel, 2001. **80**(10): p. 1447-1455.
88. Pacyna, E.G., et al., *Mercury emissions to the atmosphere from anthropogenic sources in Europe in 2000 and their scenarios until 2020.* Science of the Total Environment, 2006. **370**(1): p. 147-156.
89. Pirrone, N., et al., *Global mercury emissions to the atmosphere from anthropogenic and natural sources.* Atmospheric Chemistry and Physics, 2010. **10**(13): p. 5951-5964.

90. Vejahati, F., Z. Xu, and R. Gupta, *Trace elements in coal: Associations with coal and minerals and their behavior during coal utilization–A review*. Fuel, 2010. **89**(4): p. 904-911.
91. Wang, J., et al., *Mercury removals by existing pollutants control devices of four coal-fired power plants in China.* Journal of Environmental Sciences, 2011. **23**(11): p. 1839-1844.
92. Pacyna, E.G., et al., *Global emission of mercury to the atmosphere from anthropogenic sources in 2005 and projections to 2020.* Atmospheric Environment, 2010. **44**(20): p. 2487-2499.
93. Africa, P.S., *http://www.zeroco2.no/projects/south-africa, Accessed 10 April 2013* 2013.
94. Institute, E.P.R., *Power Generation Technology Data for Integrated Resource Plan of South Africa.* . EPRI, Palo Alto, CA:, 2010.
95. Hall, I., J. Eslait, and P. Den Hoed. *Khanyisa IPP a 450 MW CFB project: Practical challenges*. in *proceeding of IFSA 2011 conference, SAIMM*. 2011.
96. Aziz, T. and M. Dittus, *Kuyasa mine-mouth coal-fired power project: Evaluation of circulating fluidized-bed technology.* Proceedings of Industrial Fluidization South Africa, 2011: p. 11-29.
97. Masekoameng, K.E., J. Leaner, and J. Dabrowski, *Trends in anthropogenic mercury emissions estimated for South Africa during 2000–2006.* Atmospheric Environment, 2010. **44**(25): p. 3007-3014.
98. Wingrove, H., *Overview of Air Quality and Emission Standards in South Africa. Envirenment affaires and development planning, Mercury Emissions Inventory Workshop 19 August* 2011.
99. Pretorius, I., et al., *A perspective on South African coal fired power station emissions.* Journal of Energy in Southern Africa, 2015. **26**(3): p. 27-40.
100. I.S.O., *Determination of the petrographic composition of the coals* International standard office, 1985. **7404 - 2**
101. I.S.O., *Maceral group analysis.* International standard office, 1994. **7404 - 3**.
102. I.S.O., *Random reflectance measurments.* International standard office, 1994. **7404 - 5**.
103. I.S.O., *Determination of coals organic/inorganic associations* International standard office, 1988. **7404 – 4**.
104. Vainikka, P., et al., *Halide aerosols in circulating fluidised bed co-combustion. Role of coal bound kaolin.* Fuel processing technology, 2011. **92**(9): p. 1738-1749.
105. Lind, T., *Ash formation in circulating fluidised bed combustion of coal and solid biomass*. 1999: Technical Research Centre of Finland.
106. Gayan, P., et al., *Circulating fluidised bed co-combustion of coal and biomass.* Fuel, 2004. **83**(3): p. 277-286.
107. Tourunen, A., J. Saastamoinen, and H. Nevalainen, *Experimental trends of NO in circulating fluidized bed combustion.* Fuel, 2009. **88**(7): p. 1333-1341.
108. Koukouzas, N., et al., *Quantitative evaluation of minerals in fly ashes of biomass, coal and biomass–coal mixture derived from circulating fluidised bed combustion technology.* Journal of Hazardous Materials, 2009. **169**(1): p. 100-107.
109. Guo, Q. and J. Werther, *Influence of a gas maldistribution of distributor design on the hydrodynamics of a CFB riser*. Chemical Engineering and Processing: Process Intensification, 2008. **47**(2): p. 237-244.
110. Yates, J., *Effect of temperature and pressure.* CHEMICAL INDUSTRIES-NEW YORK-MARCEL DEKKER-, 2003: p. 129-154.

111. Prins, W., et al., *Devolatilization and ignition of coal particles in a two-dimensional fluidized bed.* Combustion and flame, 1989. **75**(1): p. 57-79.
112. Riaza, J., et al., *Single particle ignition and combustion of anthracite, semi-anthracite and bituminous coals in air and simulated oxy-fuel conditions.* Combustion and Flame, 2014. **161**(4): p. 1096-1108.
113. Watanabe, N., et al., *Combustible and incombustible speciation of Cl and S in various components of municipal solid waste.* Waste management, 2004. **24**(6): p. 623-632.
114. Kim, S.-T., W. Scaroni, and M. Fatemi-Badi, *Effect of Maceral Composition and Vitrinite Reflectance on the Combustion Behavior of Six hvA Bituminous Coals.* Prepr. Pap., Am. Chem. Soc., Div. Fuel Chem.;(United States), 1988. **33**(CONF-8809272-).
115. Sanyal, A., *Role of Macerals- An Underappreciated Coal Quality Parameter for Unburned Carbon Characterisation And Control.* Third DOE conference on unburned carbon on utility fly ash, Pittsburg 13- 14 May, 1977.
116. Sanyal, A., *Role of coal macerals in combustion.* Journal of the Institute of Energy, 1983. **56**: p. 92-5.
117. Oboirien, B., et al., *Study on the structure and gasification characteristics of selected South African bituminous coals in fluidised bed gasification.* Fuel processing technology, 2011. **92**(4): p. 735-742.
118. Redemann, K., E.-U. Hartge, and J. Werther, *Ash management in circulating fluidized bed combustors.* Fuel, 2008. **87**(17): p. 3669-3680.
119. Zhao, J., et al., *Gas concentration profiles and NO x formation in circulating fluidized bed combustion.* Fuel, 1997. **76**(9): p. 853-860.
120. Williams, A., M. Pourkashanian, and J. Jones, *Combustion of pulverised coal and biomass.* Progress in Energy and Combustion Science, 2001. **27**(6): p. 587-610.
121. Jensen, A., et al., *Formation and reduction of NO x in pressurized fluidized bed combustion of coal.* Fuel, 1995. **74**(11): p. 1555-1569.
122. Aho, M.J. and P.M. Pirkonen, *Effects of pressure, gas temperature and CO 2 and O 2 partial pressures on the conversion of coal-nitrogen to NO, N 2 O and NO 2.* Fuel, 1995. **74**(11): p. 1677-1681.
123. Åmand, L.-E., B. Leckner, and K. Dam-Johansen, *Influence of SO2 on the NON2O chemistry in fluidized bed combustion: 1. Full-scale experiments.* Fuel, 1993. **72**(4): p. 557-564.
124. Liu, H. and B.M. Gibbs, *The influence of limestone addition at different positions on gaseous emissions from a coal-fired circulating fluidized bed combustor.* Fuel, 1998. **77**(14): p. 1569-1577.
125. Krawczyk, E., M. Zajemska, and T. Wyleciał, *The chemical mechanism of SOx formation and elimination in coal combustion process.* CHEMIK nauka-technika-rynek, 2013. **1**(67): p. 856-862.
126. Shun, D., et al., *Kinetic Study of Sulfur Dioxide Elimination by Limestone through the Lab Scale Circulating Fluidized Bed Combustor.* Advances in Materials Physics and Chemistry, 2013. **2**(04): p. 189.
127. Lyngfelt, A., B. Leckner, and T. Mattisson, *A fluidized-bed combustion process with inherent CO 2 separation; application of chemical-looping combustion.* Chemical Engineering Science, 2001. **56**(10): p. 3101-3113.
128. Lupiáñez, C., et al., *Experimental study of SO 2 and NO x emissions in fluidized bed oxy-fuel combustion.* Fuel processing technology, 2013. **106**: p. 587-594.
129. Shimizu, T., et al., *Effect of SO2 removal by limestone on NOx and N2O emissions from a bubbling fluidized-bed combustor.* Fuel, 1992. **71**(7): p. 841-844.

130. Abanades, J.C., *The maximum capture efficiency of CO 2 using a carbonation/calcination cycle of CaO/CaCO 3.* Chemical Engineering Journal, 2002. **90**(3): p. 303-306.
131. Rodríguez, N., et al., *Comparison of experimental results from three dual fluidized bed test facilities capturing CO 2 with CaO.* Energy Procedia, 2011. **4**: p. 393-401.
132. Klika, Z., L. Bartoňová, and D. Spears, *Effect of boiler output on trace element partitioning during coal combustion in two fluidised-bed power stations.* Fuel, 2001. **80**(7): p. 907-917.
133. Tavoulareas, E.S. and W. Jozewicz, *Multipollutant emission control technology options for coal-fired power plants*. 2005: US Environmental Protection Agency, Office of Research and Development and Office of Air and Radiation.
134. Pavlish, J.H. and e. al, *Status review of mercury control options for coal-fired power plants.* Fuel Processing Technology, 2003. **82**(2): p. 89-165.
135. Streets, D.G., et al., *Anthropogenic mercury emissions in China.* Atmospheric environment, 2005. **39**(40): p. 7789-7806.
136. Belaid, M., et al. *Potential and technical basis for utilising coal beneficiation discards in power generation by applying circulating fluidised bed boilers*. 2013. International Conference on Chemical, Ecology and Environmental Sciences (ICEES'2013).
137. North, B., A. Engelbrecht, and B. Oboirien, *Feasibility study of electricity generation from discard coal.* Journal of the Southern African Institute of Mining and Metallurgy, 2015. **115**(7): p. 573-580.
138. Nzove, S. and H. Ndiritu. *Clean Coal Utilization for Power Generation: A Review*. in *Proceedings of Sustainable Research and Innovation Conference*. 2013.
139. I.E.A., *Projected costs of generating electrcity.* Available at www.IEA.com accessed 11 March 2016, 2010.
140. Duan, L., et al., *O 2/CO 2 coal combustion characteristics in a 50kW th circulating fluidized bed.* International Journal of Greenhouse Gas Control, 2011. **5**(4): p. 770-776.
141. Jaggi, N. and D. Vij, *Fourier transform infrared spectroscopy*, in *Handbook of Applied Solid State Spectroscopy*. 2006, Springer. p. 411-450.
142. Thermonicolet, *FTIR working principle* Available on www.thermonicolet.com accessed May 2016, 2016.
143. Simonescu, C.M., *Application of FTIR spectroscopy in environmental studies*. 2012: INTECH Open Access Publisher.
144. Ayling, B., et al. *QEMSCAN (Quantitative evaluation of minerals by scanning electron microscopy): capability and application to fracture characterization in geothermal systems*. in *Proc, Thirty-Seventh Workshop on Geotherm Reserv Eng. Stanford, California: Stanford University*. 2012.
145. Pascoe, R., M. Power, and B. Simpson, *QEMSCAN analysis as a tool for improved understanding of gravity separator performance.* Minerals engineering, 2007. **20**(5): p. 487-495.
146. Permchart, W. and V.I. Kouprianov, *Emission performance and combustion efficiency of a conical fluidized-bed combustor firing various biomass fuels.* Bioresource technology, 2004. **92**(1): p. 83-91.
147. Bergmann, J.L., *Combustion Analysis.* Flanders, NJ, USA, 2006.
148. Gungor, A., *Analysis of combustion efficiency in CFB coal combustors.* Fuel, 2008. **87**(7): p. 1083-1095.
149. Dispersion, A., *Conversions and Formulas.* available on www.air-dispersion.com accessed 18 February, 2016.